TA7
C6
CER 83-84/10
copy 2

WIND-TUNNEL STUDIES FOR SAND RESEARCH PROJECT

by

J. E. Cermak,[1] H. W. Shen,[2]
and J. A. Peterka[3]

FLUID MECHANICS AND WIND ENGINEERING PROGRAM

COLLEGE OF ENGINEERING

COLORADO STATE UNIVERSITY
FORT COLLINS, COLORADO

Engineering Sciences
DEC 1 1983
Brown Library

CER83-84JEC-HWS-JAP10

WIND-TUNNEL STUDIES FOR SAND RESEARCH PROJECT

by

J. E. Cermak,[1] H. W. Shen,[2]
and J. A. Peterka[3]

Prepared for

Research Institute
University of Petroleum and Minerals
Dhahran, Saudi Arabia

Project No. 5-3-9017

Fluid Mechanics and Diffusion Laboratory
Fluid Mechanics and Wind Engineering Program
Department of Civil Engineering
Colorado State University
Fort Collins, Colorado 80523

July 1983 CER83-84JEC-HWS-JAP-10

---

[1]Director, Fluid Dynamics and Diffusion Laboratory
[2]Professor, Department of Civil Engineering
[3]Professor, Department of Civil Engineering

TABLE OF CONTENTS

Section		Page
	LIST OF FIGURES	ii
	LIST OF TABLES	vii
1.0	INTRODUCTION	1
	1.1 Authorization	1
	1.2 Specific Tasks	1
	1.3 Wind-Tunnel Configuration	2
	1.4 Test Instrumentation	6
2.0	REPORT ORGANIZATION	9
3.0	ROADWAY/EMBANKMENT TESTS	10
	3.1 Purpose	10
	3.2 Test Configuration	10
	3.3 Test Procedures	10
	3.4 Test Results	13
	3.5 Conclusions	33
4.0	FENCE TESTS	38
	4.1 Purpose	38
	4.2 Test Configurations	38
	4.3 Test Procedures	41
	4.4 Test Results	42
	4.5 Conclusions and Commentary	63
5.0	SAND TRAP CALIBRATIONS	66
	5.1 Purpose	66
	5.2 Test Configuration	66
	5.3 Test Procedures	66
	5.4 Test Results	68
	5.5 Conclusions and Commentary	79
6.0	CHEMICALLY TREATED SAND	82
	6.1 Purpose	82
	6.2 Preliminary Discussions and Tests	82
	6.3 Test Configuration	83
	6.4 Test Procedures	83
	6.5 Test Results	85
	6.6 Conclusions and Commentary	94
7.0	REFERENCES	98

LIST OF FIGURES

Figure		Page
1-1	Meteorological Wind Tunnel, Fluid Dynamics and Diffusion Laboratory, Colorado State University	3
1-2	Plan view of entrance and upwind portion of MWT test section	4
1-3	Elevation view of downwind portion of MWT test section	5
1-4	Sand size distribution	7
3-1	Cross section of roadway and embankment model installed in wind tunnel (all dimensions in cm)	11
3-2	Plan view of roadway location within meteorological wind tunnel	12
3-3	Sand deposition rate on upwind side of roadway with free-stream velocity of 7 m/s	14
3-4	Sand deposition rate on upwind side of roadway with free-stream velocity of 14 m/s	15
3-5	Sand accumulation profiles for upwind roadway embankment (configuration #3) with a 7 m/s free-stream velocity	16
3-6	Sand accumulation profiles for upwind roadway embankment (configuration #3) with a 14 m/s free-stream velocity	17
3-7	Sand deposition upwind from Roadway Configuration No. 3 (after 4:45 hours of running time with a 14 m/s wind speed)	20
3-8	Side view showing the migration of sand over Roadway Configuration No. 3 (with a wind speed of 14 meters per second)	20
3-9a	Mean velocity and turbulence intensity profiles from sand-bed to a height of 130 cm at a position 3.66 m upwind of roadway (Pos. A) with a 7 m/s free-stream velocity	21
3-9b	Mean velocity and turbulence intensity profiles from surface to a height of 110 cm above roadway shoulder (Pos. B) with a 7 m/s free-stream velocity . .	22
3-9c	Mean velocity and turbulence intensity profiles from surface to a height of 110 cm above roadway median (Pos. C) with a 7 m/s free-stream velocity . . .	23

Figure		Page
3-10a	Mean velocity and turbulence intensity profiles from sand-bed to a height of 110 cm at a position 3.66 cm upwind of roadway (Pos. A) with a 14 m/s free-stream velocity	24
3-10b	Mean velocity and turbulence intensity profiles from surface to a height of 110 cm above roadway shoulder (Pos. B) with a 14 m/s free-stream velocity	25
3-10c	Mean velocity and turbulence intensity profiles from surface to a height of 110 cm above roadway median (Pos. C) with a 14 m/s free-stream velocity	26
3-11a	Mean velocity and turbulence intensity profiles from sand-bed to a height of 20 cm at a position 3.66 m upwind of roadway (Pos. A) with a 7 m/s free-stream velocity	27
3-11b	Mean velocity and turbulence intensity profiles from surface to a height of 20 cm above roadway shoulder (Pos. B) with a 7 m/s free-stream velocity	28
3-11c	Mean velocity and turbulence intensity profiles from surface to a height of 20 cm above roadway median (Pos. C) with a 7 m/s free-stream velocity	29
3-12a	Mean velocity and turbulence intensity profiles from sand-bed to a height of 20 cm at a position 3.66 m upwind of roadway (Pos. A) with a 14 m/s free-stream velocity	30
3-12b	Mean velocity and turbulence intensity profiles from surface to a height of 20 cm above roadway shoulder (Pos. B) with a 14 m/s free-stream velocity	31
3-12c	Mean velocity and turbulence intensity profiles from surface to a height of 20 cm above roadway median (Pos. C) with a 14 m/s free-stream velocity	32
3-13	Sand transport profiles over roadway with a 7 m/s free-stream wind velocity (aspirating probe measurements)	34
3-14	Sand transport profiles over roadway with a 14 m/s free-stream wind velocity (aspirating probe measurements)	35
3-15	Sand transport rate over roadway compared with amount of sand trapped by Shen vertical sand trap . . .	36
4-1	One-eighth (0.3175 cm) inch vertical slat fence with 60 percent porosity	39

Figure		Page
4-2	Plan view of long single fence installed across tunnel at 45° angle to wind	40
4-3	Plan view of short single fence installed within tunnel at 45° angle to wind	41
4-4	Sand accumulation on downwind side of long 45° fence	43
4-5	Sand accumulation on upwind side of long 45° fence	44
4-6a	Sand accumulation profiles for two-dimensional fence at 45° to 9 m/s wind	45
4-6b	Sand accumulation profiles at six cross sections around two-dimensional fence at 45° to 9 m/s wind (18 hours running time)	46
4-7	Sand accumulation around 45-degree inclined long fence (after 20+00 hours running time)	47
4-8	Sand accumulation on downwind side of short 45° fence	49
4-9	Sand accumulation on upwind side of short 45° fence	50
4-10	Sand accumulation profiles for 86 cm fence at 45° to prevailing 9 m/s wind	51
4-11	Sand accumulation: Downwind from 45-degree inclined short fence	52
4-12	Sand accumulation downwind from double fences (first test)	54
4-13	Sand accumulation between double fences (first test)	55
4-14	Sand accumulation upwind from double fences (first test)	56
4-15	Sand accumulation profiles for double fences (first test)	57
4-16	Sand accumulation between and downwind from double fences	58
4-17	Sand accumulation downwind from double fences (second test)	59

Figure		Page
4-18	Sand accumulation between double fences (second test)	60
4-19	Sand accumulation upwind from double fences (second test)	61
4-20	Sand accumulation profiles in vicinity of double fences (second test)	62
4-21	Downwind (a), between (b), and upwind (c) comparisons of sand deposition for two series of double fence tests	64
5-1	Plan view of USGS vertical and 34 mm I.D. vertical sand trap locations within MWT test section	67
5-2	Characteristic curves for the large azimuthal sand trap	72
5-3	Characteristic curve for large azimuthal sand trap per centimeter of intake width	73
5-4	Sand collection rate of horizontal traps at heights from 1-5 cm compared with characteristic curve for azimuthal sand trap	74
5-5	Comparison of cylindrical trap collection rates with those of large azimuthal trap	75
5-6	Comparison of sand collection rate for aspirating probe, Dr. Shen's trap and large azimuthal trap	76
5-7	Comparison of sand accumulation rates from azimuthal trap with those from aspirator probe	77
5-8	Relationship of azimuthal trap and aspirator probe accumulation rates as a function of wind-speed	78
5-9	Calibration curve for large azimuthal sand trap	80
6-1	Plan and elevation views of 20 cm stabilized sand strips in tunnel test section	84
6-2a	Mean velocity and turbulence intensity profiles from the surface to 110 cm at a position 1 m upwind from simulated dune	86
6-2b	Mean velocity and turbulence intensity profiles from the surface to 130 cm at a position 20 cm up stoss side of simulated dune	87

Figure		Page
6-2c	Mean velocity and turbulence intensity profiles from the surface to 150 cm at a position midway up stoss side of simulated dune	88
6-2d	Mean velocity and turbulence intensity profiles from the surface to 90 cm at a position 20 cm below crest on stoss side of simulated dune	89
6-3a	Mean velocity and turbulence intensity profiles from the surface to 20 cm at a position 1 m upwind from simulated dune	90
6-3b	Mean velocity and turbulence intensity profiles from the surface to 20 cm at a position 20 cm up stoss side of simulated dune	91
6-3c	Mean velocity and turbulence intensity profiles from the surface to 20 cm at a position midway up stoss side of simulated dune	92
6-3d	Mean velocity and turbulence intensity profiles from the surface to 20 cm at a position 20 cm below crest on stoss side of simulated dune	93
6-4	Upwind side of ramp (simulated dune) after 5½ hours of running time at 9 m/s wind speed	95

LIST OF TABLES

Table		Page
3-1	Sand accumulation (cm^3) per centimeter of width, calculated for a distance of 5.76 m upwind from the road shoulder	18
3-2	Total sand transport rate in grams/minute per centimeter of width at Positions A, B, and C	33
4-1	Sand accumulation (cm^3) per centimeter of width upwind and downwind from the single fence positioned across the tunnel at 45° to the wind	47
4-2	Sand accumulation (cm^3) per centimeter of width upwind and downwind from the short single fence positioned 45° to the wind	48
4-3	Sand accumulation (cm^3) per cm of width downwind, between and upwind from the double fences (first series)	52
4-4	Sand accumulation (cm^3) per centimeter of width upwind, downwind and between double fences (second series)	53
5-1	Sand accumulation rates measured for USGS Sand Trap at free-stream velocities and alignments from Tunnel center-line indicated	69
5-2	Sand accumulation rates measured for horizontal sand traps at free-stream velocities and heights indicated	70
5-3	Calculated efficiency of azimuthal sand trap	79
6-1	Sand erosion (cm) between stabilized strips on a level surface and on a simulated dune stoss face, for a 9 m/s wind velocity	97

WIND-TUNNEL STUDIES

FOR SAND RESEARCH PROJECT

1.0 INTRODUCTION

1.1 Authorization

As authorized by a formal contract between Colorado State University's Department of Civil Engineering and the Research Institute, University of Petroleum and Minerals, Dhahran, Saudi Arabia, dated 19 May 1983, wind-tunnel studies for the Madinat Al-Jubayl As-Sigaiyah Sand Research Project were performed in the CSU Fluid Dynamics and Diffusion Laboratory (FDDL) from 16 May 1983 through 8 July 1983.

1.2 Specific Tasks

The study requirements were a continuation of wind-tunnel sand control studies completed at the FDDL in 1982 and reported by Cermak et al., in "Wind-Tunnel Research for IAP Sand Study Project," September 1982. Tasks for this study, as specified in Telex messages between UPM and CSU, dated 31 January, 8 February and 11 April 1983, and related references contained therein, were as follows:

- Calibrate large azimuthal sand trap for one direction and four wind speeds. Additional calibration of 34 mm I.D. horizontal opening cylindrical traps.
- Two-dimensional tests on roadway and embankment configuration #3 (see 1982 report) at 7 m/sec and 14 m/sec wind speeds. Measurements as in previous tests to include: i) wind velocity distribution over the roadway, ii) vertical sand distribution over the roadway and, iii) migration of sand particles over the roadway for unsteady flow conditions.

- Two-dimensional test on a double row of 60 percent porosity, one-eighth inch vertical slat fences, separated by 40 D/H ratio, at 12 m/sec speed.
- Two-dimensional test on a 60 percent porosity, one-eighth inch vertical slat, diverting fence (45° angle to wind) at 9 m/sec speed.
- Two-dimensional test on an inclined surface with a slope of 13° and length of about 2.5 meters covered with sand to 5 cm depth. Twenty cm strips of sand perpendicular to the wind direction to be covered with "Stokopol C-4140," leaving alternate 20 cm strips of the sand untreated. Test to be completed at a wind speed which was experimentally determined to initiate sand erosion.

1.3 Wind-Tunnel Configuration

The foregoing described tests were accomplished in the FDDL Meteorological Wind Tunnel (MWT), as schematically depicted in Figure 1-1, operating in the auxiliary mode. A detailed description of the MWT operation is provided by Cermak (June 1981).

The MWT entrance configuration is generally reflected in Figure 1-2. The 1.83 m wooden spires and 0.18 m trip located at the entrance were used to create a simulated atmospheric boundary layer (ABL) within the tunnel test-section. The theory of ABL simulation is addressed in publications by Cermak (September 1971, October 1982). Figure 1-3 provides graphic description of the sand-bed, sand collection trap and other details of the downwind part of the MWT test-section. Specific location of roadway, fences, traps and stabilized sand strips within the tunnel are contained in appropriate report sections.

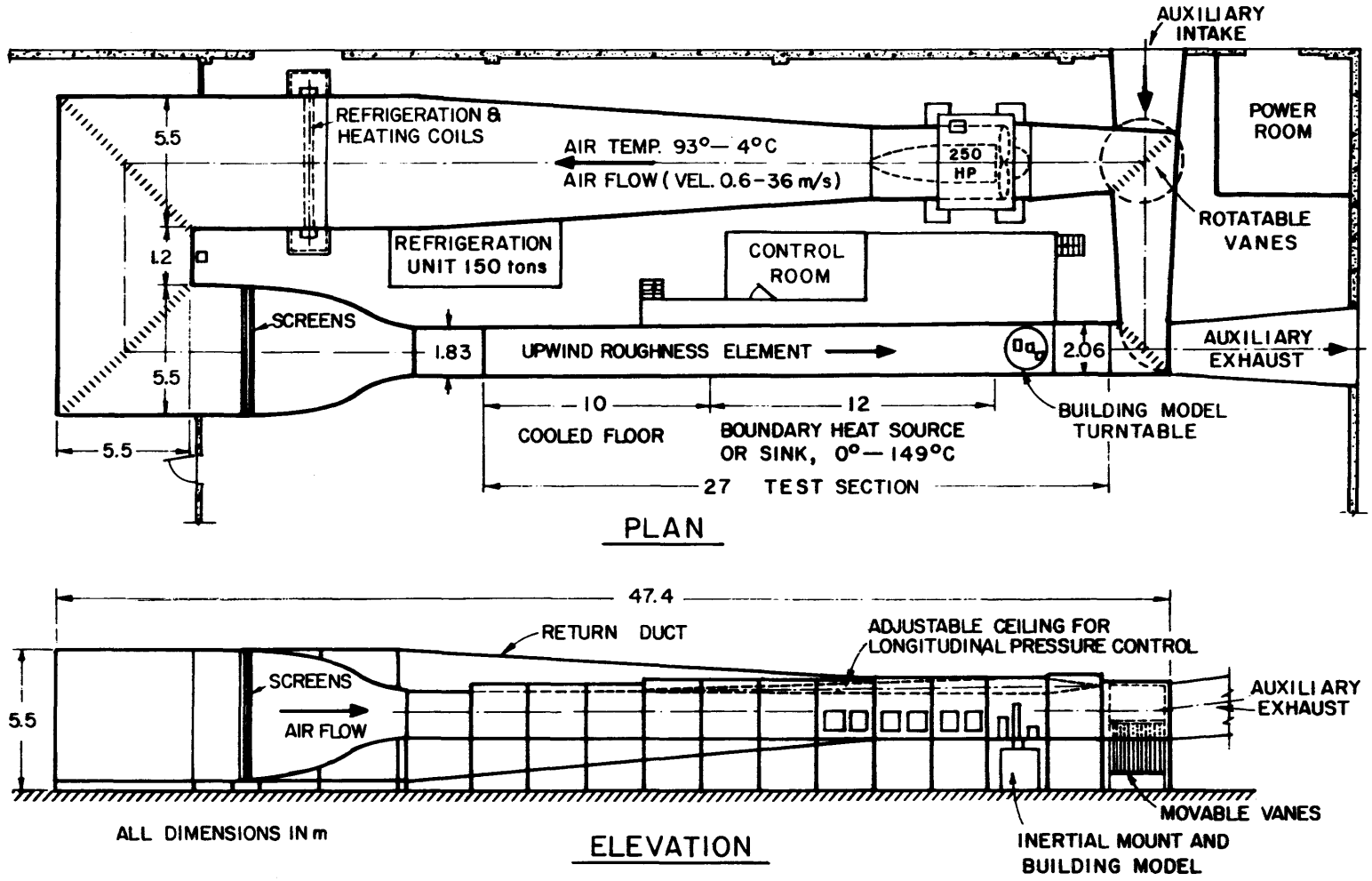

Figure 1-1. Meteorological Wind Tunnel Fluid Dynamics and Diffusion Laboratory, Colorado State University.

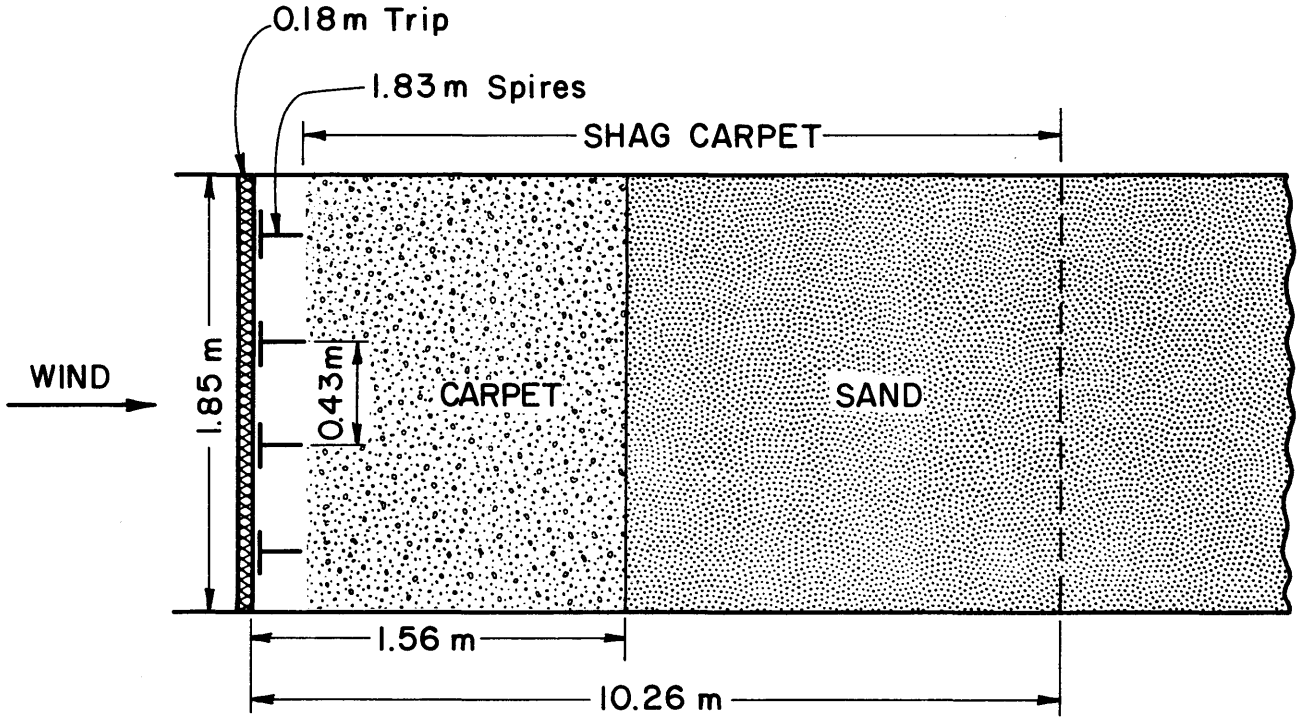

Figure 1-2. Plan view of entrance and upwind portion of MWT test section.

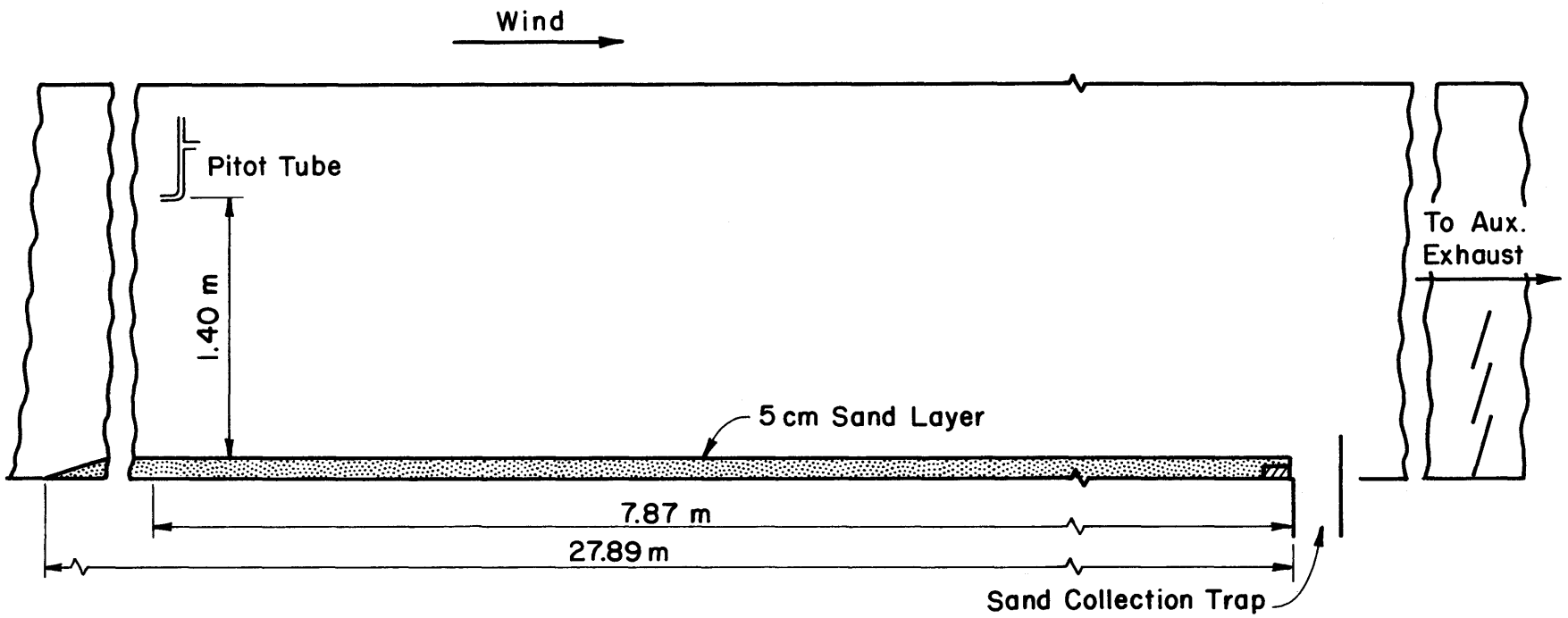

Figure 1-3. Elevation view of downwind portion of MWT test section.

Sand used for the tests was the same as that used in the 1982 wind-tunnel sand studies. Average diameter of the sand grains is about 140 microns, as indicated in the size distribution graph which comprises Figure 1-4.

1.4 Test Instrumentation

Velocity, sand accumulation and sand concentration measurements were all acquired in virtually the same manner as for the previous sand study (Cermak et al., 1982) and described in appendices to that report.

All velocity measurements were made with a Model 1610 Velocity Transducer, manufactured by TSI Incorporated. While this probe, with a time constant of approximately 0.1 second, sacrifices sensitivity to the faster turbulence frequency components, it possesses sufficient ruggedness to preclude particle induced errors in velocity responses.

A pitot tube was positioned at 145 cm above the tunnel floor and 7.87 m upwind from the sand collection trap. This location placed the pitot tube in good proximity to all the models tested and well above the ABL to insure accurate monitoring of free-stream velocities (u_∞). Pressure differentials were monitored with a Model 120 meter made by Trans-Sonics, Inc. Accuracy of the Trans-Sonics meter was verified with a Datametrics Integrating voltmeter.

Sand heights were again measured with a "point gauge" affixed to the custom-made trolley constructed especially for the 1982 sand study. As before, the largest drawback to this system of documenting sand accumulation was in the accurate selection of points on the rippled surface which represented mean heights of the sand surface.

Airborne sand distributions were once more measured with the FDDL designed isokinetic sampler. Operation of the isokinetic aspirating

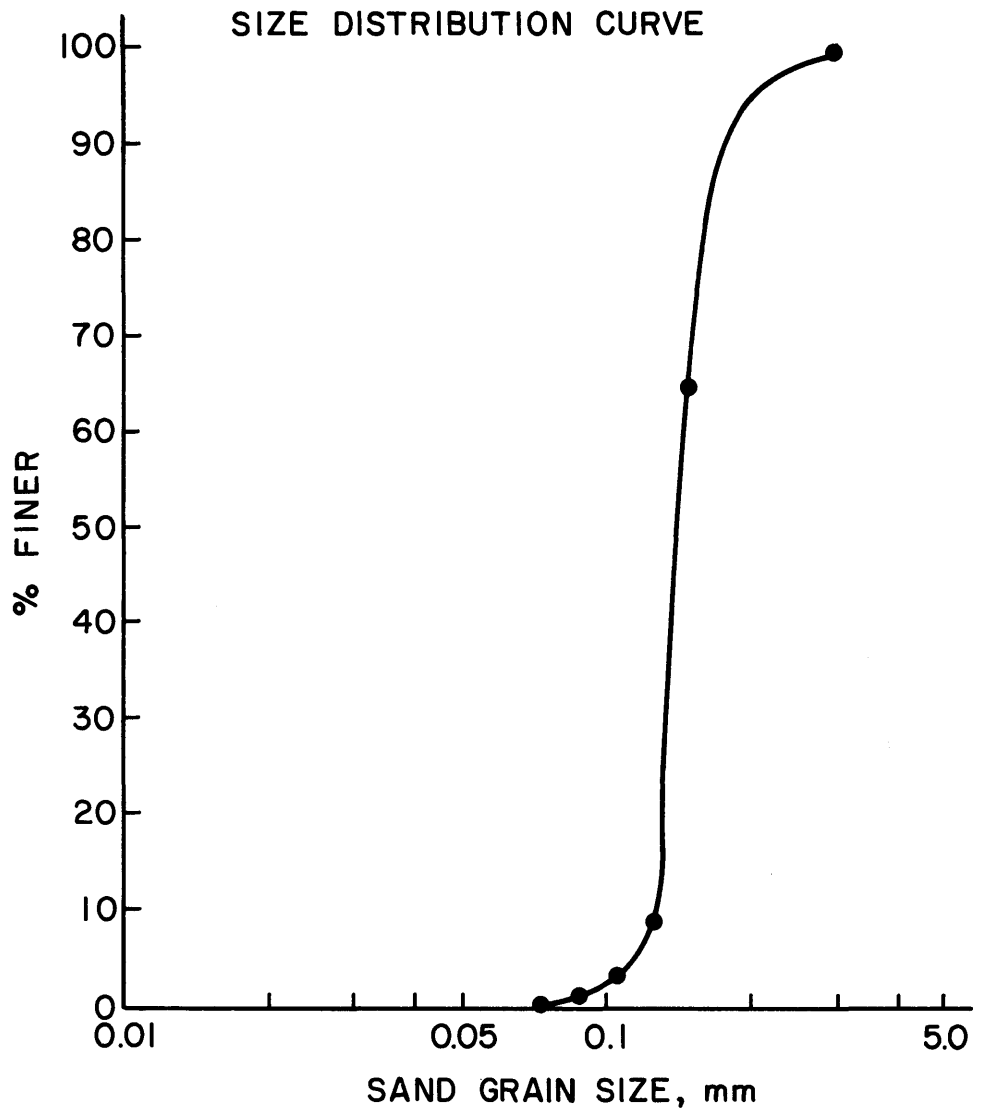

Figure 1-4. Sand size distribution.

probe was identical to that described in Appendix B of the 1982 IAP Sand Study Report, with the single exception of the probe opening. A 0.2 cm high by 1.0 cm wide rectangular opening was substituted for the circular orifice used in the earlier tests. This change permitted a more orderly analysis of the sand collected by the probe at variable heights above the sand bed surface.

2.0 REPORT ORGANIZATION

The body of this report has been divided into four separate sections which encompass the roadway, fences, sand traps and stabilized sand-strip test categories. Each of the four sections includes, as practicable: i) purpose for the tests; ii) a description of the tunnel configuration; iii) test procedures followed to include tunnel conditions and data measurement techniques/locations; iv) test results which include photo documentation as well as the tables and figures generated in the data analysis process and; v) pertinent conclusions deduced from the wind-tunnel study and related commentary.

3.0 ROADWAY/EMBANKMENT TESTS

3.1 Purpose

The wind-tunnel tests performed on roadway configuration #3 (as defined in 1982 IAP Sand Study Report) at free-stream velocities of 7 m/s and 14 m/s are a continuation of earlier studies and were intended to determine:

- Sand accumulation upwind from the roadway.
- Wind velocity distribution over the roadway.
- Vertical sand distribution over the roadway.

3.2 Tunnel Configuration

A cross-sectional sketch of the roadway model and embankment used in the tests is included as Figure 3-1. Prototype height of embankment #3 is six meters with an 18.43° angle of approach. With an assumed prototype-model ratio of 40 to 1, height of the comparable model was scaled to 15 cm. Moreover, the model roadway shoulders were covered with 0.5 mm grit, the road surface with a rubber material and the median with coarse sandpaper. Both embankments of the roadway were also coated with sandpaper.

The roadway model location in the MWT test section is depicted on Figure 3-2. The sand-bed extended approximately 20 m upwind from the roadway and was screeded to a depth of 7 cm for each of the two series of experiments. However, the 14 m/s tests caused significant deposits of the sand-bed beyond the tunnel section designed for sand entrapment and recycling. The loss of available sand prompted a decision to reduce sand-bed depth for the remainder of the tests.

3.3 Test Procedures

Roadway tests were made at free-stream velocities of 7 m/s and 14 m/s, as requested. In each case the accumulation of sand around the

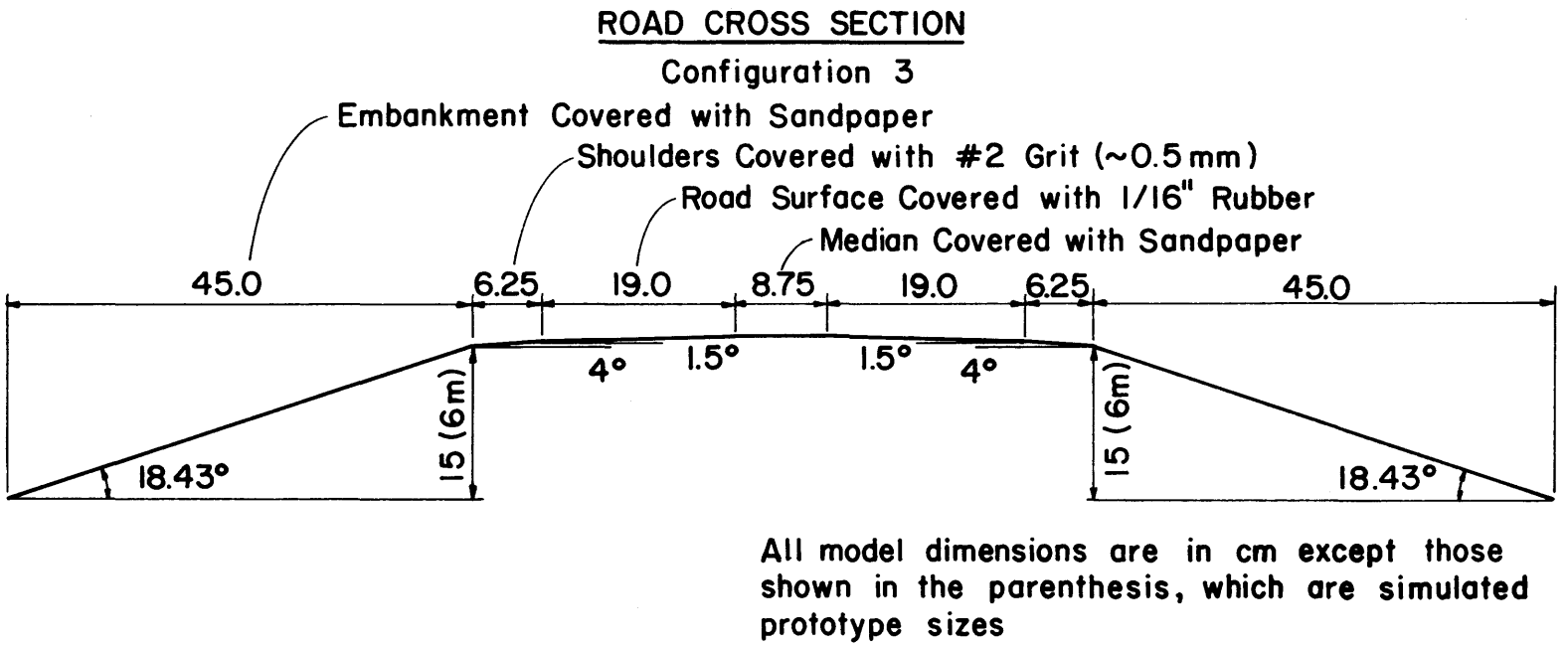

Figure 3-1. Cross section of roadway and embankment model installed in wind tunnel (all dimensions in cm).

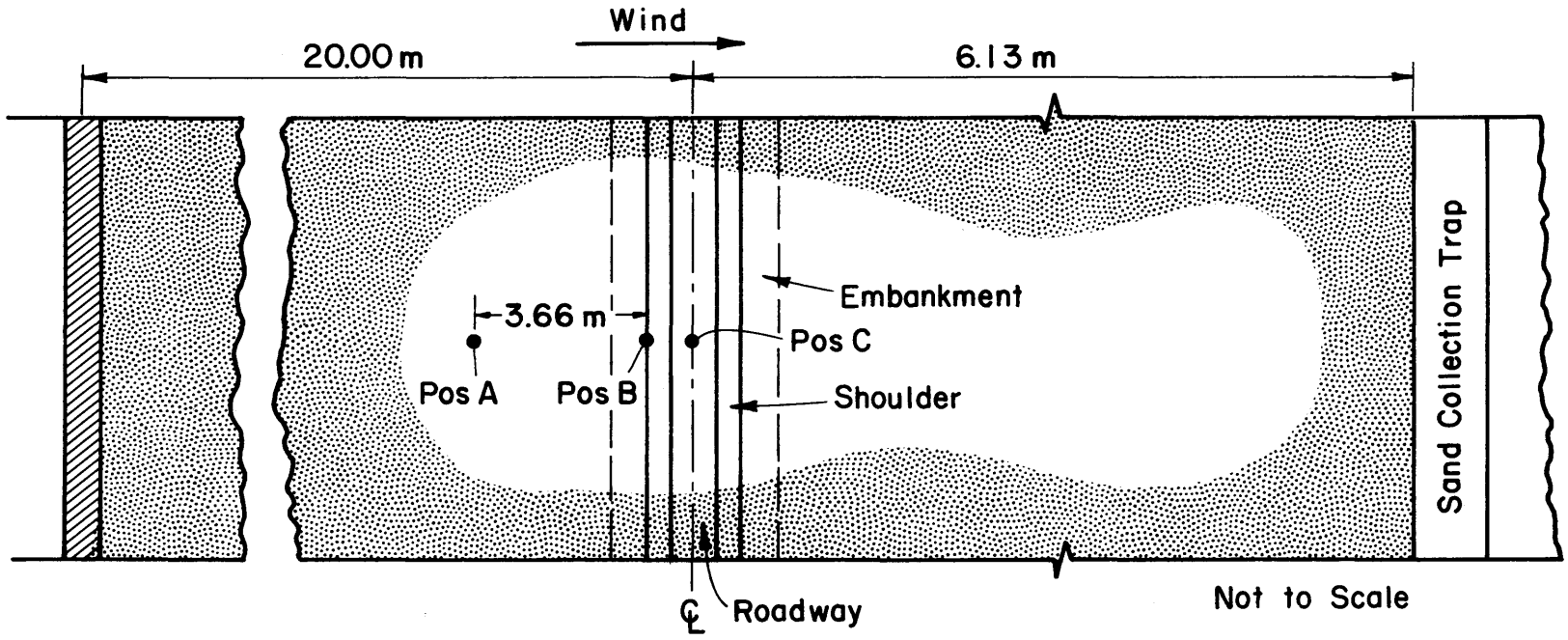

Figure 3-2. Plan view of roadway location within meteorological wind tunnel.

roadway was ascertained by measuring the sand depth along the tunnel centerline at predetermined time intervals. Measurements were continued until the shape of the deposition became stabilized.

The second step in the tests involved the taking of measurements for wind velocity profiles. Data was collected at three different locations (see Figure 3-2):

- Position A, 3.66 m upstream from the roadway shoulder,
- Position B, upstream shoulder-embankment joint,
- Position C, center of roadway median.

The resultant velocity data was also used to determine proper settings for the aspirating probe utilized to measure sand transport at the same location.

3.4 Test Results

The accumulation of sand upwind from the roadway ($x = 0$ at Position B) was calculated over a distance of 5.76 m back upstream. Table 3-1 contains a summary of the calculations, which are graphically portrayed in Figures 3-3 and 3-4. As can be seen on those plots, total depositions continued to increase throughout the tests. The rate of growth of the accumulation remains reasonably constant with time for the 7 m/s wind velocity. At the higher wind speed the rate of growth remained nearly constant for the first 200 minutes and then decreased significantly, as if an equilibrium condition was developing. Profiles of the deposition upwind from the roadway, derived from the measurements taken along the centerline of the wind tunnel, are contained on Figures 3-5 and 3-6. The slope of the upwind deposition next to the embankment appears to be approximately 7°, as measured from the horizontal, for the 7 m/s wind speed and 3° for the 14 m/s velocity. (From the 1982 study, the angle of approach was close to 6° for a speed of 12 m/s).

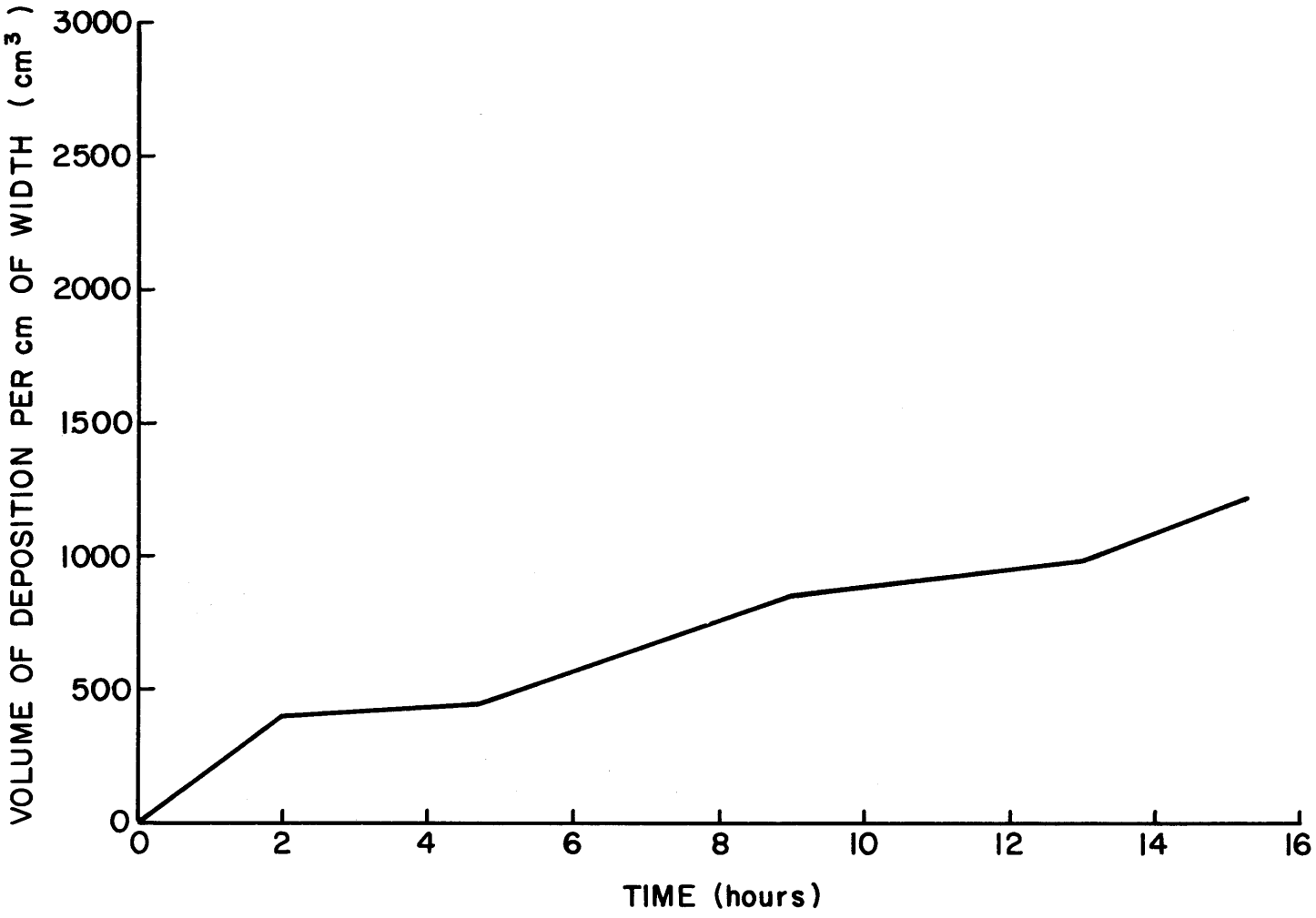

Figure 3-3. Sand deposition rate on upwind side of roadway with free-stream velocity of 7 m/s.

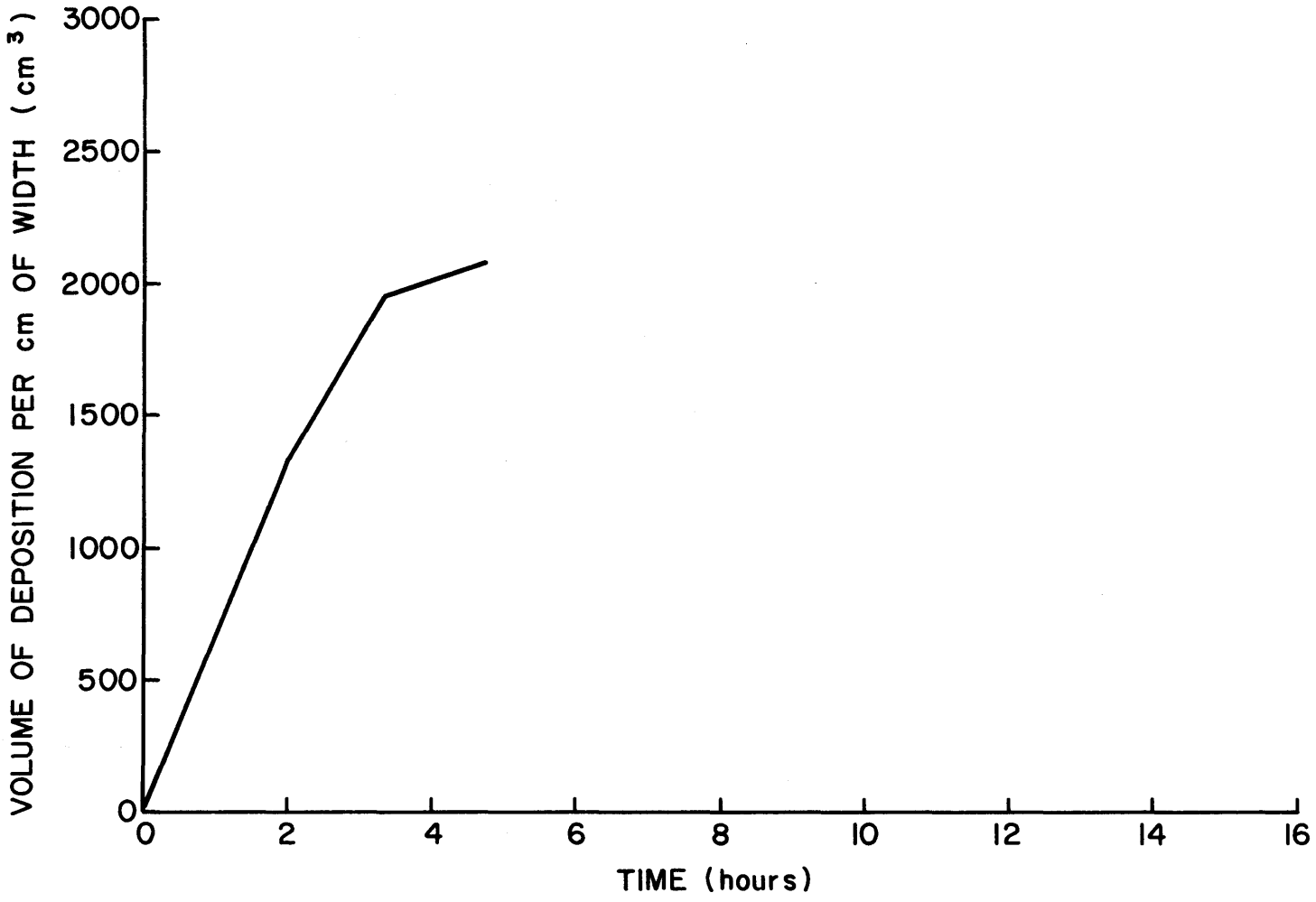

Figure 3-4. Sand deposition rate on upwind side of roadway with free-stream velocity of 14 m/s.

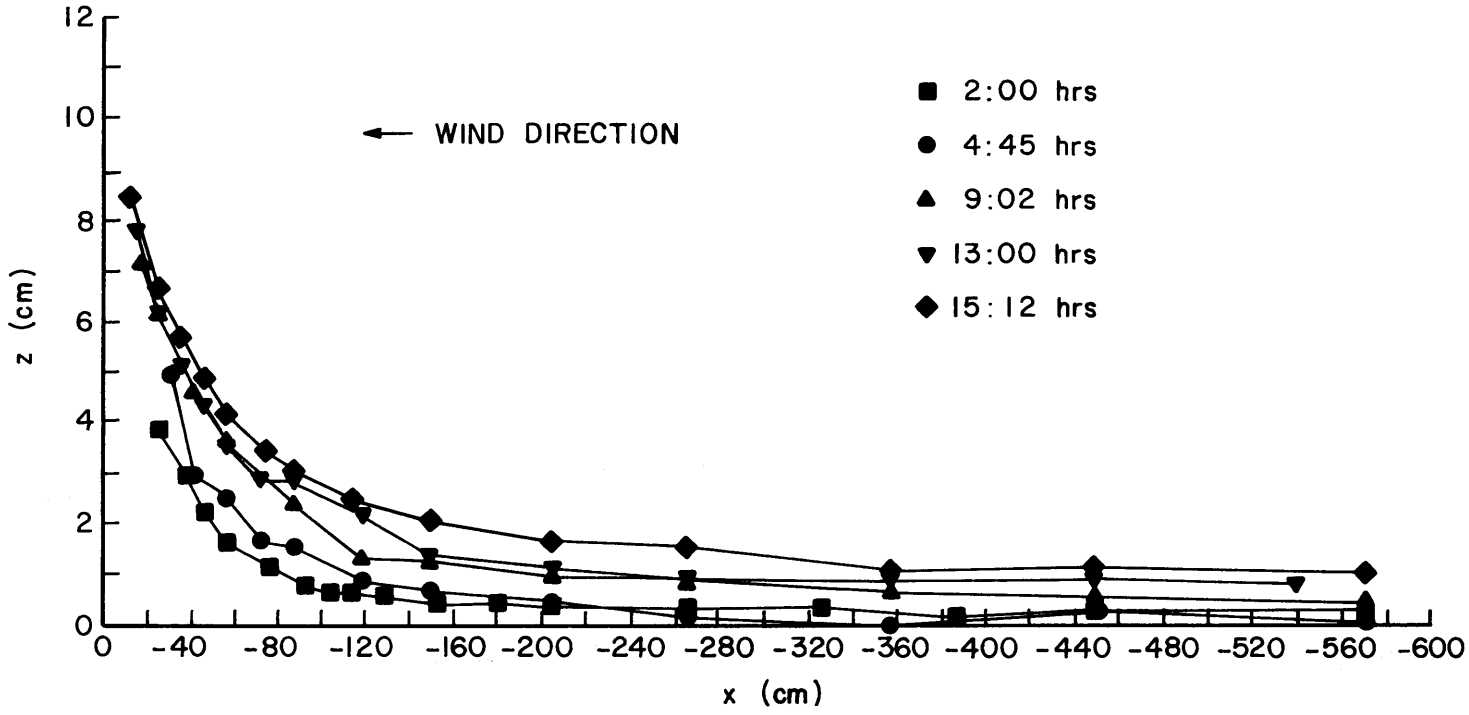

Figure 3-5. Sand accumulation profiles for upwind roadway embankment (configuration #3) with a 7 m/s free-stream velocity.

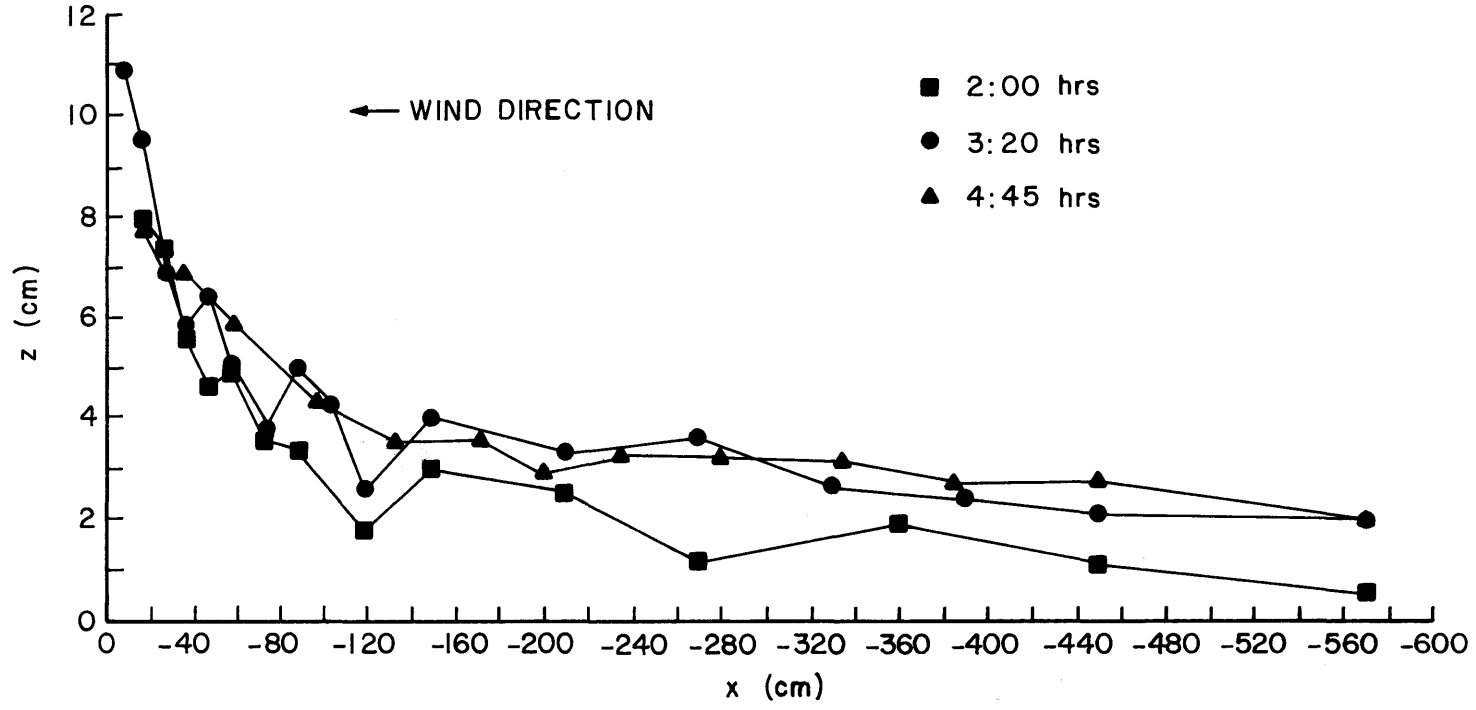

Figure 3-6. Sand accumulation profiles for upwind roadway embankment (configuration #3) with a 14 m/s free-stream velocity.

Table 3-1. Sand accumulation (cm^3) per centimeter of width, calculated for a distance of 5.76 m upwind from the road shoulder.

Time (hrs)	u_∞ (m/s)	
	7	14
2+00	400	1336
3+20	-	1952
4+45	454	2083
9+02	858	-
13+00	991	-
15+12	1228	-

Sand deposition upwind from Roadway Configuration No. 3, after four hours and 45 minutes at 14 m/s wind speed, is reflected in the photo reproduced as Figure 3-7. Sand migration across the roadway is particularly heavy at the higher wind velocity, as shown in the Figure 3-8 photo print, for the same test conditions.

Wind velocity distributions (mean velocity profiles) and turbulence intensity profiles were measured at the three locations indicated in Figure 3-2 after the sand-bed had stabilized, but prior to final sand accumulation. The profiles obtained from the surface to 110-130 cm are contained in Figures 3-9a,b,c and 3-10a,b,c for free-stream velocities of 7 m/s and 14 m/s, respectively. Expanded profiles of the lowest 20 cm are contained in Figures 3-11a,b,c and 3-12a,b,c.

The effect of the roadway embankment on the acceleration of the flow is quite evident and most noticeable in the lower two centimeters of the profiles (see Figures 3-11 and 3-12). Velocity increased from 3.5 m/s at Pos. A to 6 m/s at Pos. B, before reducing to 5 m/s at Pos. C, with a 7 m/s free-stream velocity. Similarly the wind speed

increased from 6 m/s in the flat sand-bed to 10 m/s at the top of the embankment, before moving back to 8 m/s at the median, with a 14 m/s reference velocity. That the effect is local (only occurs in close proximity to the roadway), may be confirmed in the profiles of Figures 3-9 and 3-10, where the free-stream velocity is seen to remain constant for each of the three locations at a height of 110-130 cm above the surface.

The turbulence intensity profiles reveal information similar to the mean velocity profiles. Turbulence intensity near the surface (2 cm) which was approximately 13 percent at Pos. A, decreased to about 9 percent at Pos. B before increasing to 10.5 percent at Pos. C for the 7 m/s test case. Comparable turbulence intensity with a 14 m/s reference wind speed moves from approximately 14 percent to 12 percent and back to 14 percent at 2 cm above the roadway. Turbulence above the ABL was measured at 4-5 percent for all three locations in both test series.

Figures 3-13 and 3-14 contain vertical sand distribution profiles measured with an aspirating probe at the three previously defined positions A, B and C (refer to Figure 3-2). Integrating the curves with respect to height, yields the transport rates in grams/minute/centimeter of width perpendicular to the wind direction. These calculated rates are tabulated in Table 3-2 for the 7 m/s and 14 m/s wind speeds.

The total transport rate of the undisturbed flow (position A) compares very well for both velocities with results obtained from the Shen trap during the 1982 studies. Comparisons are plotted on the graph of Figure 3-15. Lower transport rates for positions B and C, in the 7 m/s case, are attributed to the growth rate of the deposition upwind from the roadway. As noted on Figure 3-3, the growth rate remained

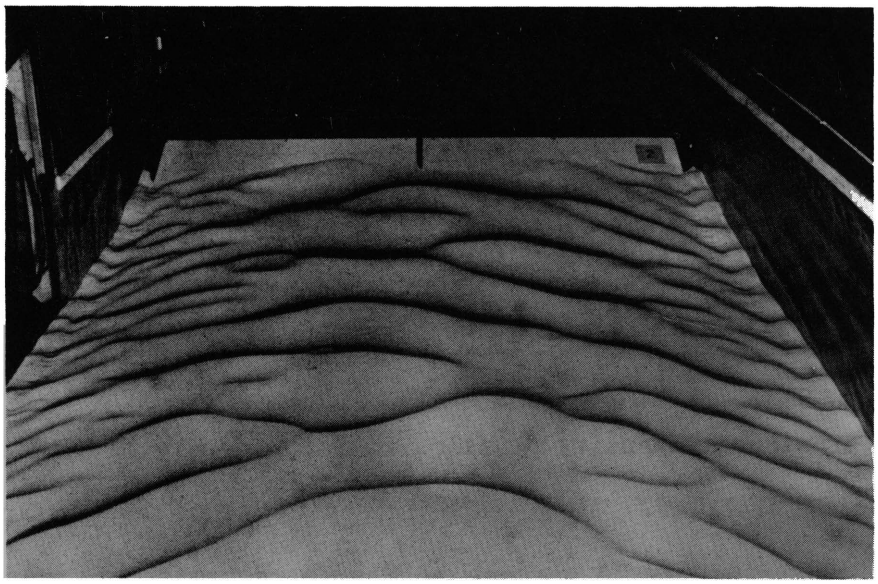

Figure 3-7. Sand deposition upwind from Roadway Configuration No. 3 (after 4:45 hours of running time with a 14 m/s wind speed).

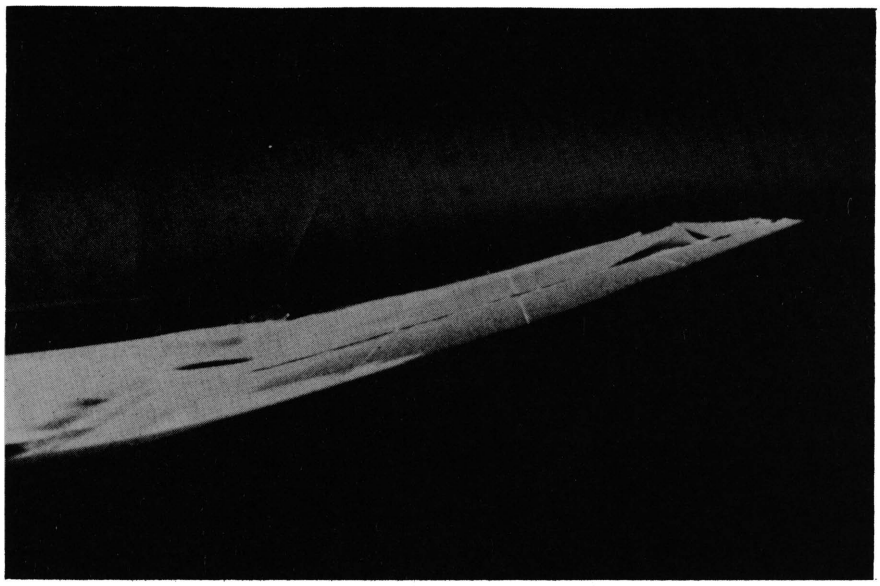

Figure 3-8. Side view showing the migration of sand over Roadway Configuration No. 3 (with a wind speed of 14 m/s).

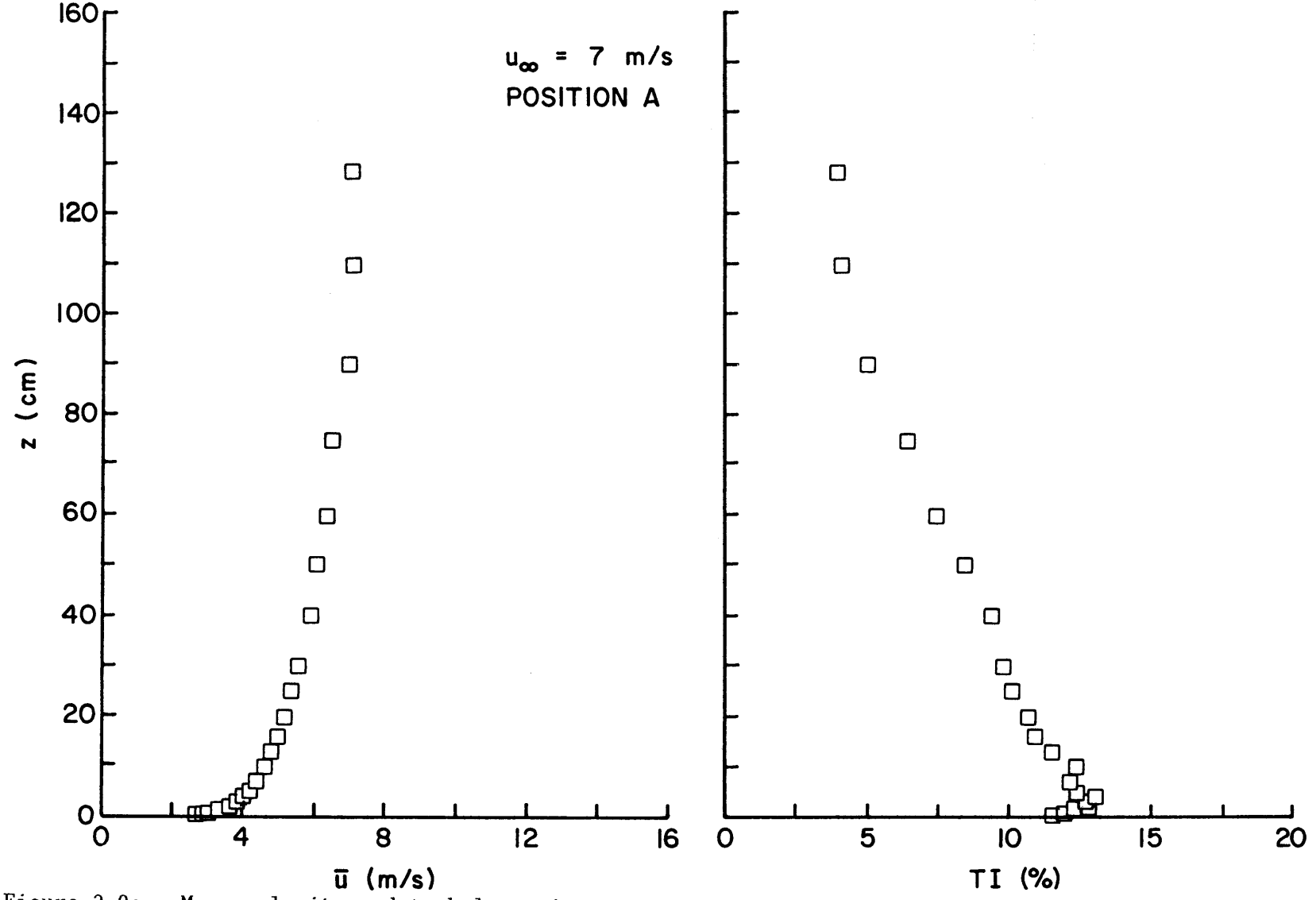

Figure 3-9a. Mean velocity and turbulence intensity profiles from sand-bed to a height of 130 cm at a position 3.66 m upwind of roadway (Pos. A) with a 7 m/s free-stream velocity.

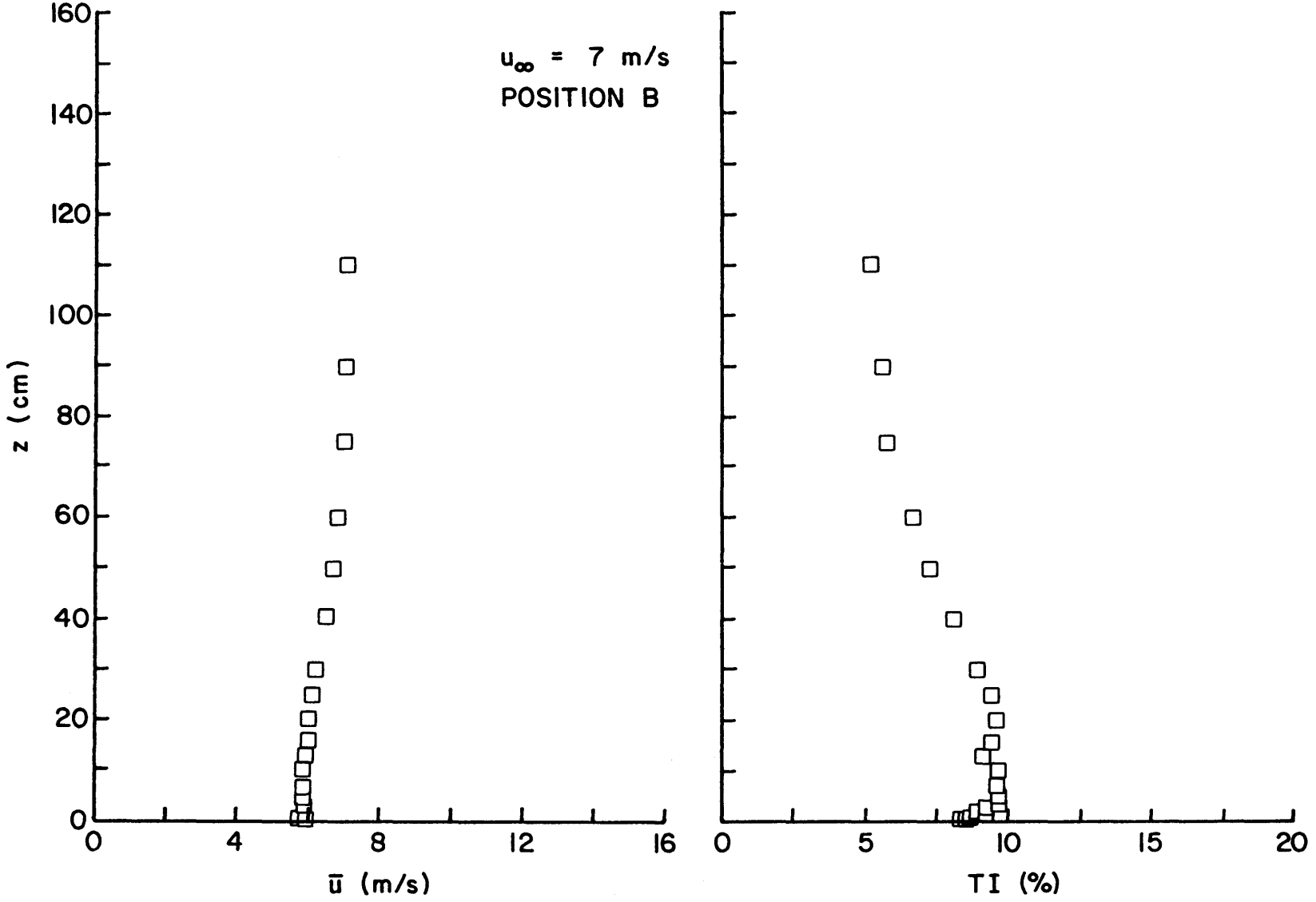

Figure 3-9b. Mean velocity and turbulence intensity profiles from surface to a height of 110 cm above roadway shoulder (Pos. B) with a 7 m/s free-stream velocity.

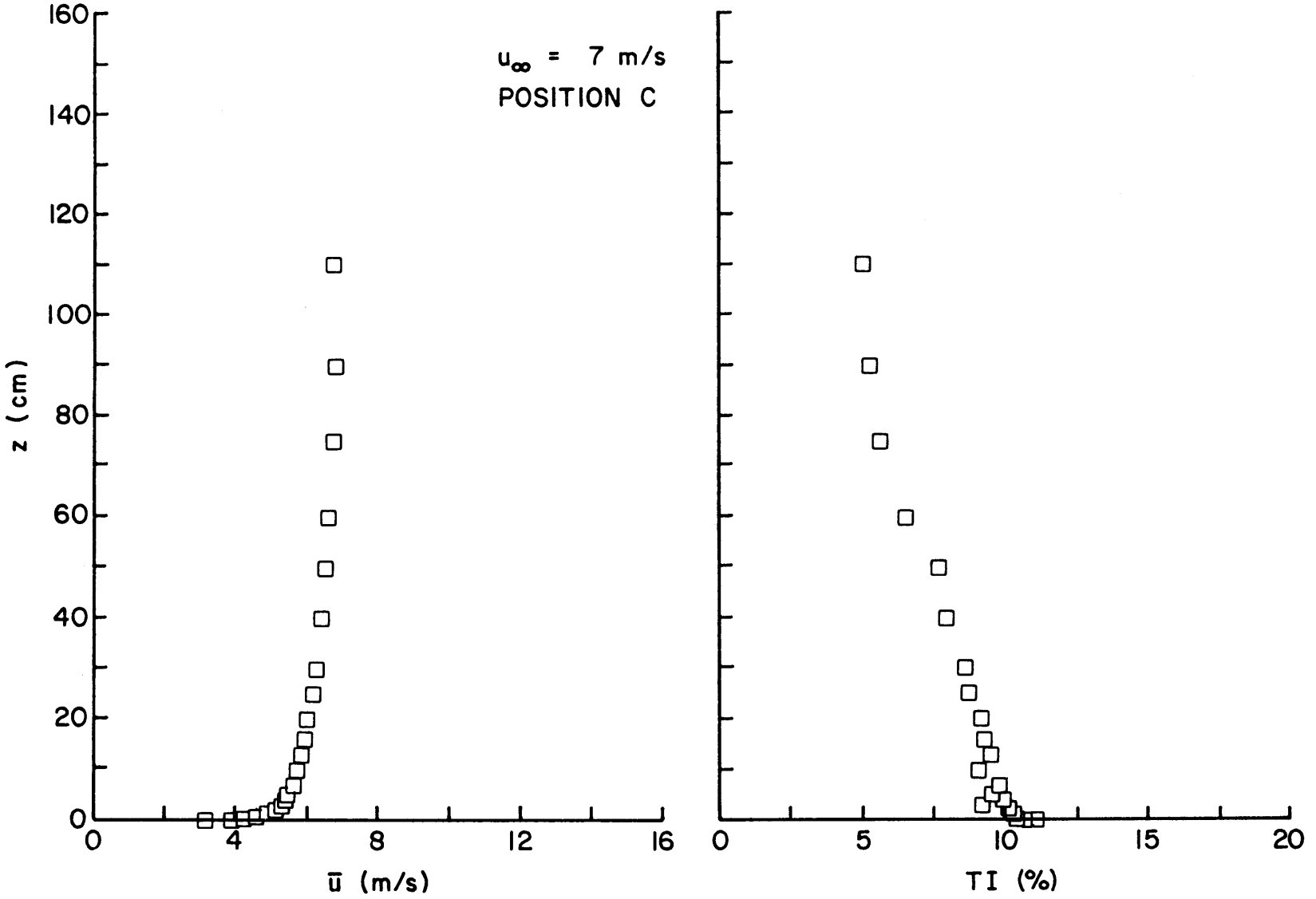

Figure 3-9c. Mean velocity and turbulence intensity profiles from surface to a height of 110 cm above roadway median (Pos. C) with a 7 m/s free-stream velocity.

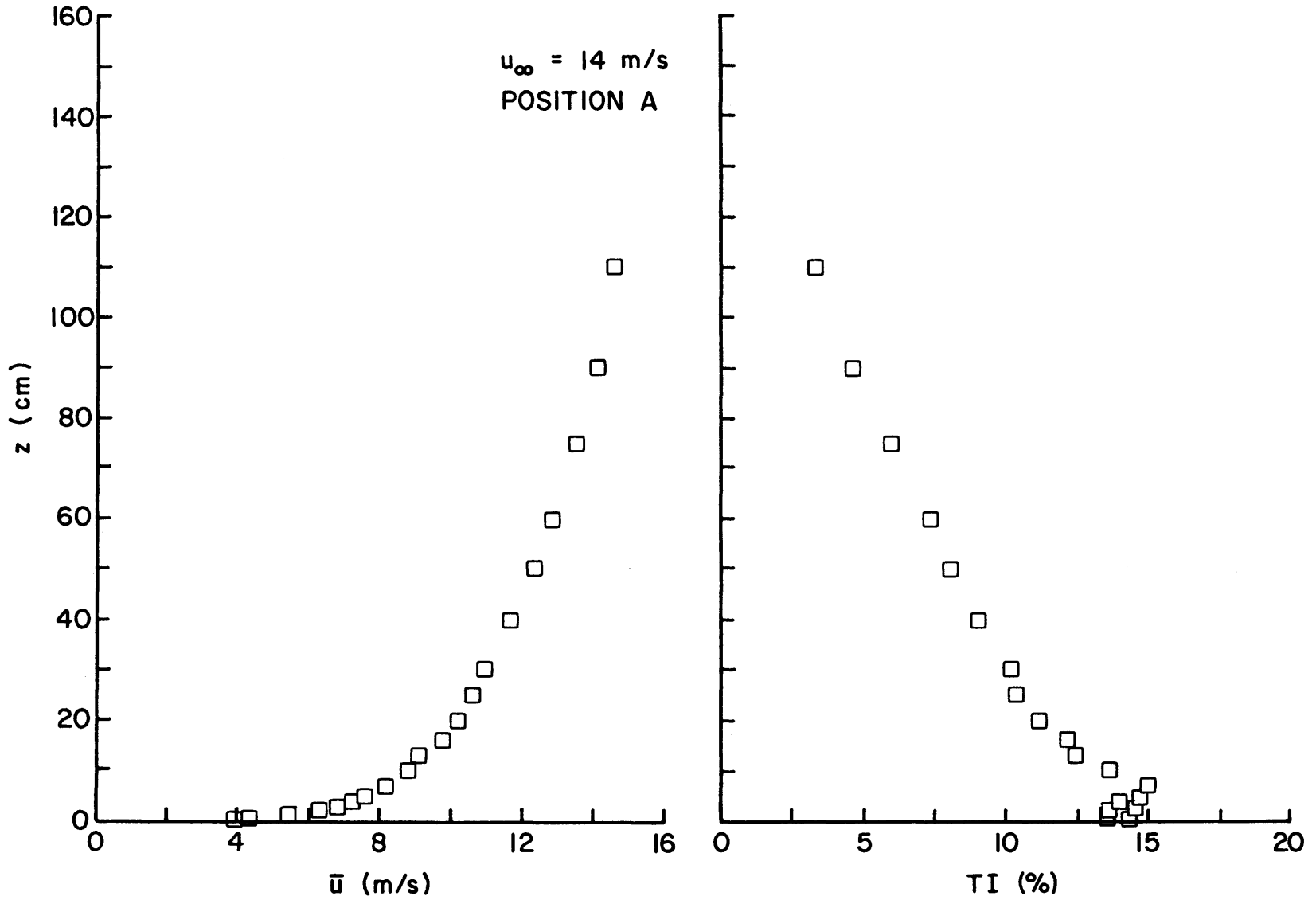

Figure 3-10a. Mean velocity and turbulence intensity profiles from sand-bed to a height of 110 cm at a position 3.66 cm upwind of roadway (Pos. A) with a 14 m/s free-stream velocity.

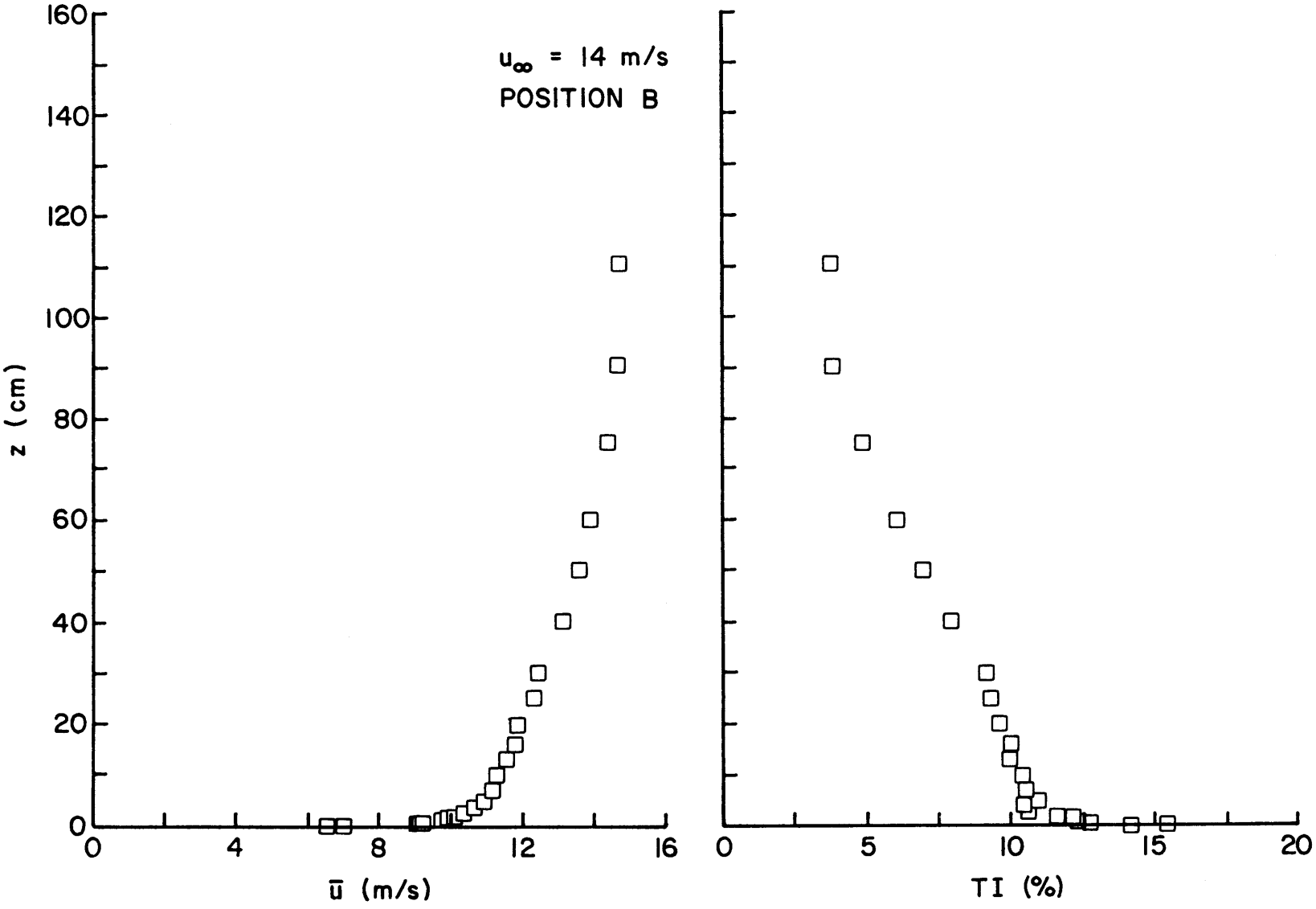

Figure 3-10b. Mean velocity and turbulence intensity profiles from surface to a height of 110 cm above roadway shoulder (Pos. B) with a 14 m/s free-stream velocity.

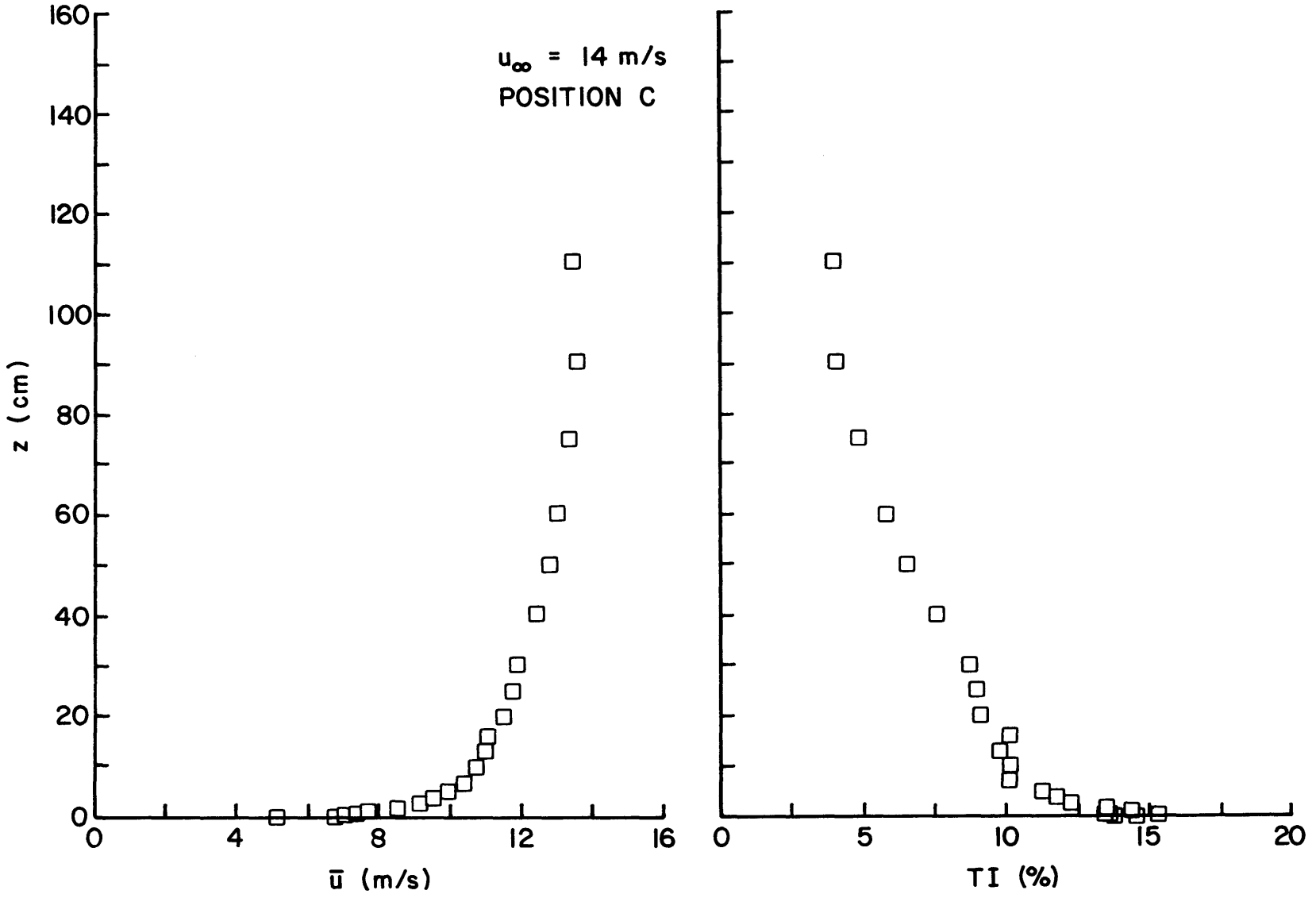

Figure 3-10c. Mean velocity and turbulence intensity profiles from surface to a height of 110 cm above roadway median (Pos. C) with a 14 m/s free-stream velocity.

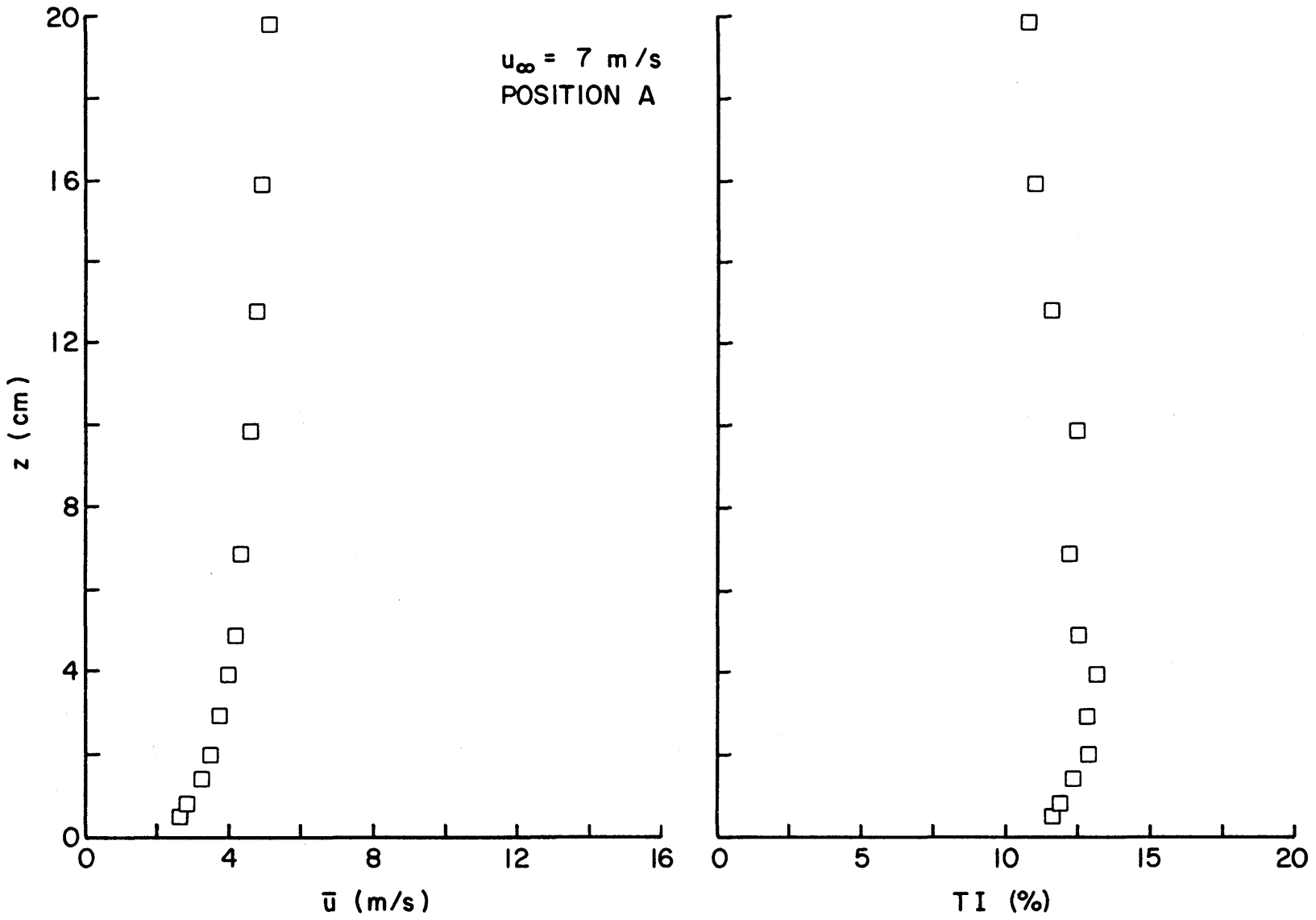

Figure 3-11a. Mean velocity and turbulence intensity profiles from sand-bed to a height of 20 cm at a position 3.66 m upwind of roadway (Pos. A) with a 7 m/s free-stream velocity.

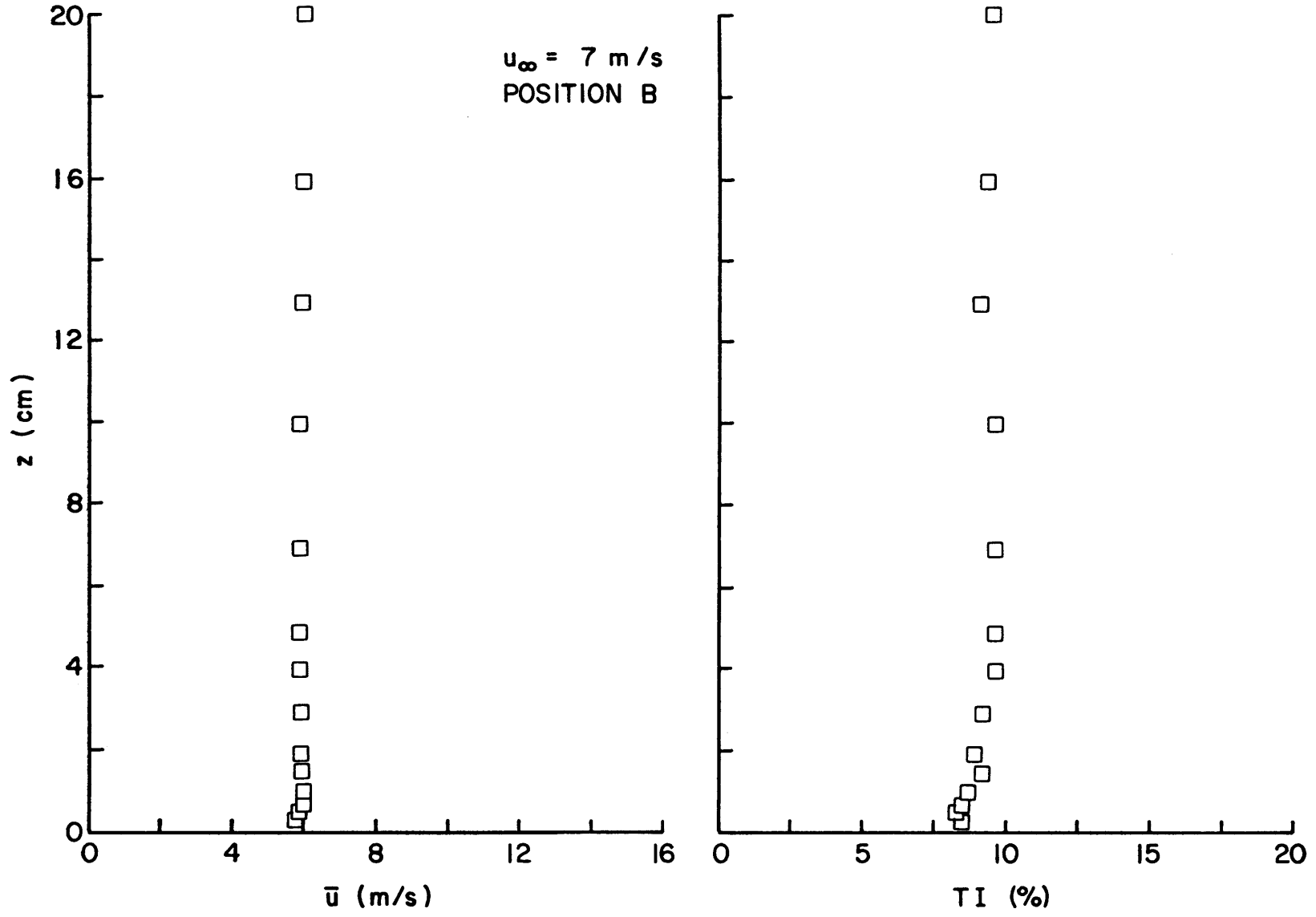

Figure 3-11b. Mean velocity and turbulence intensity profiles from surface to a height of 20 cm above roadway shoulder (Pos. B) with a 7 m/s free-stream velocity.

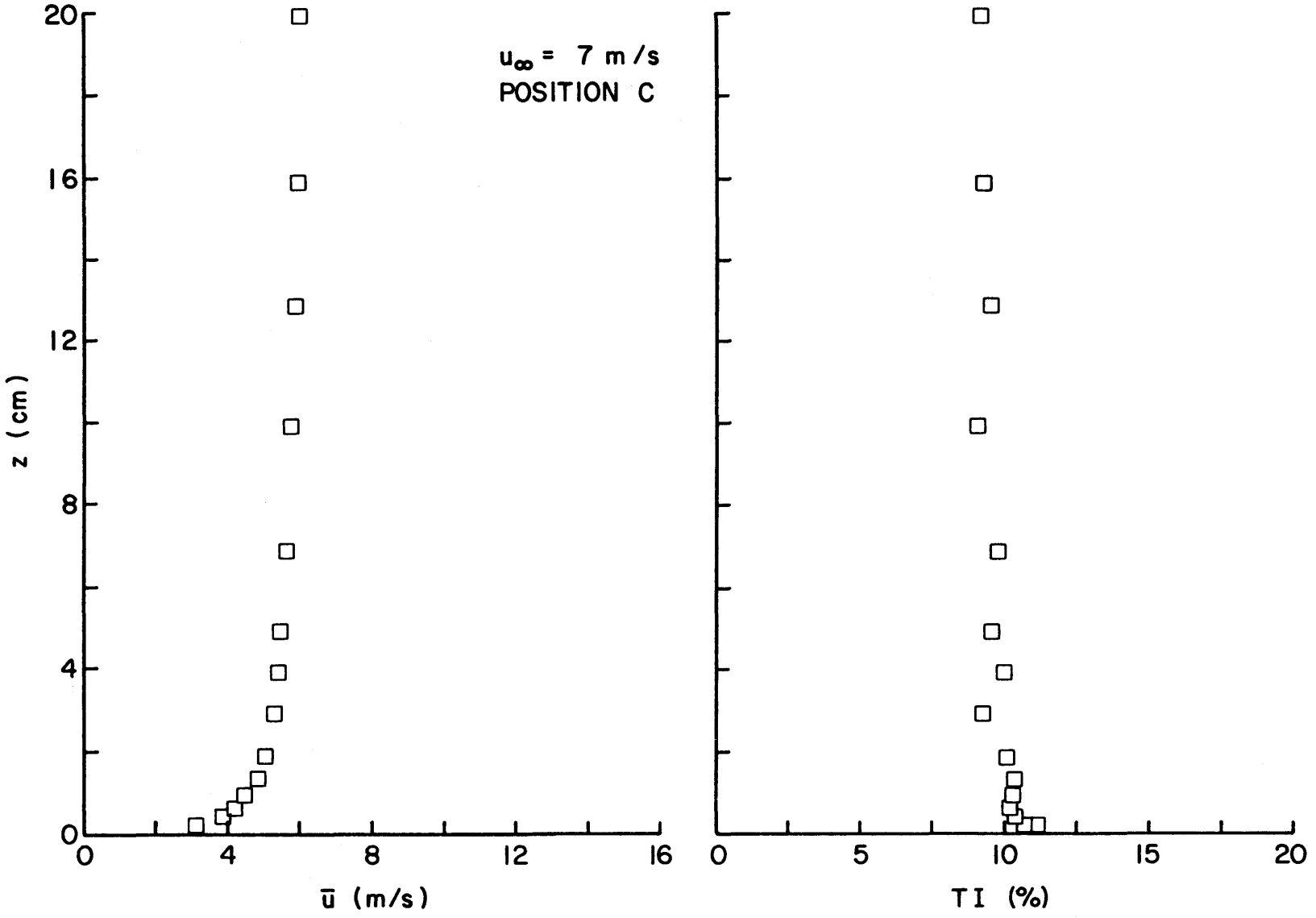

Figure 3-11c. Mean velocity and turbulence intensity profiles from surface to a height of 20 cm above roadway median (Pos. C) with a 7 m/s free-stream velocity.

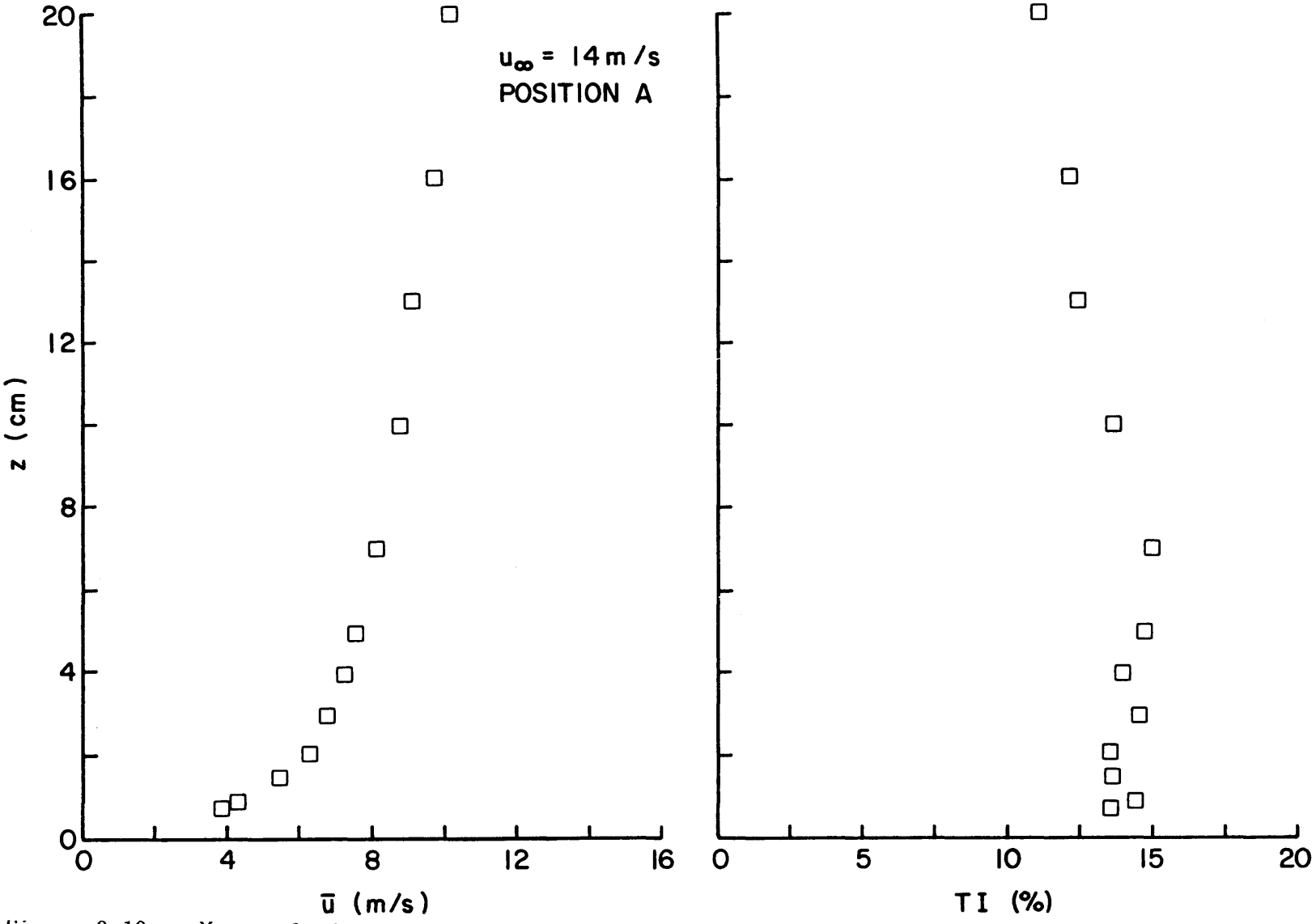

Figure 3-12a. Mean velocity and turbulence intensity profiles from sand-bed to a height of 20 cm at a position 3.66 m upwind of roadway (Pos. A) with a 14 m/s free-stream velocity.

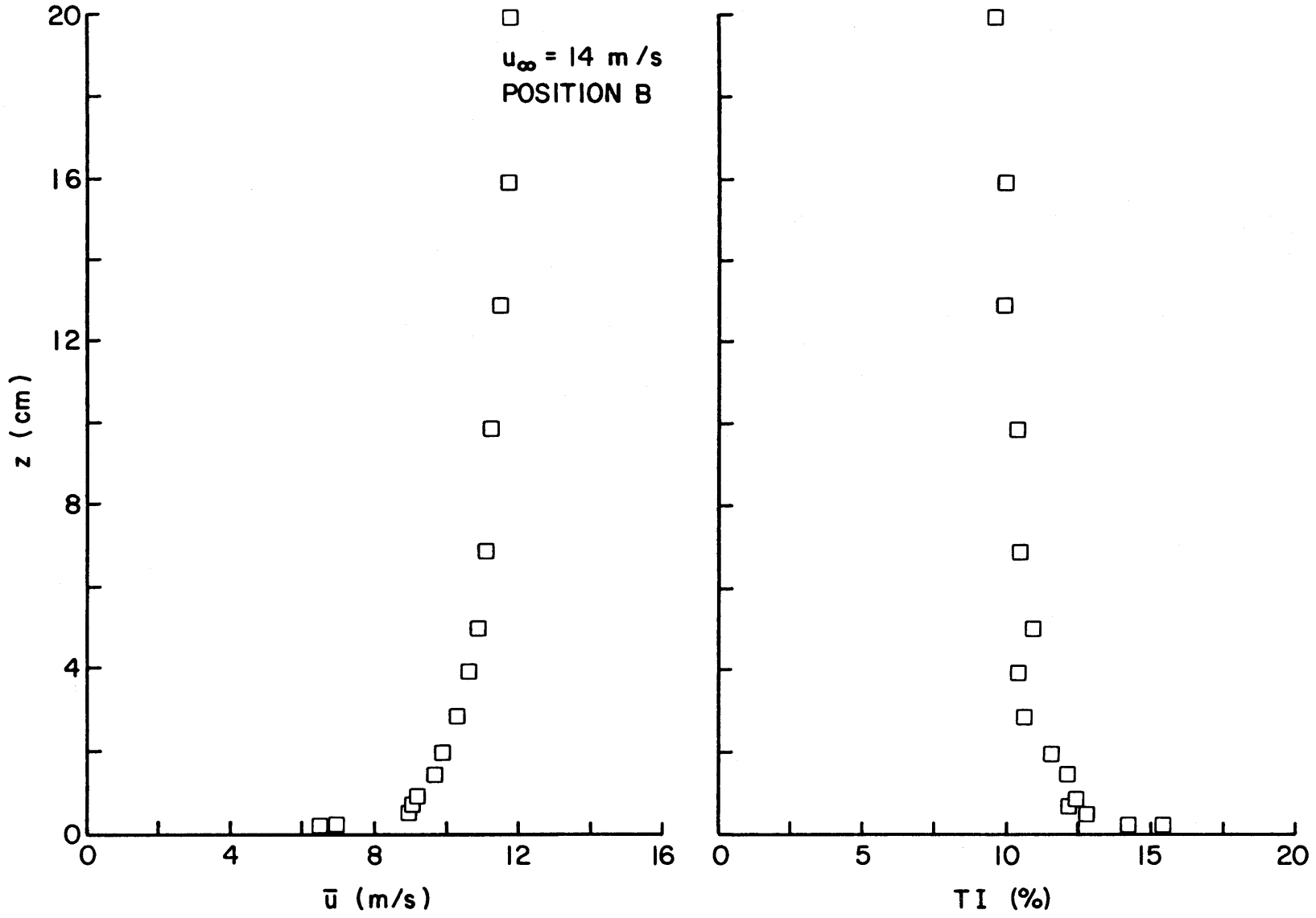

Figure 3-12b. Mean velocity and turbulence intensity profiles from surface to a height of 20 cm above roadway shoulder (Pos. B) with a 14 m/s free-stream velocity.

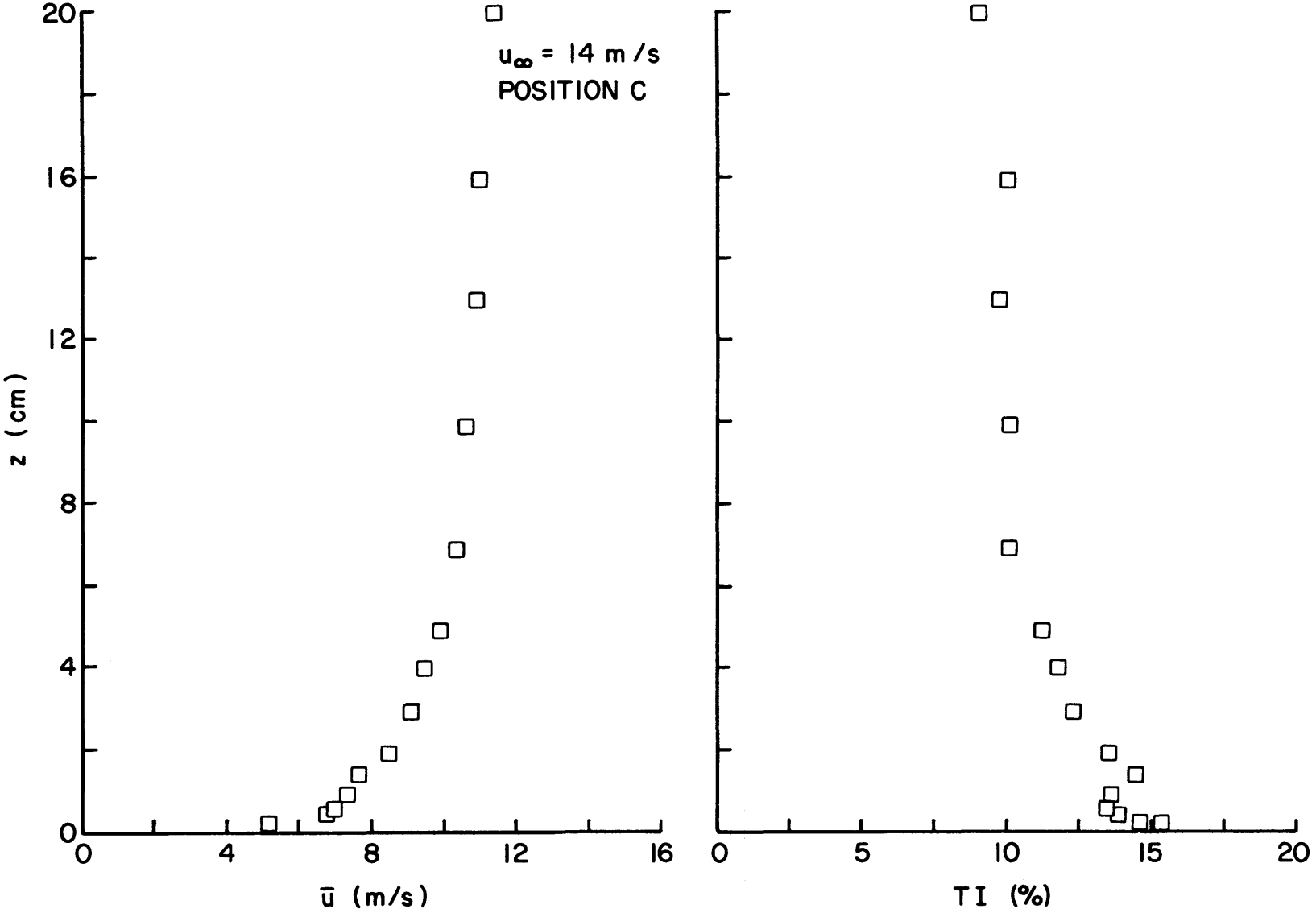

Figure 3-12c. Mean velocity and turbulence intensity profiles from surface to a height of 20 cm above roadway median (Pos. C) with a 14 m/s free-stream velocity.

Table 3-2. Total sand transport rate in grams/ minute per centimeter of width at Positions A, B, and C.

Position		Transport Rate, q (gm/min/cm)		
		A	B	C
u_∞ (m/s)	7	2.03	1.05	1.0
	14	30	31.3	32.2

fairly constant with time, indicating that a steady deposition of sand particles was occurring in the area between positions A & B. Conversely, Figure 3-4 reveals a significant decrease in the growth rate after 200 minutes of running time for the 14 m/s tests. With the area upwind from the roadway in near equilibrium the sand transport rate at all three locations should be approximately equal.

3.5 Conclusions

From this new series of tests, as from the previous tests, it can be concluded that under constant wind-speed, sand particles will be continuously deposited upstream from the roadway until sand deposition reaches the top of the roadway.

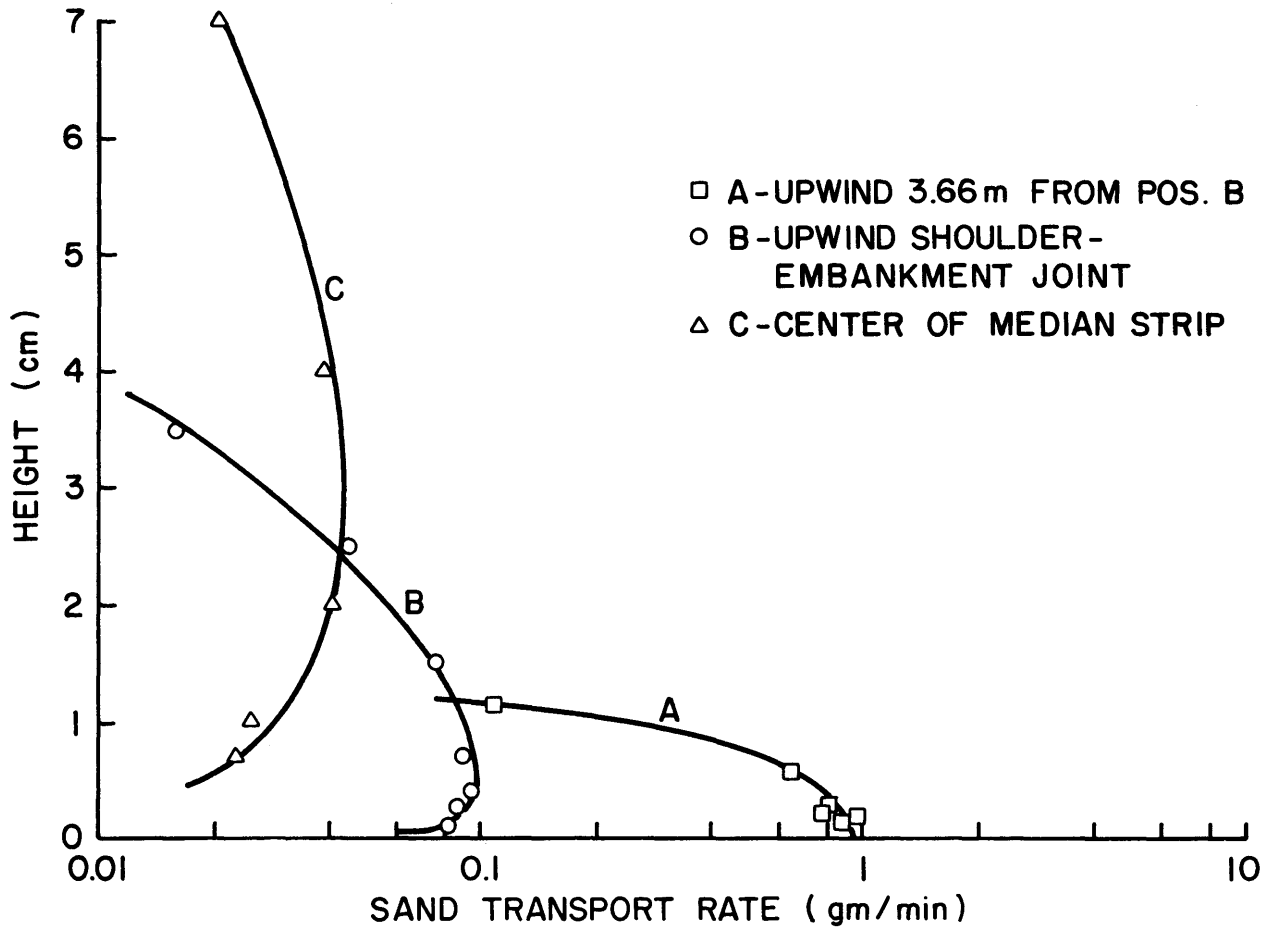

Figure 3-13. Sand transport profiles over roadway with a 7 m/s free-stream wind velocity (aspirating probe measurements).

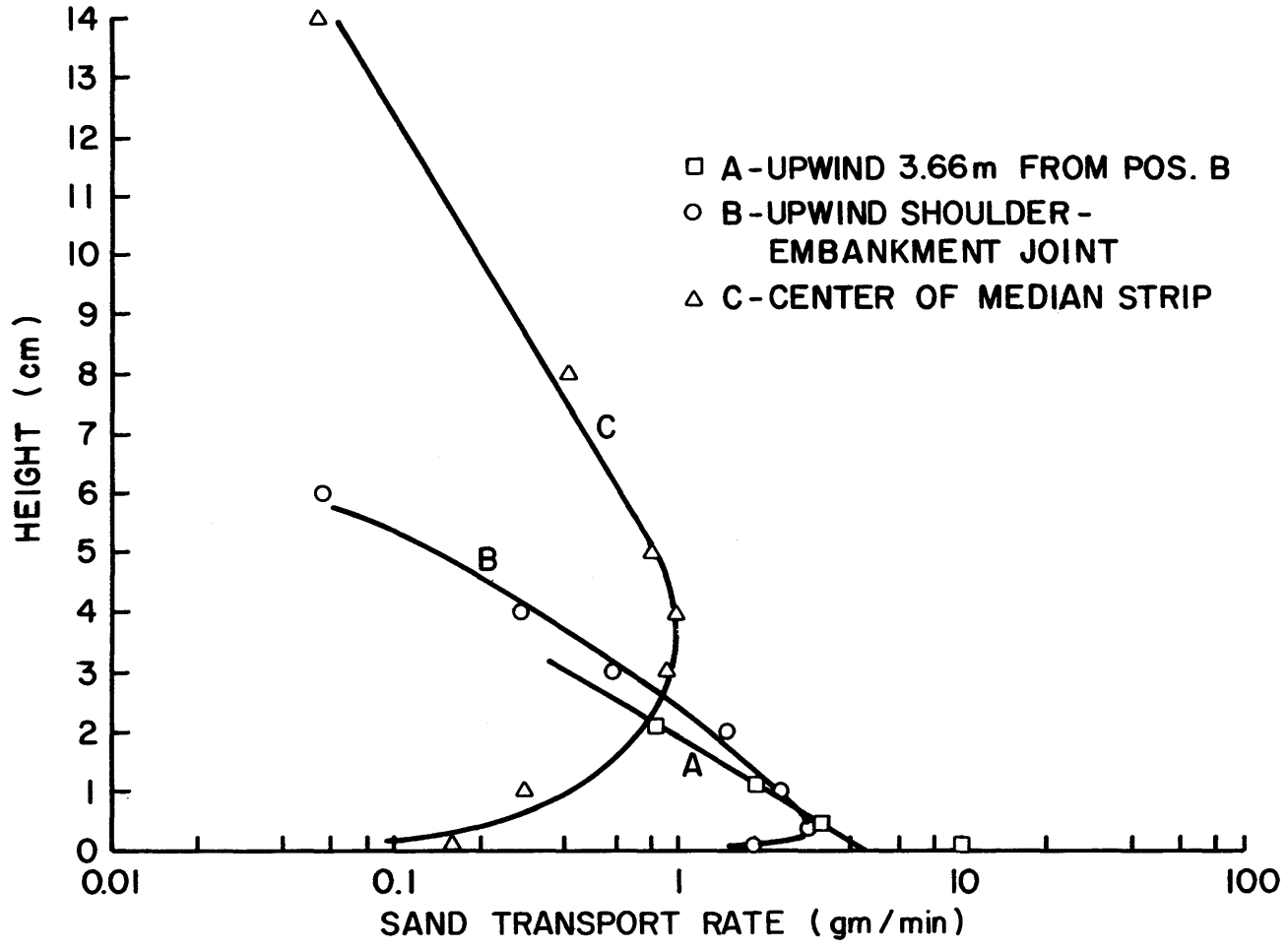

Figure 3-14. Sand transport profiles over roadway with a 14 m/s free-stream wind velocity (aspirating probe measurements).

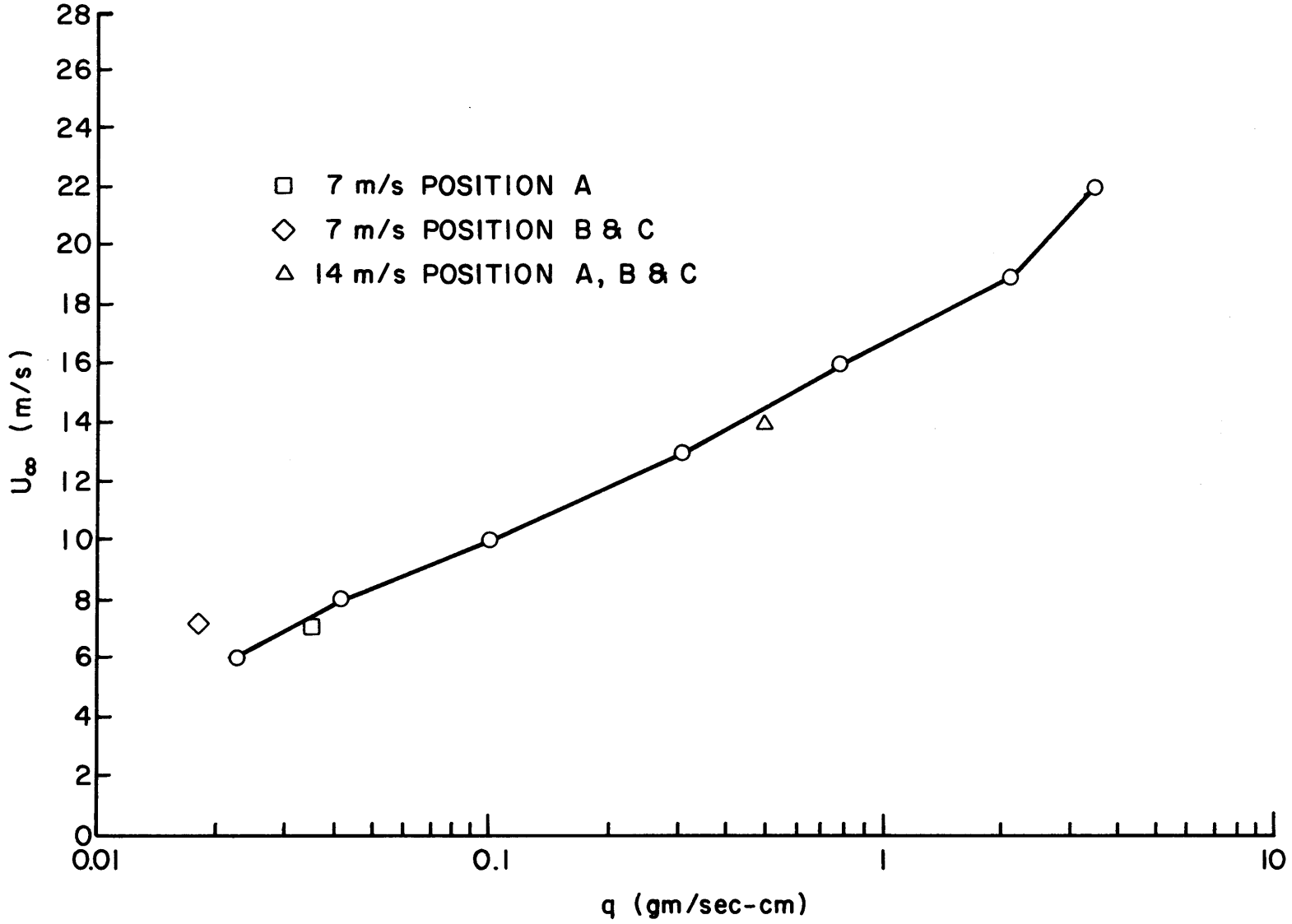

Figure 3-15. Sand transport rate over roadway compared with amount of sand trapped by Shen vertical sand trap.

It may also be concluded that for lower wind speeds (just sufficient to cause saltation) the accumulation upwind of the embankment will be substantial. At significantly higher wind speeds sufficient energy exists to elevate and transport a preponderance of the particles across the roadway.

4.0 FENCE TESTS

4.1 Purpose

The fence tests described in the 1983 telex messages constitute an extension of the 1982 sand control studies conducted on the one-eighth inch vertical slat fences of 60 percent porosity. Sand accumulation/diversion properties were to be documented at previously untested wind velocities for:

- A two-dimensional single fence placed in the tunnel at a 45° angle to the 9 m/s wind.
- A double row of fences, spaced 40 H apart, at a wind speed of 12 m/s.

Two similar tests were conducted, although not required, for comparison with data from the aforementioned tests and to obtain additional experimental information regarding sand movement/tunnel characteristics. These tests included:

- A short fence placed in the tunnel at a 45° angle to the 9 m/s wind, which covered less than half the tunnel width.
- A double row of fences, 40 H apart, installed above a modified sand-bed, and a 12 m/s test speed.

4.2 Test Configurations

The tunnel was configured in similar manner for each of the four series of fence tests, with the exception of the fence placements. The fences for each test varied only in length and were otherwise identical. The 60 percent porosity fences, constructed from 1/8" vertical strips, were 7.75 cm tall and included 5 cm high solid sub-sand barriers (a schematic of the modelled fence is included as Figure 4-1).

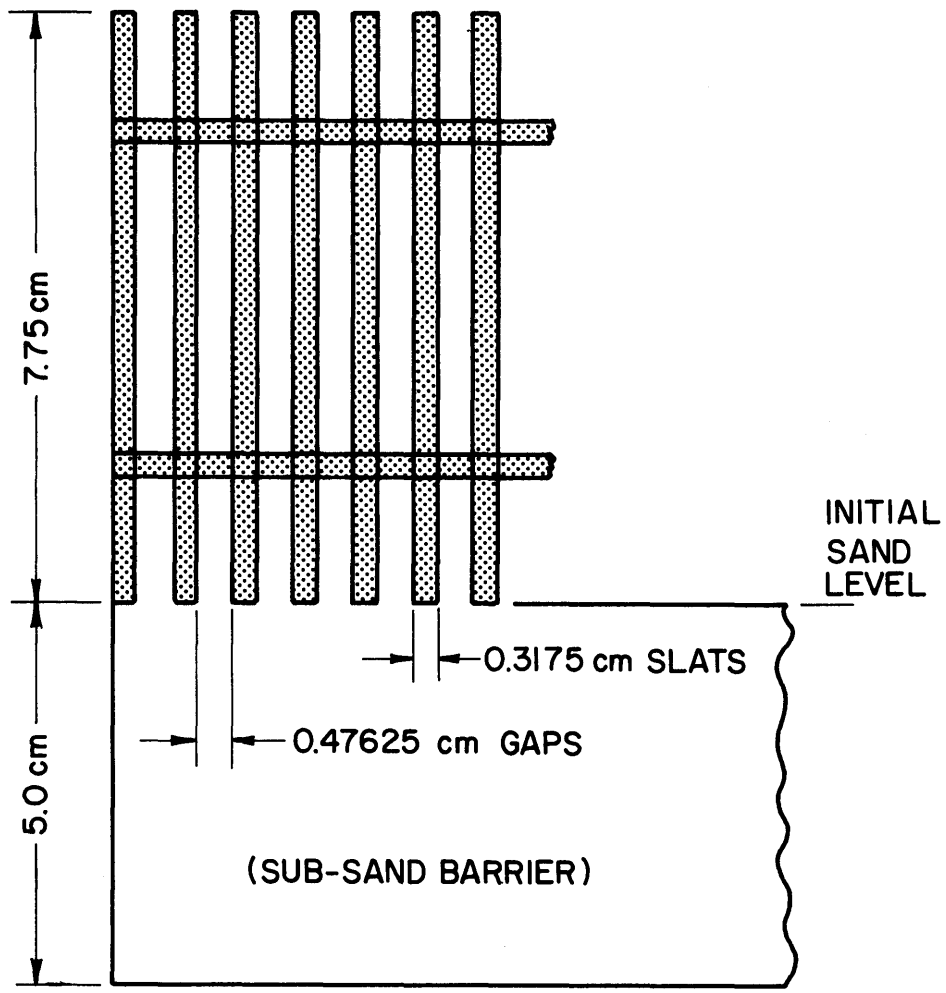

Figure 4.1. One-eighth (0.3175 cm) inch vertical slat fence with 60 percent porosity.

The sand-bed on the tunnel floor was smoothed to a depth of 5 cm (for a distance over 27 m upstream from the tunnel's sand collectors) prior to the start of each test, except for the double fences which were tested over a modified sand-bed. On this occasion the downstream and upstream fences were shimmed 2.8 cm and 4.25 cm, respectively.

In addition to the reduction in sand-bed depth from 7 cm to 5 cm, a heavy shag carpet was placed on the tunnel floor (under the sand-bed) from the spires to a point approximately 19 m upstream (see Figure 1-2).

The carpet, by trapping sand among its fibers, controlled sand scour and minimized changes in the velocity profiles.

The long single fence, tested first, was situated in the tunnel as shown in Figure 4-2. Ends of the fence touched opposite walls of the tunnel to ensure a two-dimensional effect was achieved.

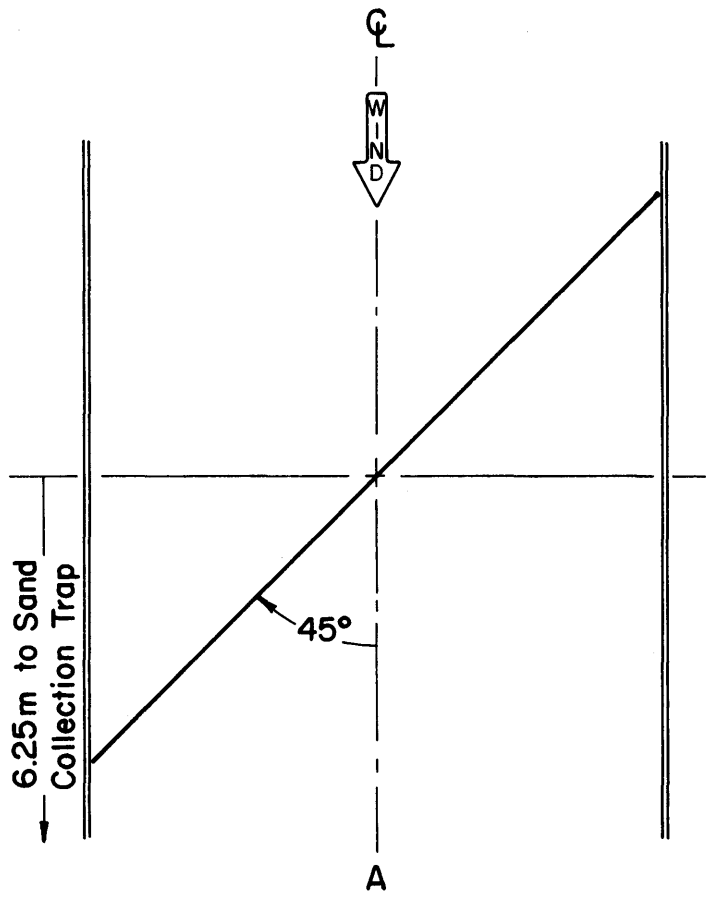

Figure 4-2. Plan view of long single fence installed across tunnel at 45° angle to wind.

The shorter fence, next tested, blocked only about one-third of the tunnel's width and provided ample room for flow around both ends of the obstacle. This fence's tunnel location is graphically detailed in Figure 4-3.

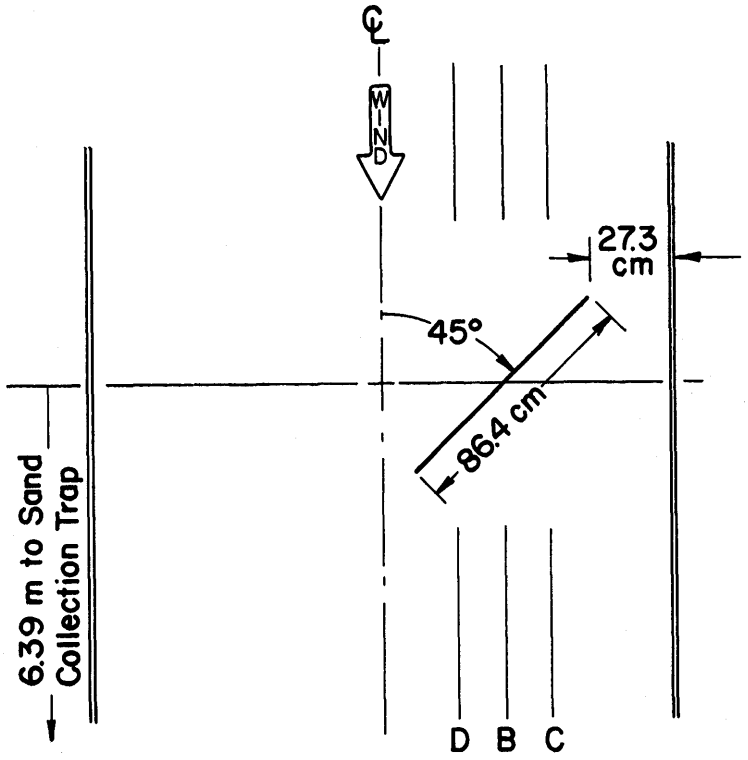

Figure 4-3. Plan view of short single fence installed within tunnel at 45° angle to wind

The double row of fences, positioned at 90° to the prevailing wind, were located 6.1 m and 9.2 m upstream from the tunnel's sand collection system, in both instances. Fences spanned the entire breadth of the tunnel to obtain the desired two-dimensional test configuration. These two series of tests were essentially performed consecutively. The tunnel was rescreeded after the first series of tests and operated for 30 hours to obtain a modified, rather than smooth, surface before installing the double fences for the second series of tests.

4.3 Test Procedures

The tunnel was operated at 9 m/s free-stream velocity for each of the single diverting fence experiments, with stops at two hour intervals to determine sand depths. Measurements were made along line A

(Fig. 4-2) for the longer fence and along line B (Fig. 4-3) for the short fence. After 18 hours of run on the long fence, six cross sections (4.57, 5.18, 5.79, 6.40, 7.01 and 7.62 m upstream) were taken of the deposition across the tunnel in the area of the fence. For the short fence, measurements parallel to the centerline were also taken (lines (C & D on Fig. 4-3) after 10 hours of tunnel operation.

A free-stream velocity of 12 m/s was established in the tunnel for each series of double fence row tests and every two hours measurements were taken of sand depth along the centerline of the tunnel. Measurements extended from 4.27 m (4.57 m) downwind to 2.99 m (12.09 m) upwind from the pair of fences for the first (second) series of tests. In addition, cross sections of sand deposition were measured every two hours at 4.57, 7.62, 12.19 and 16.76 m upstream for the second series of tests above the modified sand-bed.

4.4 Test Results

Sand accumulation rates per centimeter of width, for 4.42 m downwind and 5.94 m upwind from the center of the long diverting fence are tabulated in Table 4-1. The progressive downwind and upwind depositions about the fence are graphed on Figures 4-4 and 4-5, respectively. The longitudinal sand accumulation profiles of Figure 4-6a and cross-sectional profiles of Figure 4-6b provide graphic records of sand deposition near the fence. The longitudinal profiles indicate that sand accumulation around the long 45° fence became relatively stable after 16-18 hours of running time. The cross-sectional profiles, which were measured after 18 hours of testing, provide no indication that the two-dimensional angled fence effectively diverted any sand away from the tunnel alignment path. Figure 4-7 pictorially reveals sand deposition

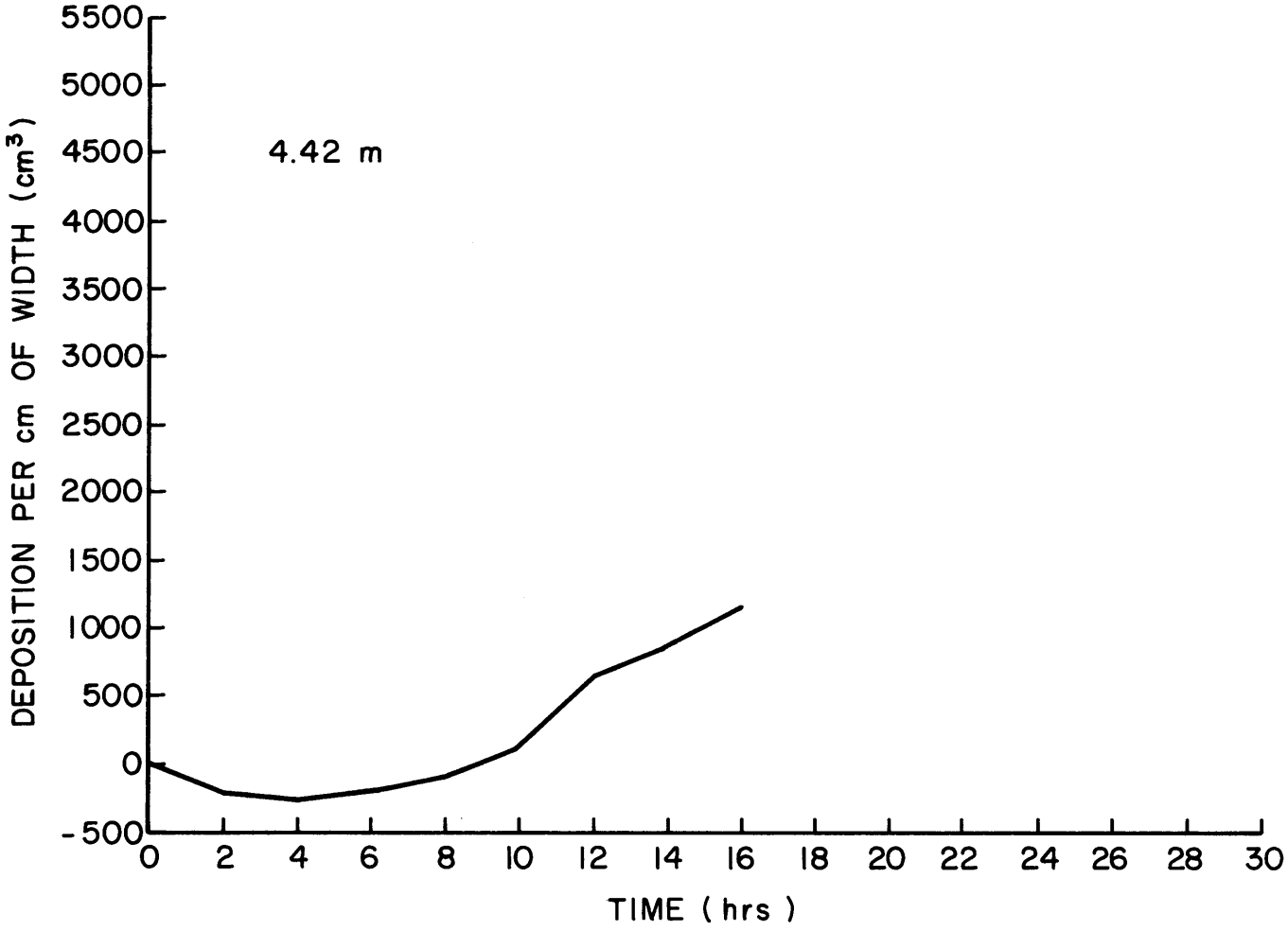

Figure 4-4. Sand accumulation on downwind side of long 45° fence.

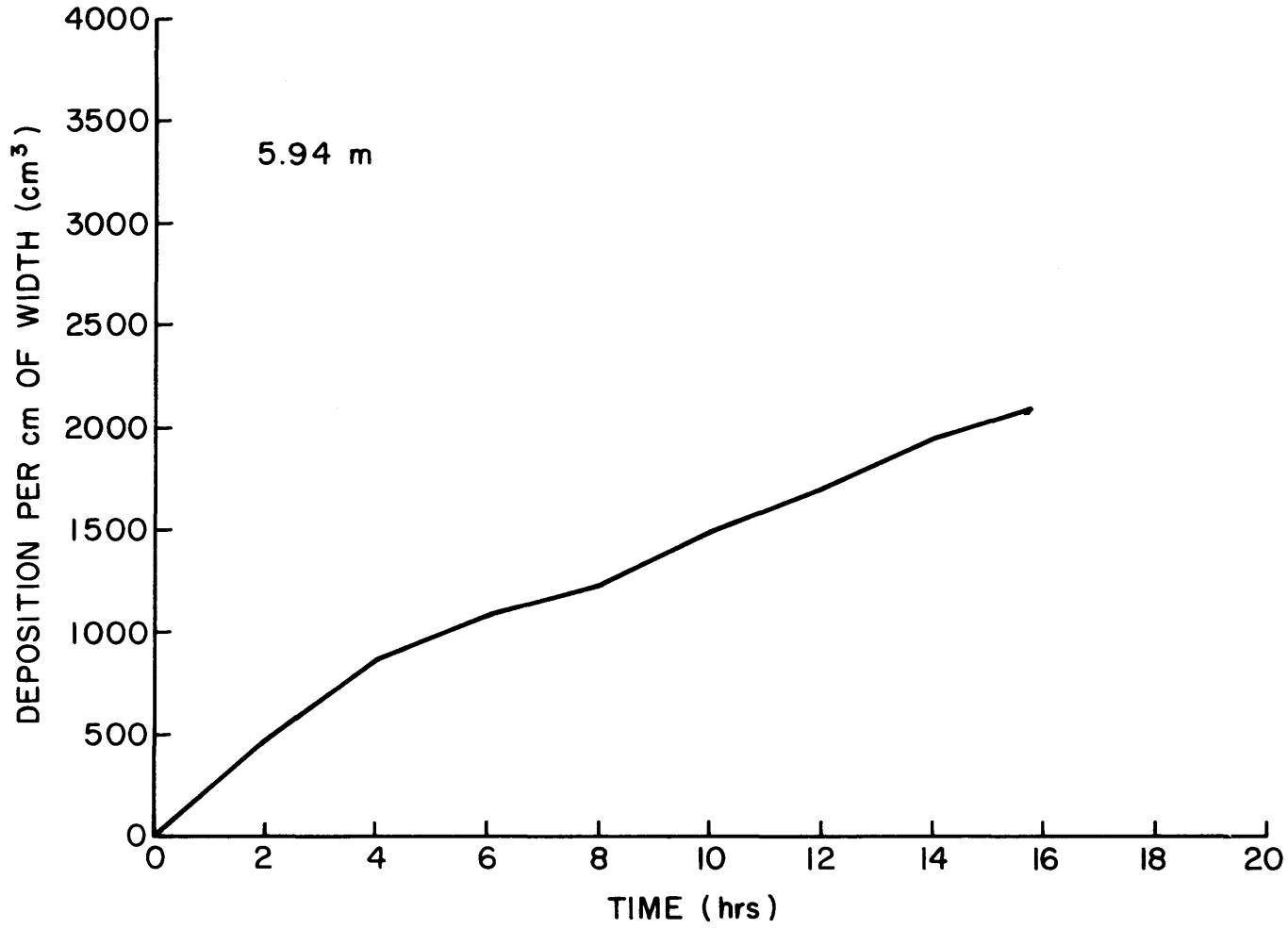

Figure 4-5. Sand accumulation on upwind side of long 45° fence.

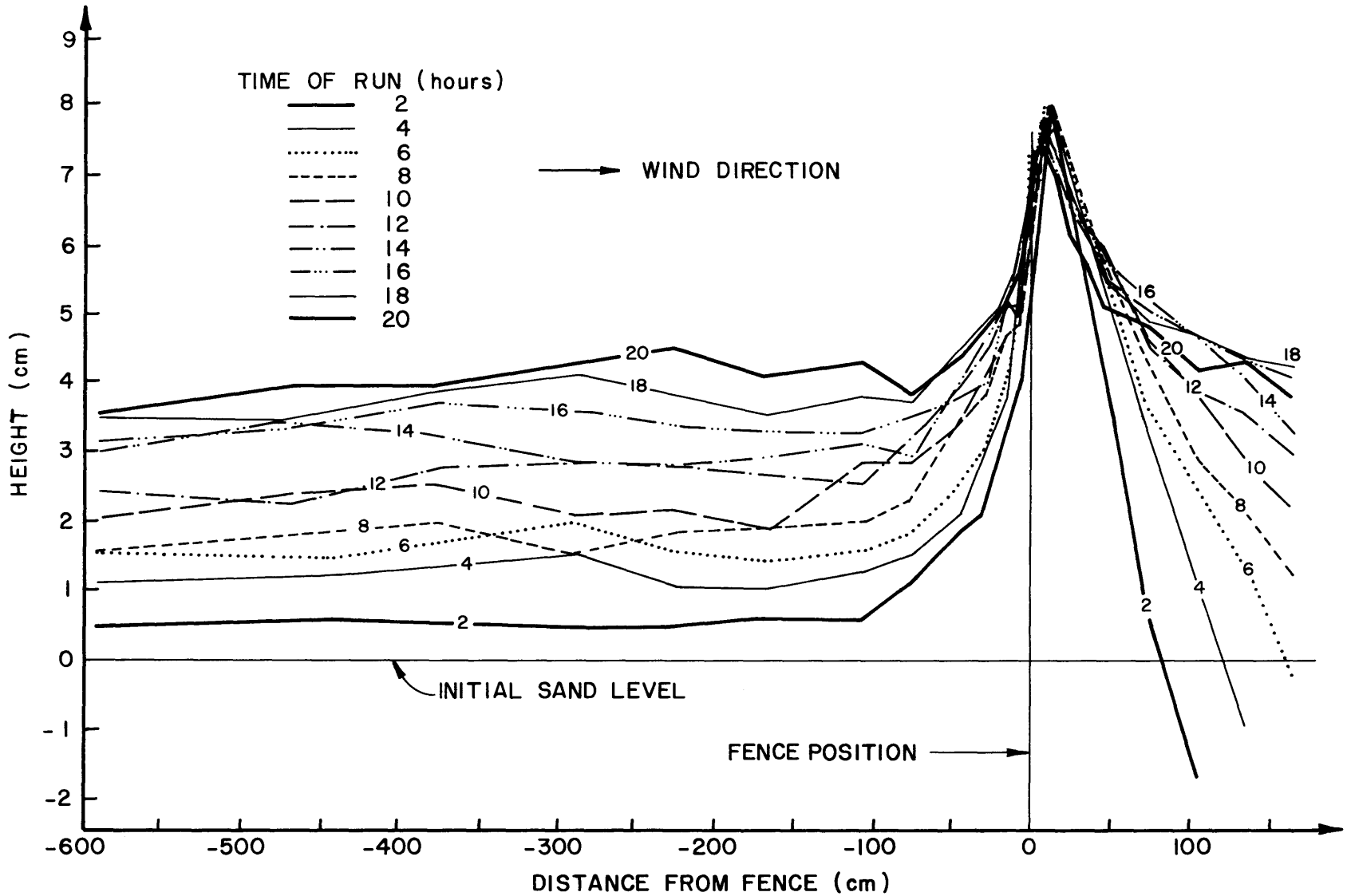

Figure 4-6a. Sand accumulation profiles for two-dimensional fence at 45° to 9 m/s wind.

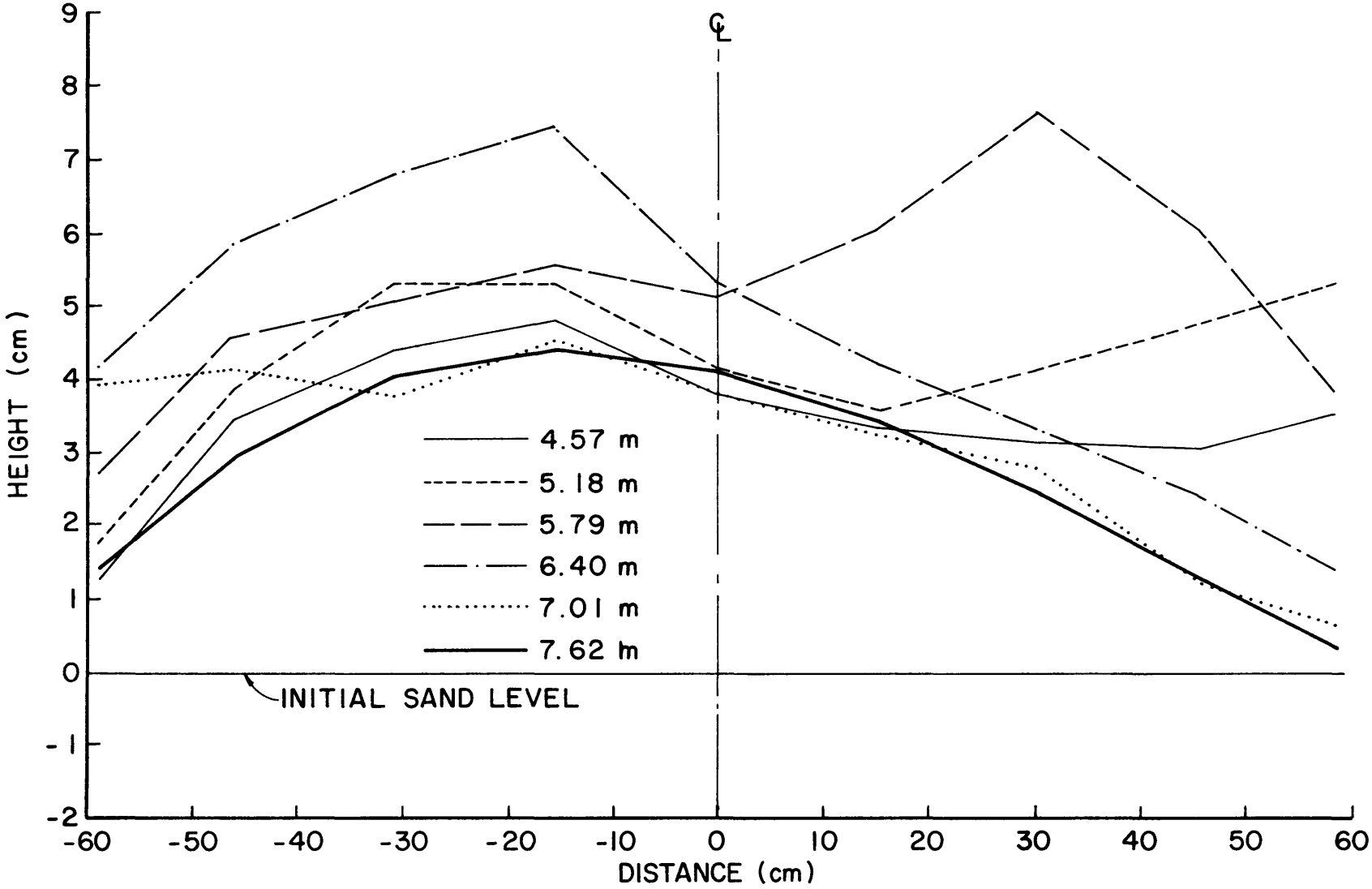

Figure 4-6b. Sand accumulation profiles at six cross sections around two-dimensional fence at 45° to 9 m/s wind (18 hours running time).

Table 4-1. Sand accumulation (cm^3) per centimeter of width upwind and downwind from the single fence positioned across the tunnel at 45° to the wind.

Time (hrs)	Downwind (4.42 m)	Upwind (5.94 m)
2+00	-206	465
4+00	-254	869
6+00	-191	1086
8+00	-77	1222
10+00	140	1488
12+00	654	1689
14+00	877	1948
16+00	1151	2112

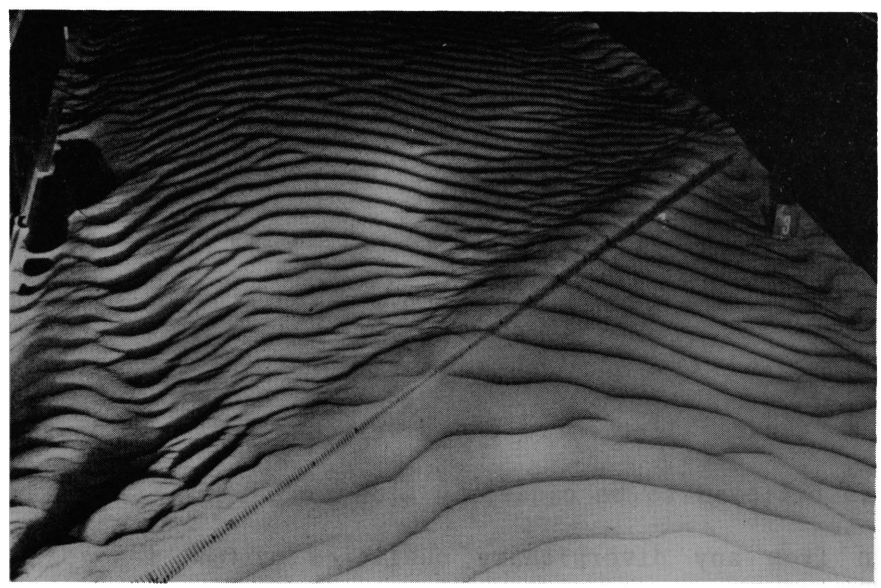

Figure 4-7. Sand accumulation around 45-degree inclined long fence (after 20+00 hours running time).

along the fence at the end of the testing period. There are no ripple, or dune, patterns discernibly misaligned from the tunnel centerline.

Accumulations of sand for 4.27 m downwind and 5.79 m upwind from the center of the short diverting fence are contained in Table 4-2. The tabulated values are portrayed in graphic form on Figures 4-8 and 4-9.

Table 4-2. Sand accumulation (cm^3) per centimeter of width upwind and downwind from the short single fence positioned 45° to the wind.

Time (hrs)	Downwind (4.27 m)	Upwind (5.79 m)
2+00	30	317
4+00	76	308
6+00	207	727
8+00	535	827
10+00	563	934

Figure 4-10 contains longitudinal profiles of sand accumulation near the short fence between 2 and 10 hours. The profiles reveal that sand accumulation around the short 45° fence was nearly stable after the ten hours of testing. The reproduced photo of Figure 4-11 reveals the sand deposition downwind from the short 45° fence which appears to have diverged from tunnel alignment. The divergence near the upwind end of the fence is believed to be caused by flow around the end of the fence, rather than from any diversionary qualities of the fence, since the misalignment disappears completely within 2 m and is never present downwind from the opposite end of the fence.

Table 4-3 contains sand accumulations downwind, between, and upwind of the double fences for a 14 hour test period which commenced with a smooth sand-bed. Graphic representation of these sand accumulations are

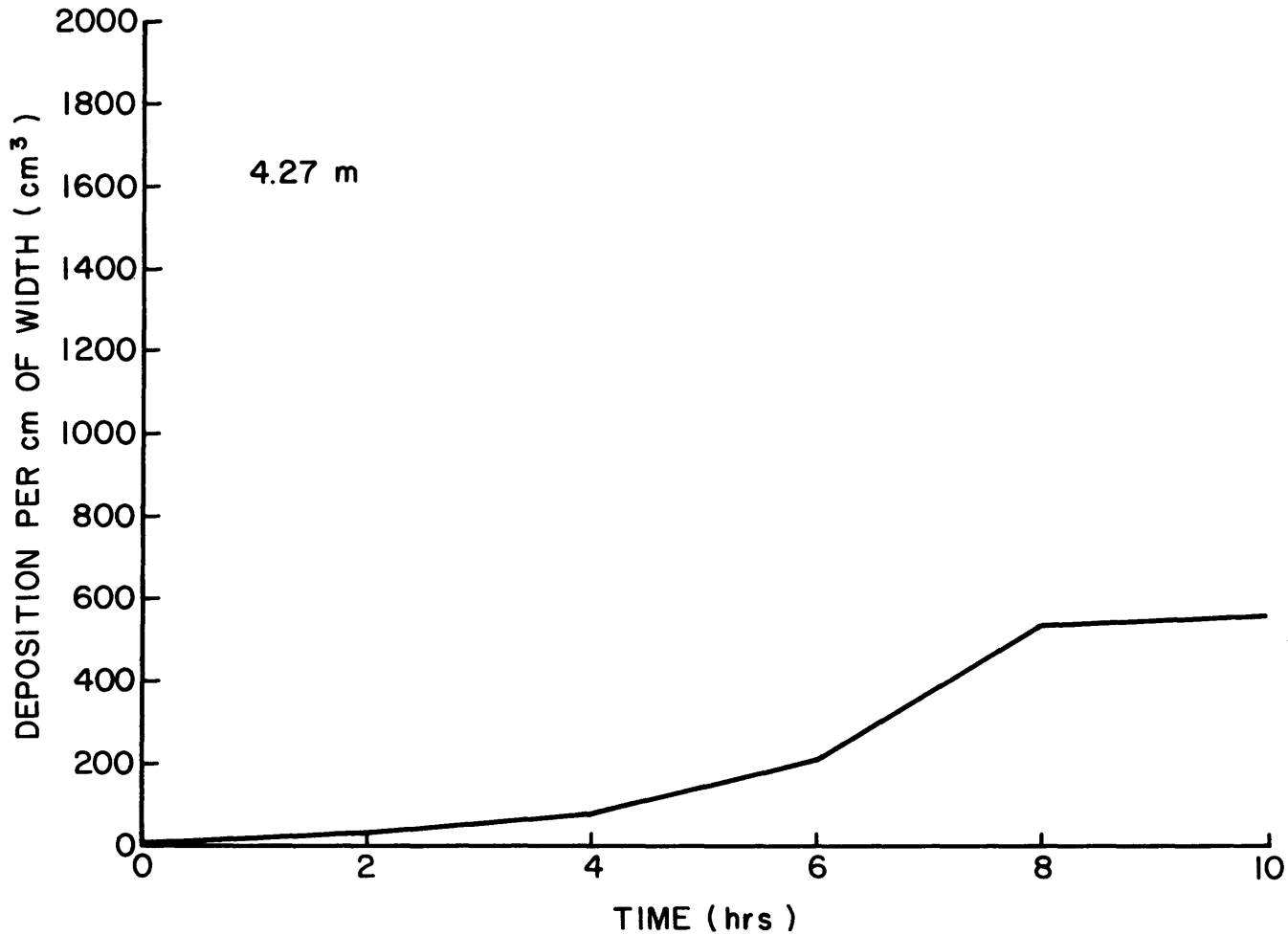

Figure 4-8. Sand accumulation on downwind side of short 45° fence.

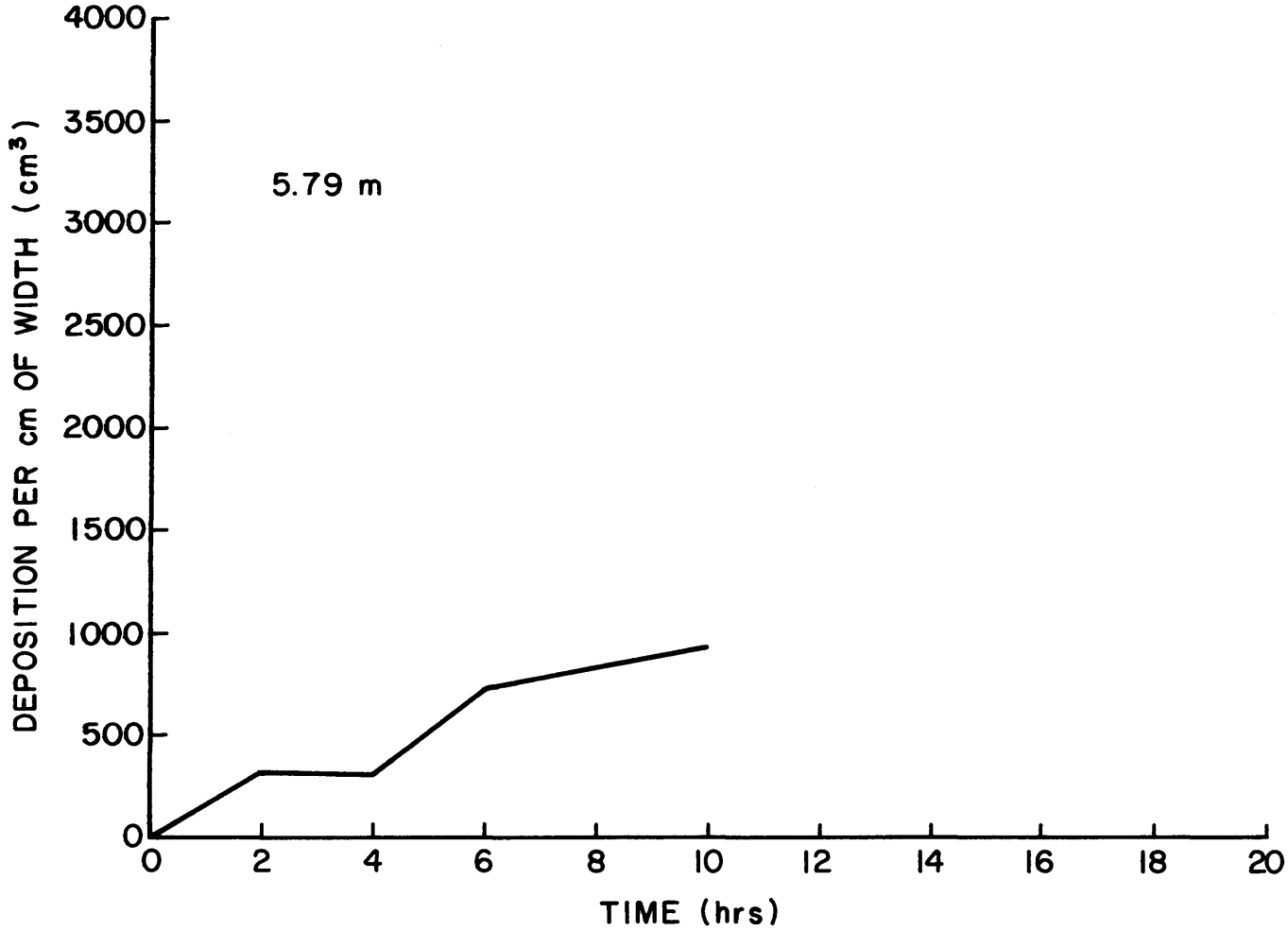

Figure 4-9. Sand accumulation on upwind side of short 45° fence.

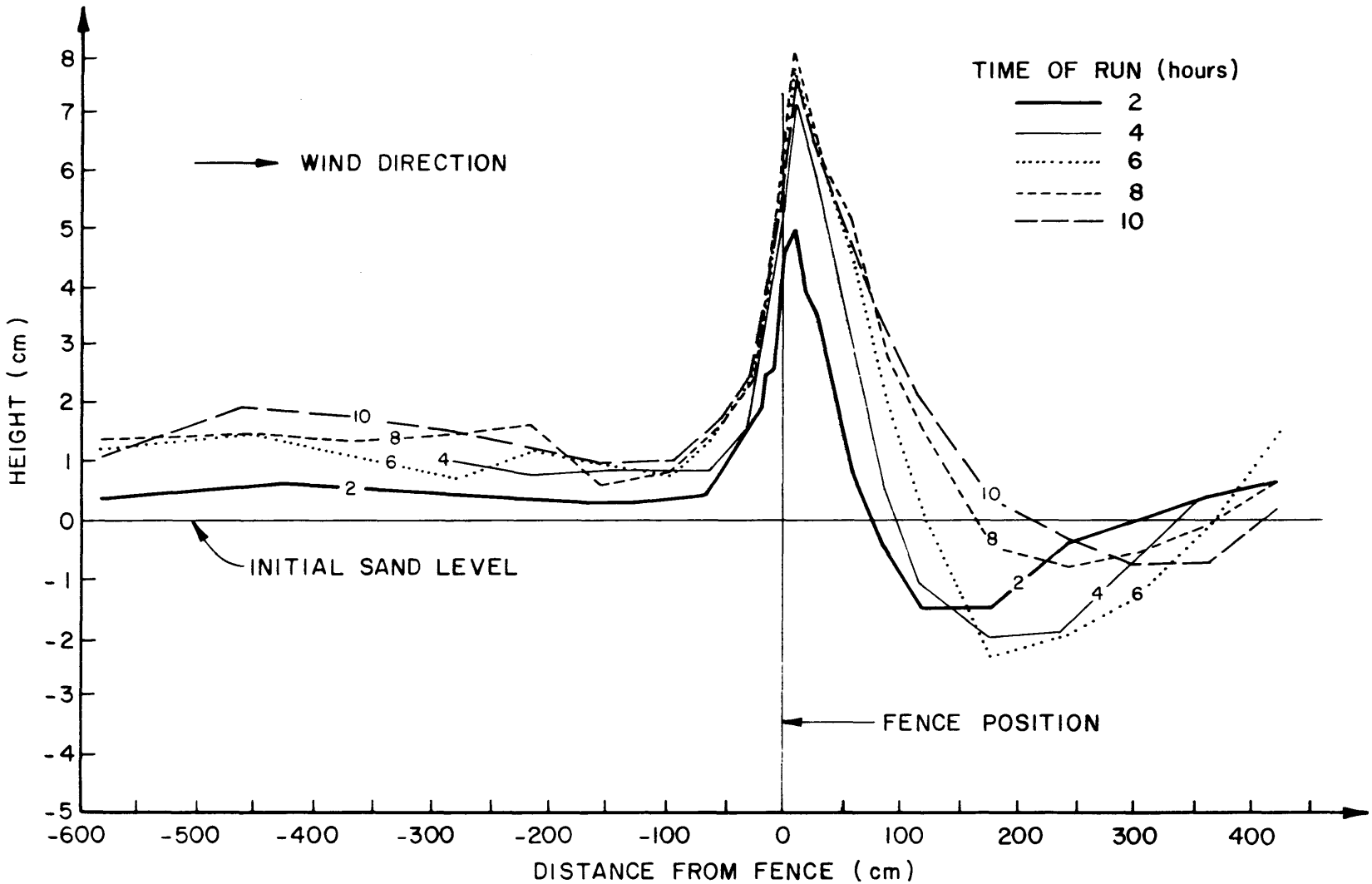

Figure 4-10. Sand accumulation profiles for 86 cm fence at 45° to prevailing 9 m/s wind.

Table 4-3. Sand accumulation (cm^3) per cm of width downwind, between and upwind from the double fences (first series).

Time (hrs)	Downwind (4.27 m)	Between (3.11 m)	Upwind (2.99 m)
2+00	-139	112	411
4+00	-246	516	421
6+00	-301	1094	1002
8+00	-167	1458	1038
10+00	382	1729	1217
12+00	920	1878	1297
14+00	1655	2019	1242

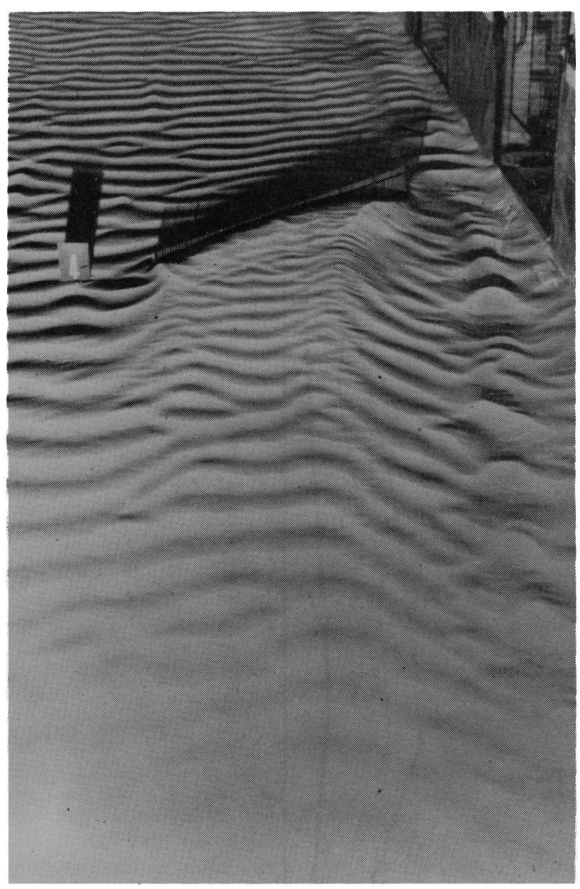

Figure 4-11. Sand accumulation: Downwind from 45-degree inclined short fence.

contained in Figures 4-12, 4-13, and 4-14. Cumulative sand accumulation profiles around the double fences for 18 hours at bi-hourly intervals are plotted on Figure 4-15. Sand accumulations between and downwind from the fences after 18 hours of tunnel operation are depicted in Figure 4-16.

Table 4-4 contains correlary sand accumulations downwind, between and upwind of the double fences for a 12-hour test period which commenced with a modified sand-bed. The table contains a base for sand depositions which had accumulated prior to the start of the double fence tests and a zero-base (in parentheses) for sand which accumulated after

Table 4-4. Sand accumulation (cm^3) per centimeter of width upwind, downwind and between double fences (second series).

Time (hrs)	Downwind (4.57 m)	Between (3.1 m)	Upwind (12.09 m)
Base	924 (0)	1560 (0)	4950 (0)
2+00	943 (19)	1653 (93)	5307 (357)
4+00	874 (-50)	2106 (546)	5619 (669)
6+00	640 (-284)	2427 (867)	5705 (755)
8+00	892 (-32)	2749 (1189)	5399 (499)
10+00	1403 479	2806 (1246)	5442 (492)
12+00	1858 934	2724 (1164)	5181 (231)

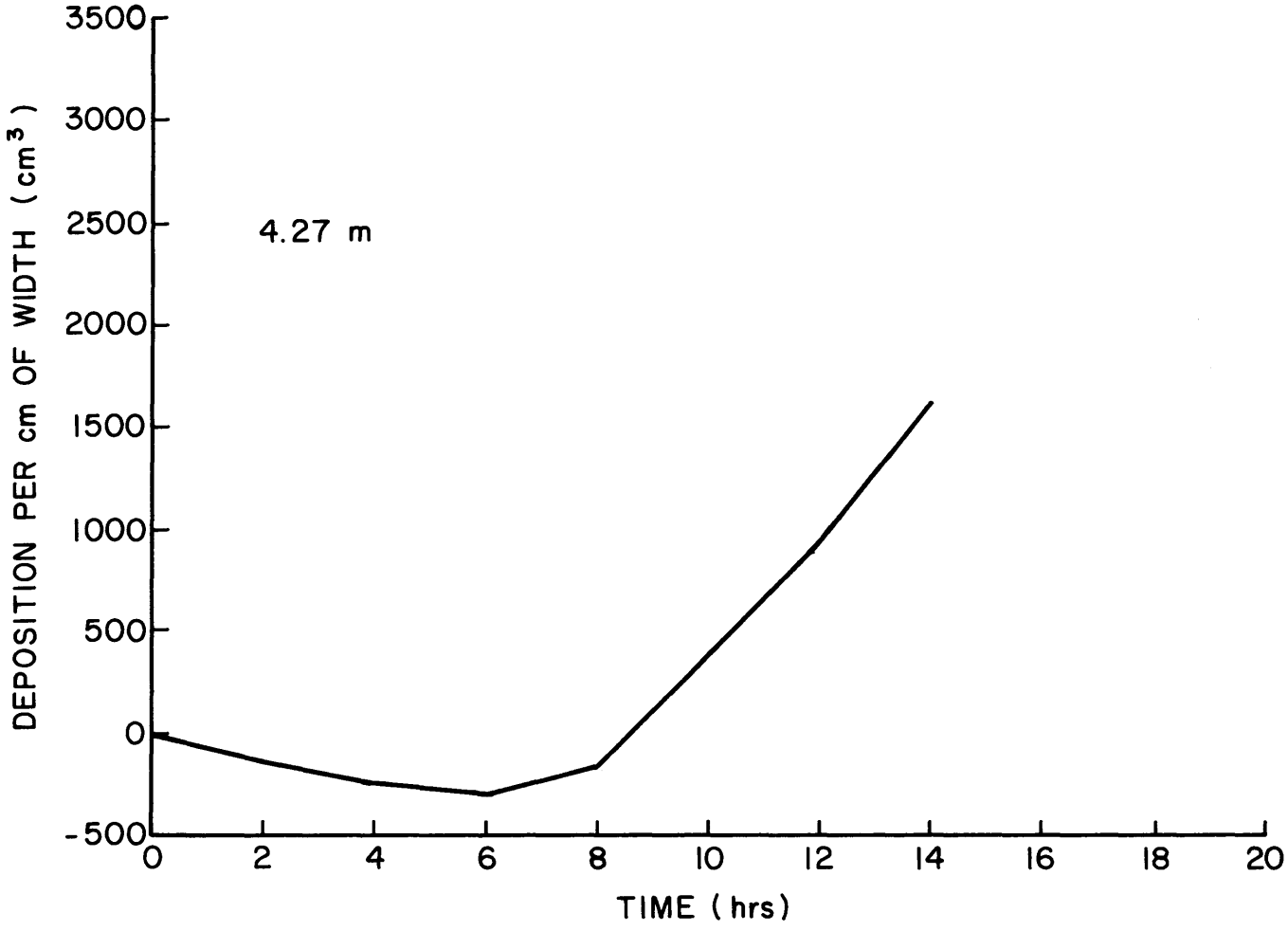

Figure 4-12. Sand accumulation downwind from double fences (first test).

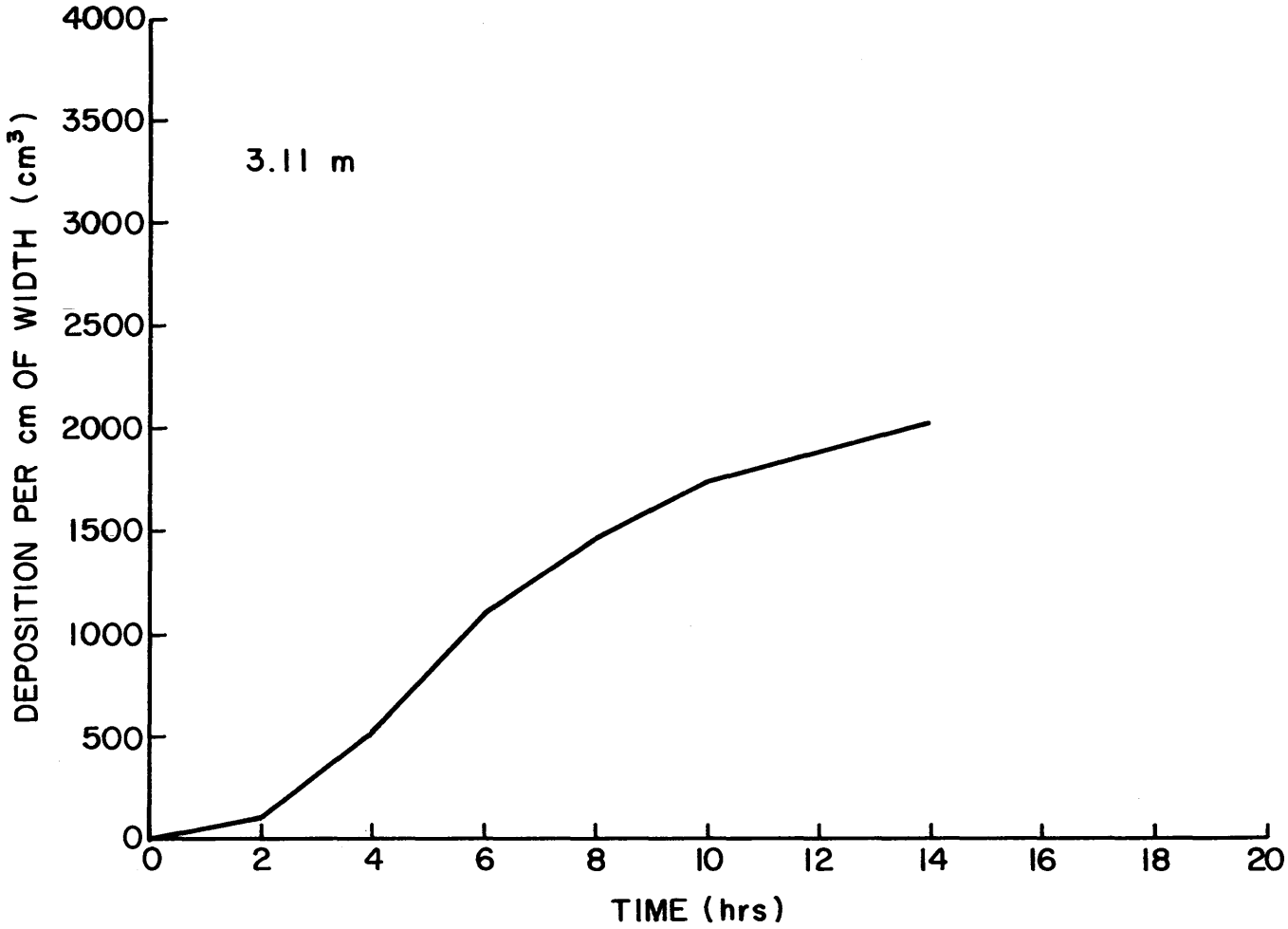

Figure 4-13. Sand accumulation between double fences (first test).

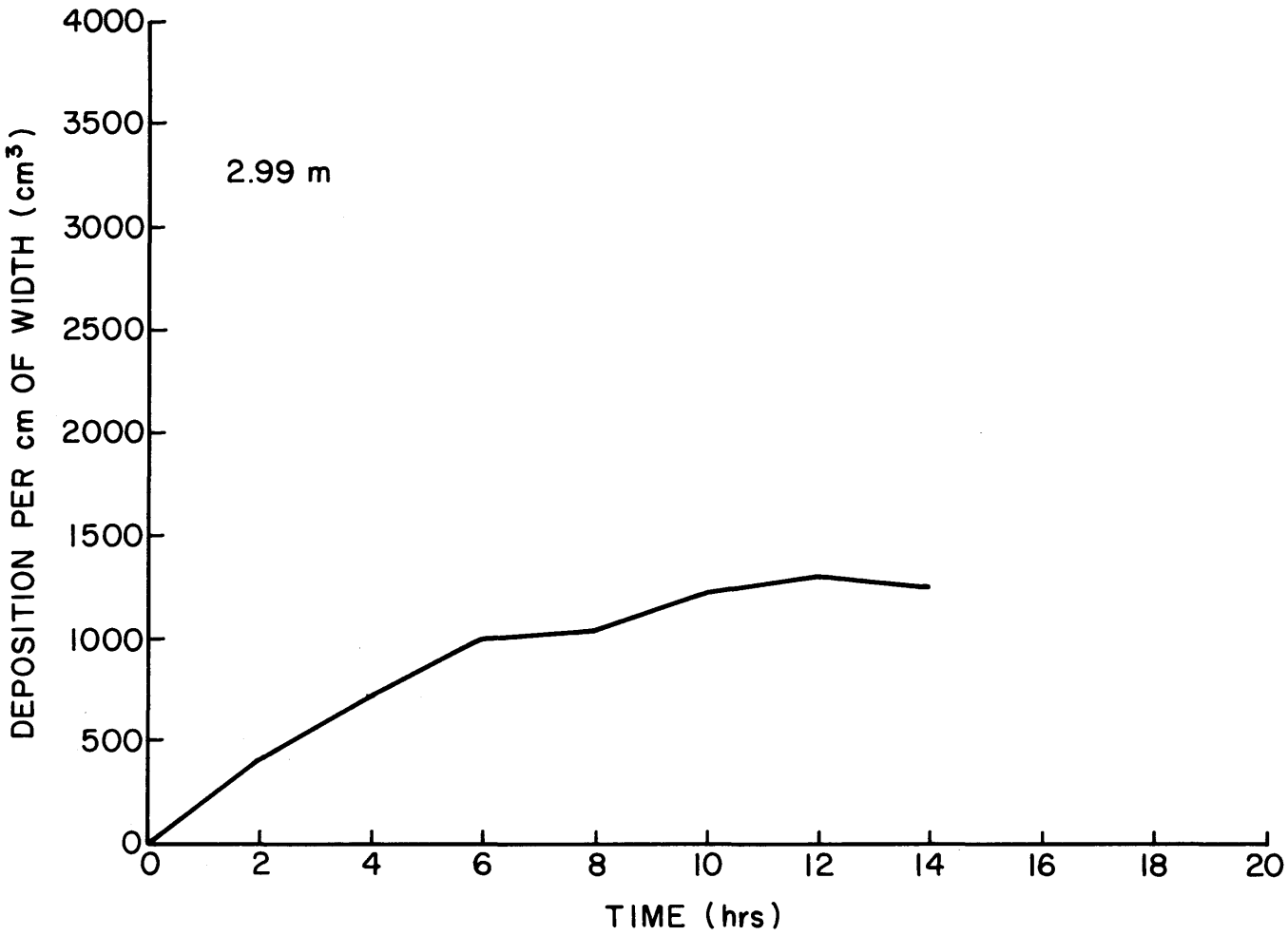

Figure 4-14. Sand accumulation upwind from double fences (first test).

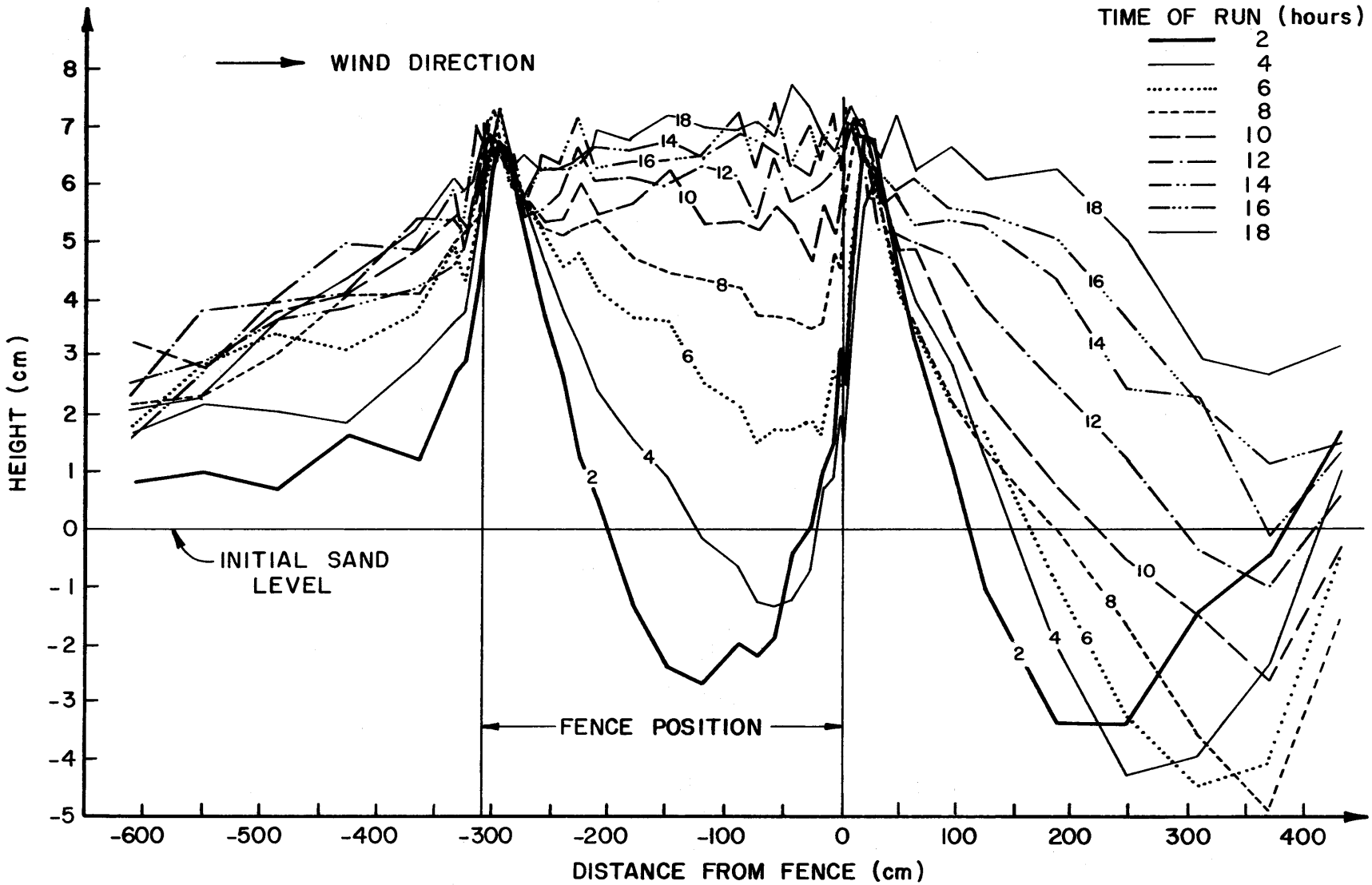

Figure 4-15. Sand accumulation profiles for double fences (first test).

fence installation. Figures 4-17, 4-18, and 4-19 contain graphs of sand depositions at the three positions, while Figure 4-20 contains the comparable longitudinal profiles for the 12 hours of testing.

Figure 4-16. Sand accumulation between and downwind from double fences.

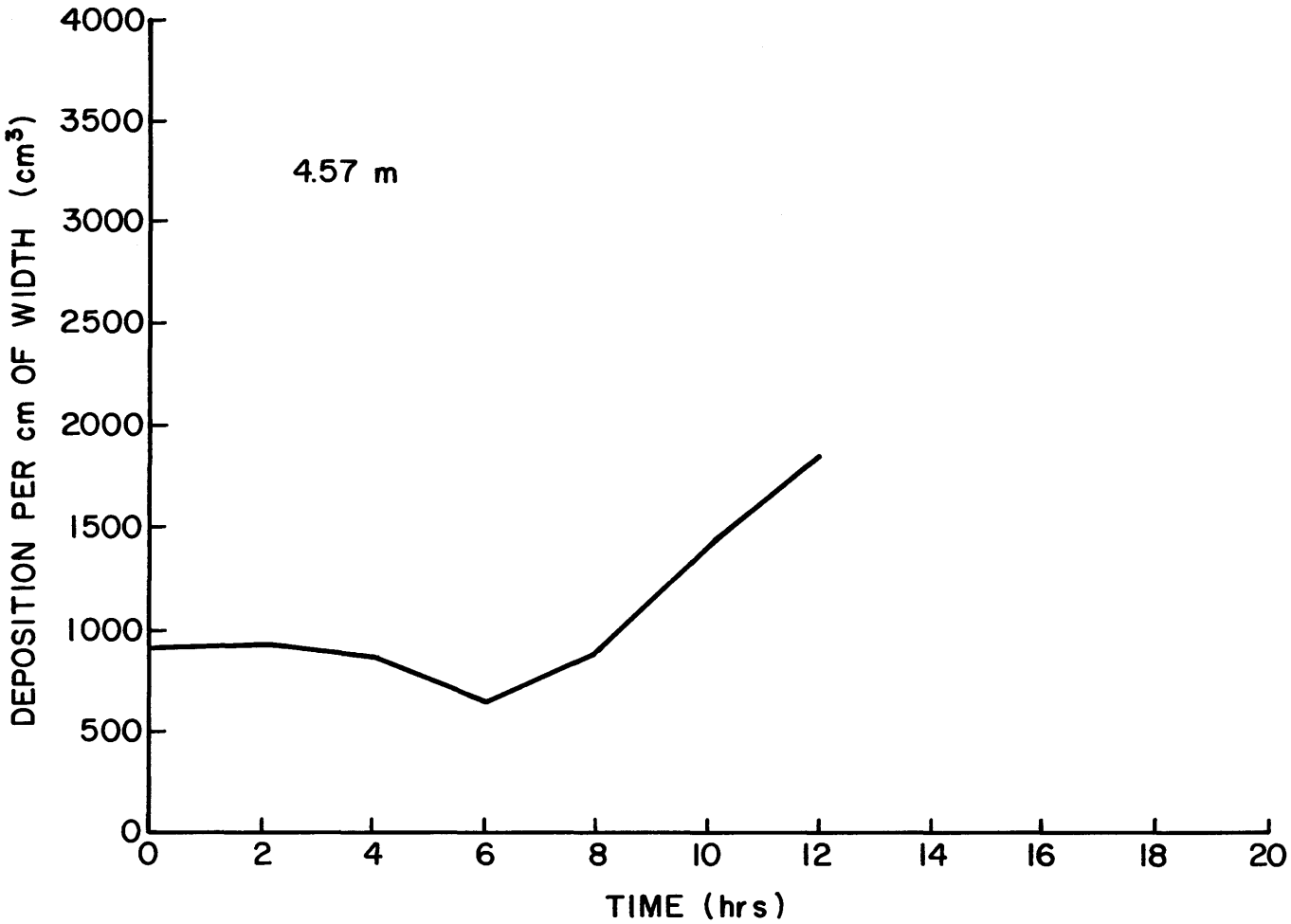

Figure 4-17. Sand accumulation downwind from double fences (second test).

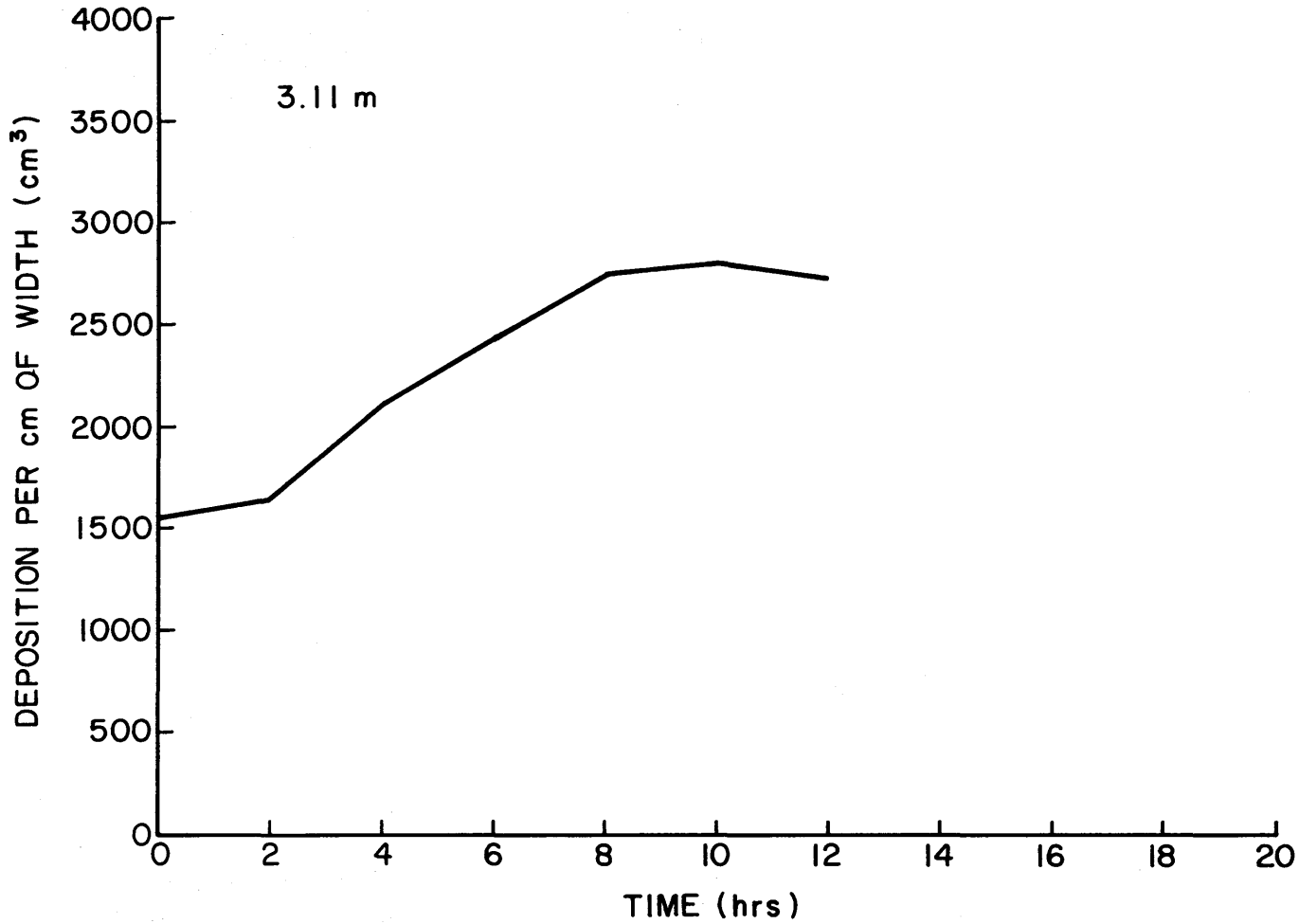

Figure 4-18. Sand accumulation between double fences (second test).

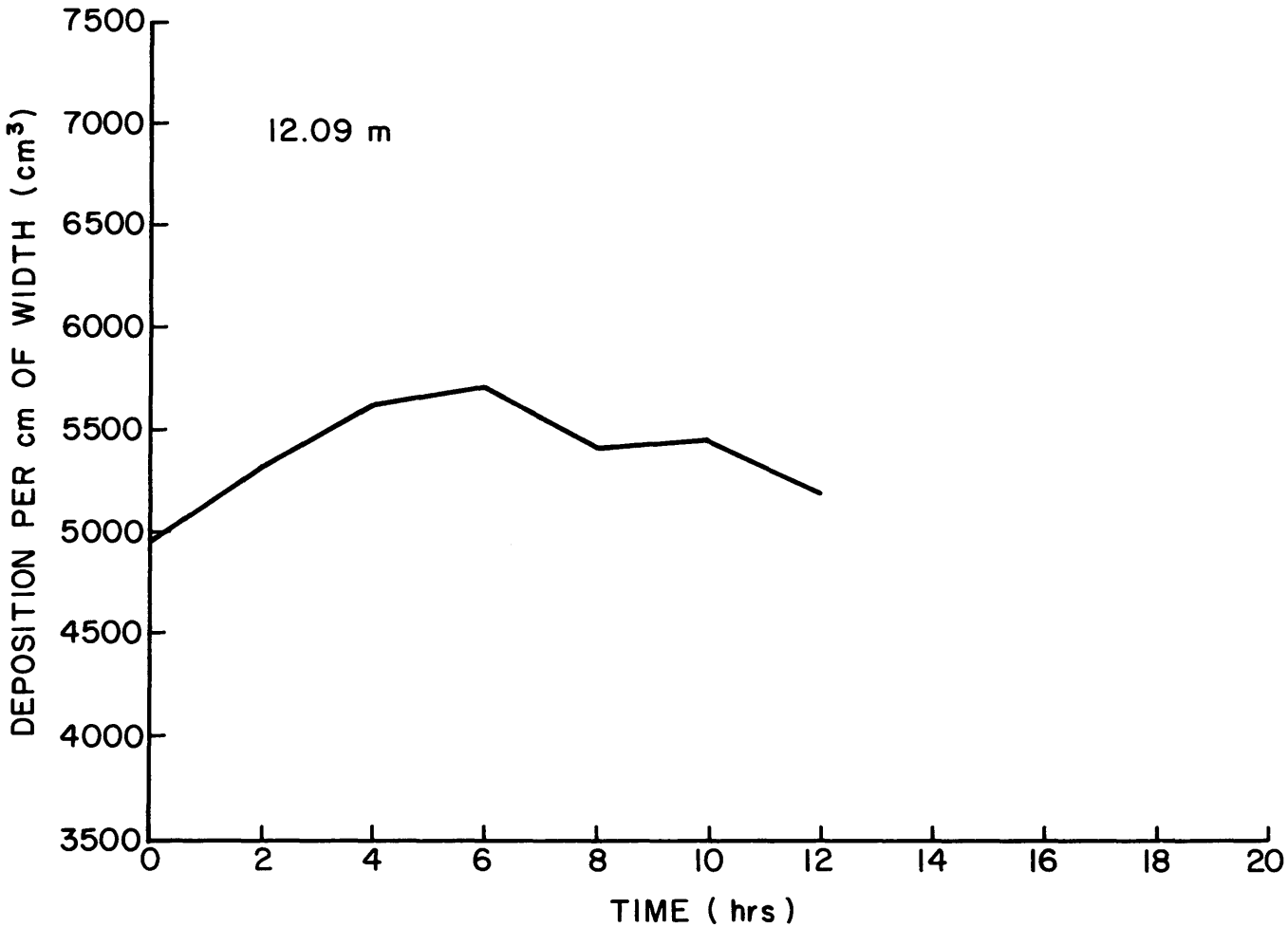

Figure 4-19. Sand accumulation upwind from double fences (second test).

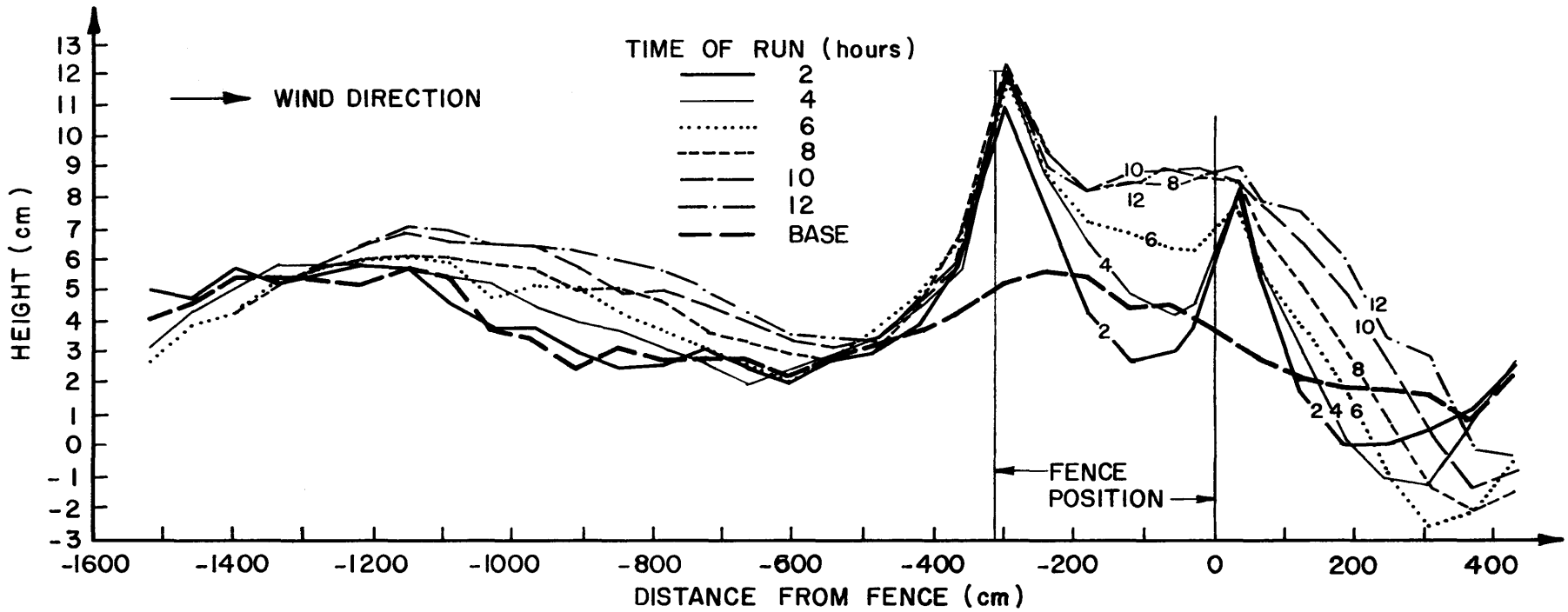

Figure 4-20. Sand accumulation profiles in vicinity of double fences (second test).

Figures 4-21a (downwind), 4-21b (between), and 4-21c (upwind), contain an interesting comparison of the double fence data. The solid lines depict the sand accumulation rates (also reported in Figures 4-12, 4-13, and 4-14) for the fence tests commencing from a flat tunnel. The dashed lines depict the comparable tests started from the modified sand-bed and corrected for sand accumulations attributed to tunnel operation prior to installation of the fences. The downwind plots show remarkable similarity and the rates were calculated over nearly equal distances of 4.27 and 4.57 m. Deposition rates between the fences also show good correlation as the digression from the solid line graph, for the later stages of double fences installed upon a modified base, is attributed to the method of fence installation which accounts for the area becoming stabilized sooner. (The relatively crowned cross section of the modified sand-bed and flat bottom of the fences required a compromised installation which resulted in fences slightly less than 7.75 cm in height at the tunnel centerline). The upwind plots of the two double fence tests also show early similarity. The first series was measured for only 2.99 m upwind, while the second series of measurements extended for 12.09 m upwind and encompassed a rather stable segment of the sand-bed (see Figures 4-19 and 4-20.).

4.5 Conclusions and Commentary

Data from the laboratory tests made with single fences positioned 45° to the prevailing wind did not produce any results which would support field attempts to divert blowing sand with strategically positioned fences.

Interaction of the double row of fences was effective, as the entire area between the fences trapped large quantities of sand in a

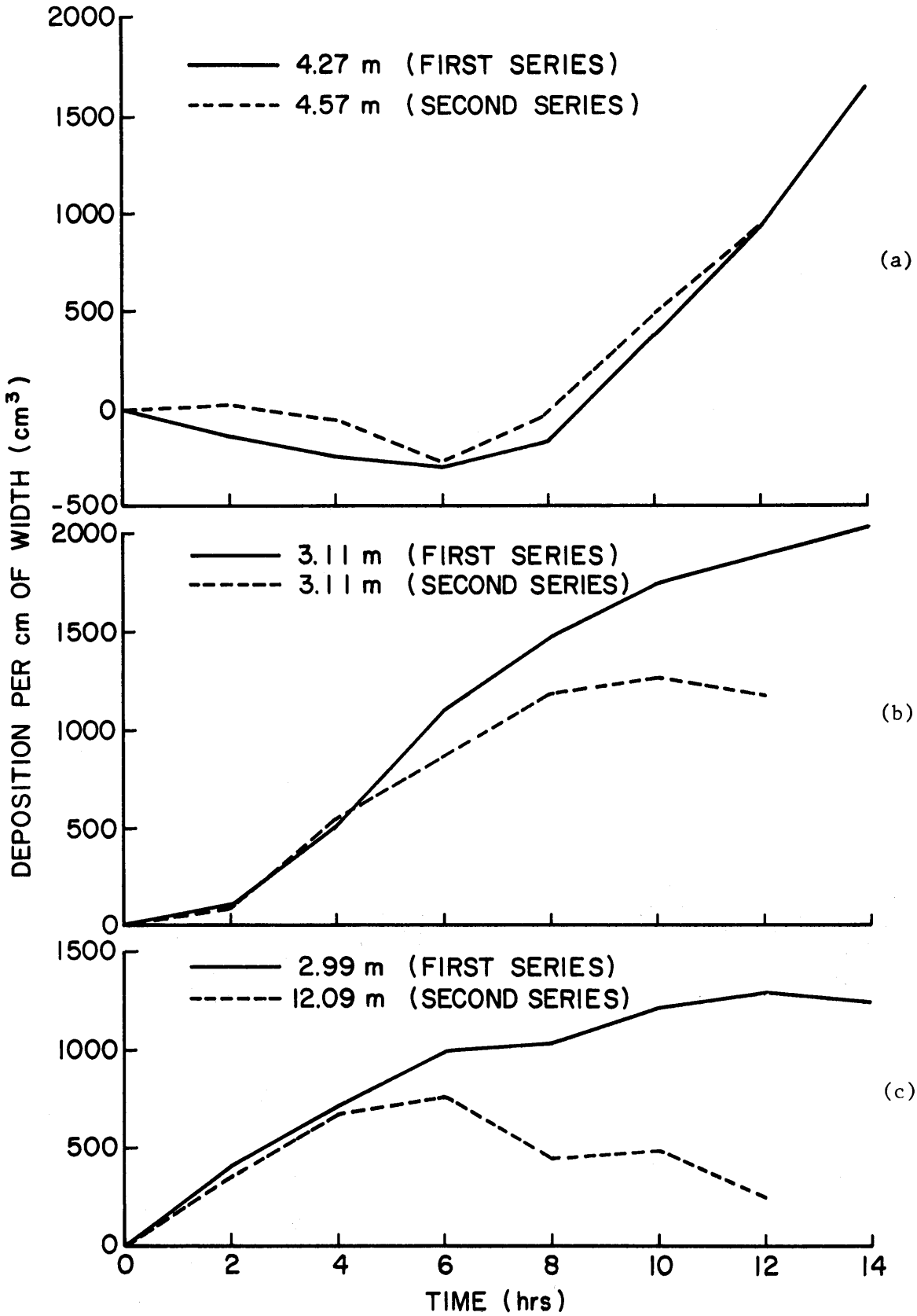

Figure 4-21. Downwind (a), between (b), and upwind (c) comparisons of sand deposition for two series of double fence tests.

relatively uniform manner. A spacing between the fences of approximately 40 fence heights still appears to be effective.

Data from the two series of double fence tests indicates that the initiation of tests from a modified sand-bed has little, if any, effect upon the resultant data.

5.0 SAND TRAP CALIBRATIONS

5.1 Purpose

This series of tests was designed to determine the efficiency of the large azimuthal USGS sand trap at four different wind speeds for one wind direction. Additional calibrations of the 34 mm I.D. horizontal cylinders were also to be incorporated into the tests, if possible.

5.2 Test Configuration

A 91.5 cm square by 5 cm high platform (containing a circular cut-out to accommodate the azimuthal sand trap) was centered on the tunnel floor approximately 4.7 m upwind from the end of the MWT test section. The sand-bed surrounding the platform, and to a position 20 m upstream, was screeded to a depth of 5 cm. The sand trap supplied by the Denver-based manufacturer was inserted in the supporting platform without the subsurface compartmented collection system used in the desert. In its place a funnel was attached to the underside of the trap base which completely covered the horizontal opening under the vertical intake and connected to a twenty-liter glass jar (beneath the tunnel) by a length of tygon tubing.

The 34 mm I.D. horizontal traps were situated as depicted on Figure 5-1, which also provides a plan view of the azimuthal trap's location.

5.3 Test Procedures

Sand trap calibration tests were conducted at free-stream wind speeds of 7, 9, 12 and 14 m/s. The sand-bed was smoothed and the characteristic ripples permitted to fully redevelop prior to each series of tests. Tests on the horizontal traps, at heights ranging from one

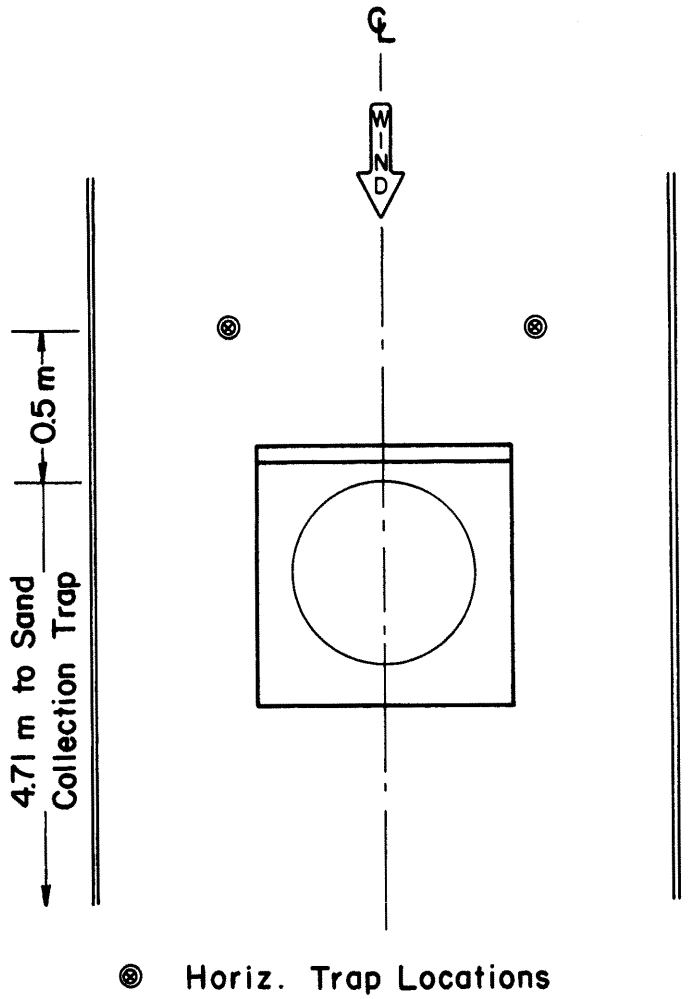

Figure 5-1. Plan view of USGS vertical and 34 mm I.D. vertical sand trap locations within MWT test section.

to ten centimeters, were accomplished simultaneously with the azimuthal trap tests. Sampling times ranged from fifteen minutes up to one hour, with the longer durations necessary at the lower wind speeds. The azimuthal trap's collection rate was measured with the vertical intake aligned to the wind and also with ten and twenty-degree off-sets. The tests at each condition were repeated from two to five times, in most instances.

5.4 Test Results

The wind speeds, sampling times, measured accumulations, and calculated collection rates in grams/minute acquired from the trap calibration tests, are tabulated in Tables 5-1 and 5-2. Collection rates for the azimuthal trap at the 0°, 10° and 20° off-sets for each of the four wind-speeds are plotted on Figure 5-2. A ten-degree misalignment of the azimuthal trap reduced its efficiency by 45-50 percent, while a twenty-degree off-set decreased sand collection by 76-86 percent.

The azimuthal trap collection rates for each aligned (zero-degree offset) test were multiplied by two (x2) to provide a per centimeter width collection rate for the trap. These rates are plotted on Figure 5-3 to produce a curve of that trap's sand collection characteristics.

Figure 5-4 provides graphic description of the horizontal sand trap accumulation rates contained in the previously referenced Table 5-2. This figure also contains the characteristic curve of the azimuthal trap for comparative purposes.

Efficiency of the horizontal trap, as compared to the azimuthal trap, is portrayed on Figure 5-5. Horizontal trap collection rates at the various heights and wind speeds contained in Table 5-2 were divided by the average collection rates for comparable wind speeds from Table 5-1 to determine the percentage of efficiency. As previously mentioned in the 1982 Sand Study Report, the horizontal traps did not produce consistent values. While a general relationship of efficiency to trap height is discernible from Figure 5-5, the variation in repeatability covers several orders of magnitude.

Table 5-1. Sand accumulation rates measured for USGS Sand Trap at free-stream velocities and alignments from Tunnel center-line indicated.

Wind Speed (meters/sec)	Direction (degrees)	Run Time (min)	Weight (grams)	Rate (gm/min)
7.0	0	30	5.59	0.186
	0	30	5.46	0.182
	0	60	8.96	0.149
	10	60	4.19	0.070
	10	45	3.10	0.069
	20	60	2.38	0.040
	20	60	1.22	0.020
9.0	0	30	22.76	0.759
	0	30	21.25	0.708
	0	60	40.50	0.675
	0	30	17.83	0.594
	10	30	9.22	0.307
	10	30	9.18	0.306
	10	45	12.87	0.286
	20	30	6.12	0.204
	20	45	5.41	0.120
12.0	0	30	72.48	2.416
	0	15	35.62	2.375
	0	30	70.38	2.346
	0	30	67.05	2.235
	10	30	30.02	1.001
	10	30	29.80	0.993
	20	30	9.88	0.329
	20	30	9.80	0.327
14.0	0	15	85.07	5.671
	0	30	139.50	4.650
	10	30	90.87	3.029
	10	15	40.86	2.724
	10	15	40.76	2.717
	20	30	26.28	0.876

Table 5-2. Sand accumulation rates measured for hortizontal sand traps at free-stream velocities and heights indicated.

Wind Speed (m/sec)	Height (cm)	Run Length (min)	Weight (grams)	Rate (gm/min)
7	1	60	9.83	0.164
	1	30	3.83	0.128
	1	60	2.30	0.038
	1	60	2.15	0.036
	2	180	2.47	0.014
	5	60	0.16	0.003
9	1.5	30	1.69	0.056
	1.5	60	3.08	0.051
	2	30	2.40	0.080
	2	60	3.02	0.050
	2	30	1.00	0.033
	2	30	0.95	0.032
	5	30	0.07	0.002
	5	60	0.05	0.001
	5	60	0.05	0.001
	5	60	0.04	0.001
	5	60	0.02	0.000
12	2	60	10.64	0.177
	2	30	3.06	0.102
	2	30	2.59	0.086
	2	30	2.27	0.076
	2.6	15	3.38	0.225
	2.6	30	1.47	0.049
	3.5	30	3.36	0.112
	4	15	0.33	0.022
	5	30	1.26	0.042
	5	60	0.33	0.006
	5	30	0.11	0.004
	5	30	0.09	0.003

Table 5-2. (continued)

Wind Speed (m/sec)	Height (cm)	Run Length (min)	Weight (grams)	Rate (gm/min)
14	2	30	63.00	2.100
	2	15	16.70	1.113
	2	15	13.10	0.873
	2	15	6.08	0.405
	3	30	11.48	0.383
	3	30	8.35	0.278
	5	15	1.22	0.081
	5	30	1.83	0.061
	5	30	1.28	0.043
	5	30	1.13	0.038
	5	30	0.07	0.002
	10	60	0.00	0.000

A comparison of the sand transport rate (gm/min/cm), as measured with the aspirating probe, the Shen trap, and the large azimuthal trap, at similar wind speeds, is presented in Figure 5-6. (See Table 6 on page 30 of 1982 report for source of aspirating probe and Shen trap data). Figure 5-7 contains a comparison of the aspirator and azimuthal trap accumulation rates on an expanded scale. Table 5-3 contains values of the points plotted on Figure 5-7, as well as interpolated values (in parentheses) for those wind speeds from 6-14 m/s where measurements were not taken. The table also contains a calculation of azimuthal trap efficiency, which was obtained by dividing azimuthal trap accumulation rates with those rates obtained from the aspirator at similar velocities.

Relationship of the aspirator probe and azimuthal trap accumulation rates are plotted on the log-log graph of Figure 5-8. There appears to be a nearly linear relationship between the two rates over the range of velocities where the measurements were taken.

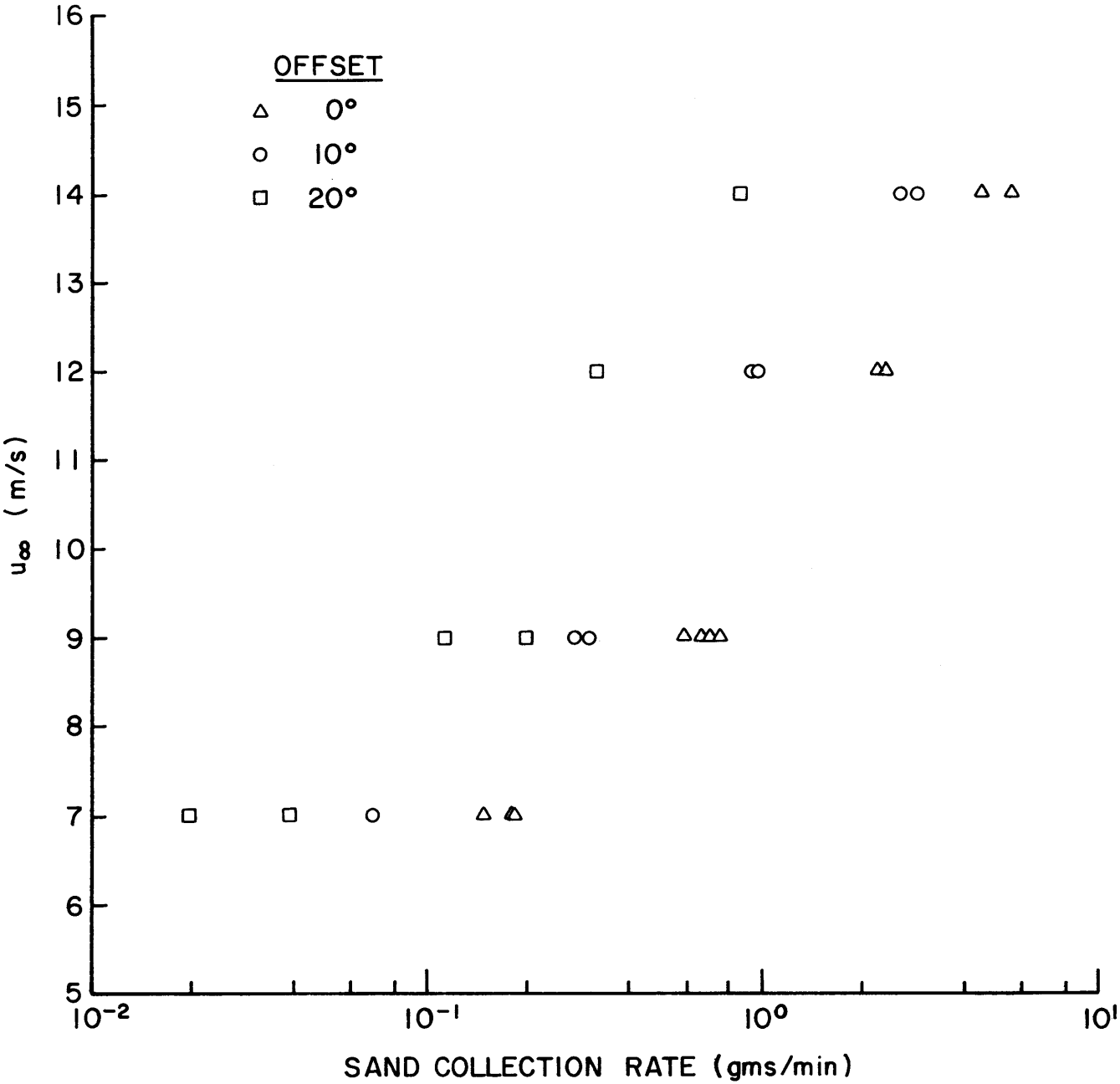

Figure 5-2. Characteristic curves for the large azimuthal sand trap.

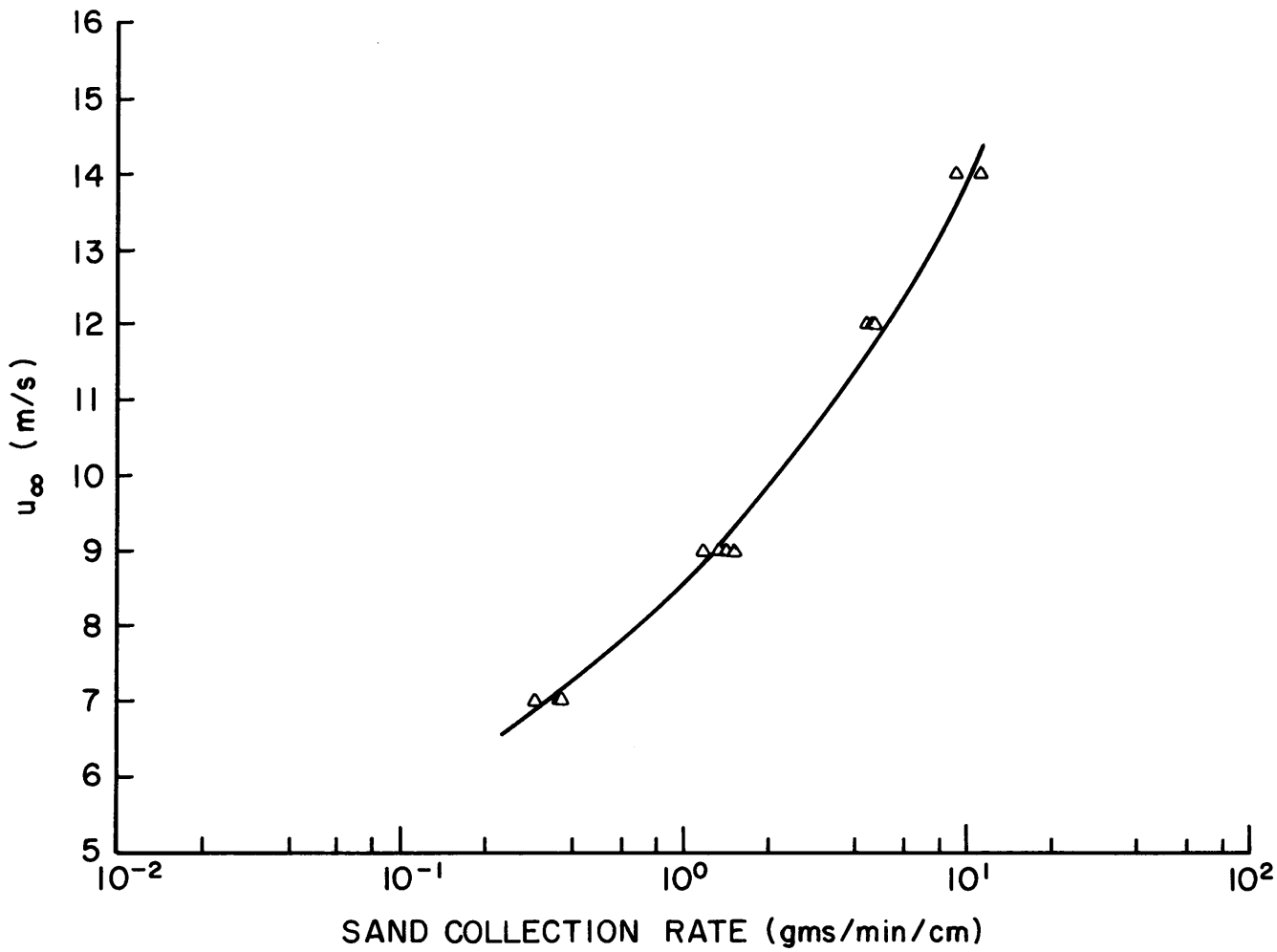

Figure 5-3. Characteristic curve for large azimuthal sand trap per centimeter of intake width.

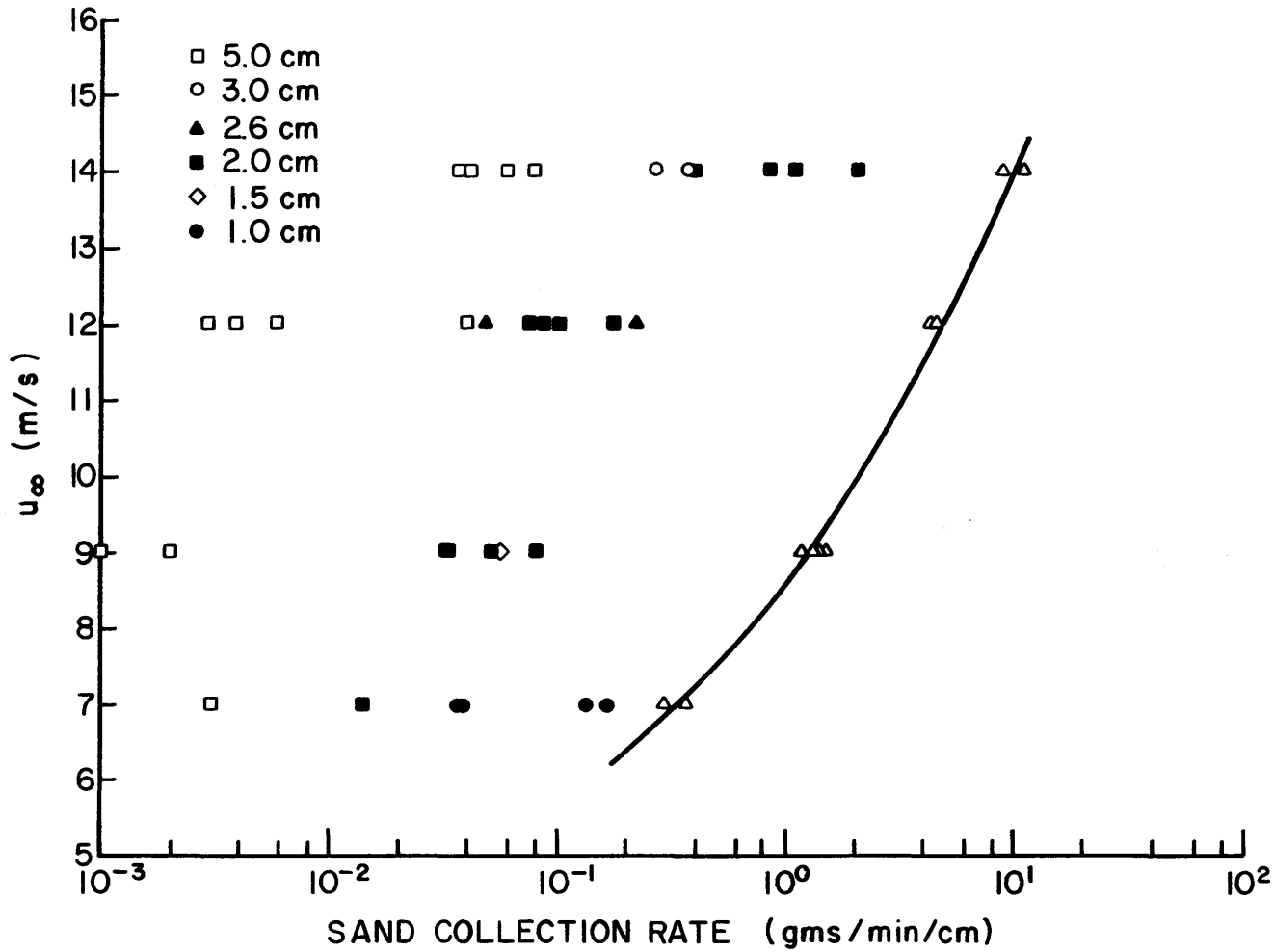

Figure 5-4. Sand collection rate of horizontal traps at heights from 1-5 cm compared with characteristic curve for azimuthal sand trap.

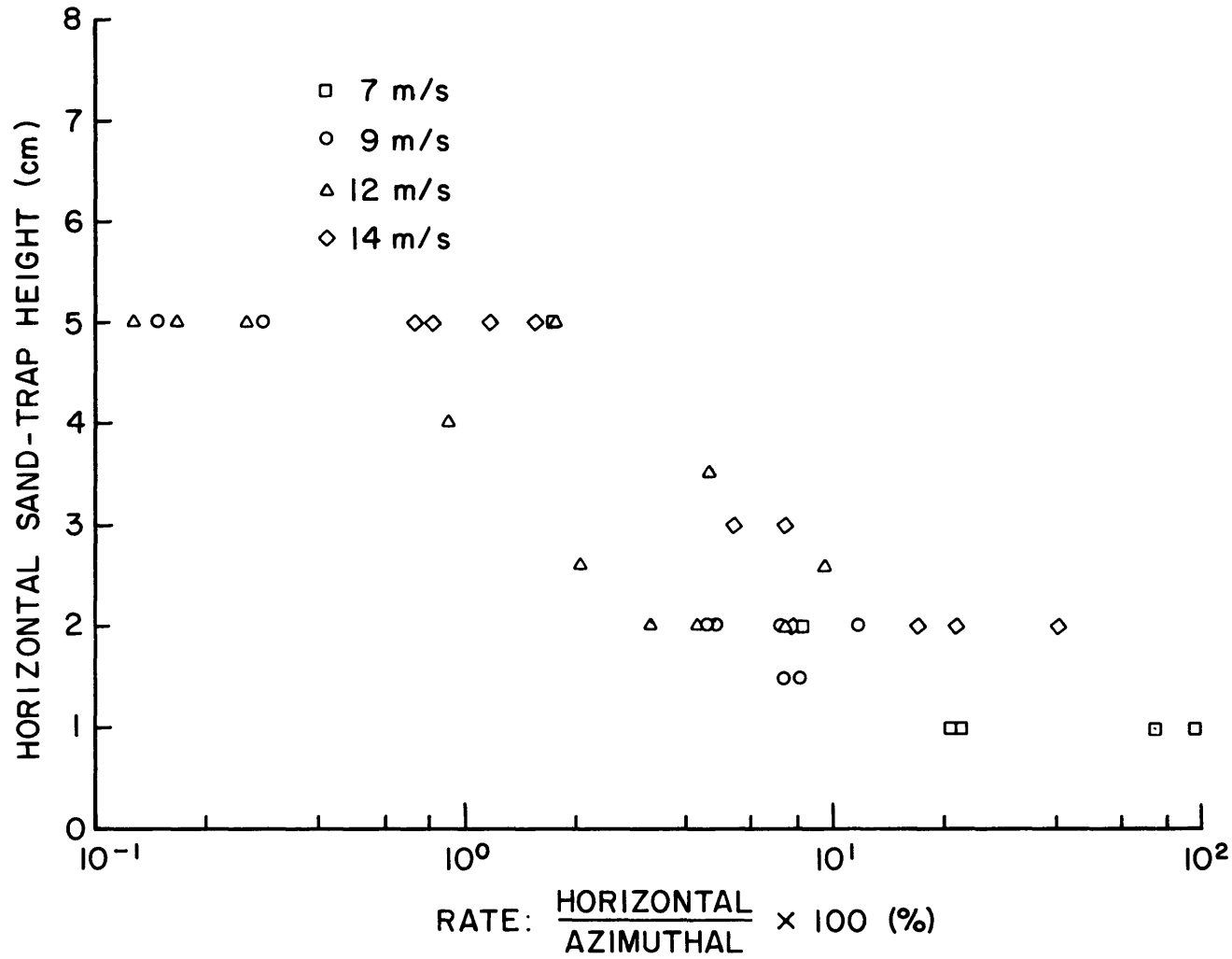

Figure 5-5. Comparison of cylindrical trap collection rates with those of large azimuthal trap.

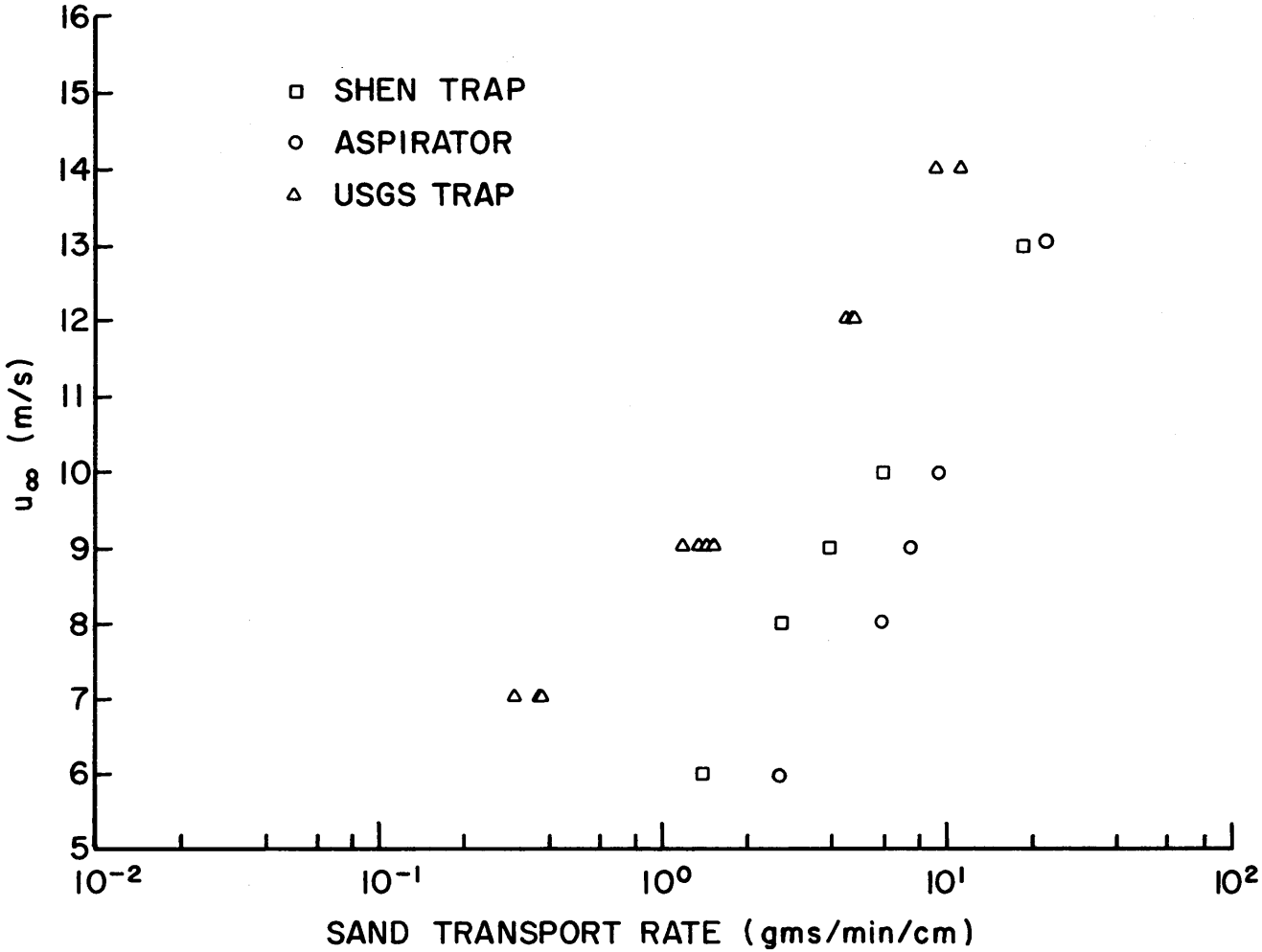

Figure 5-6. Comparison of sand collection rate for aspirating probe, Dr. Shen's trap and large azimuthal trap.

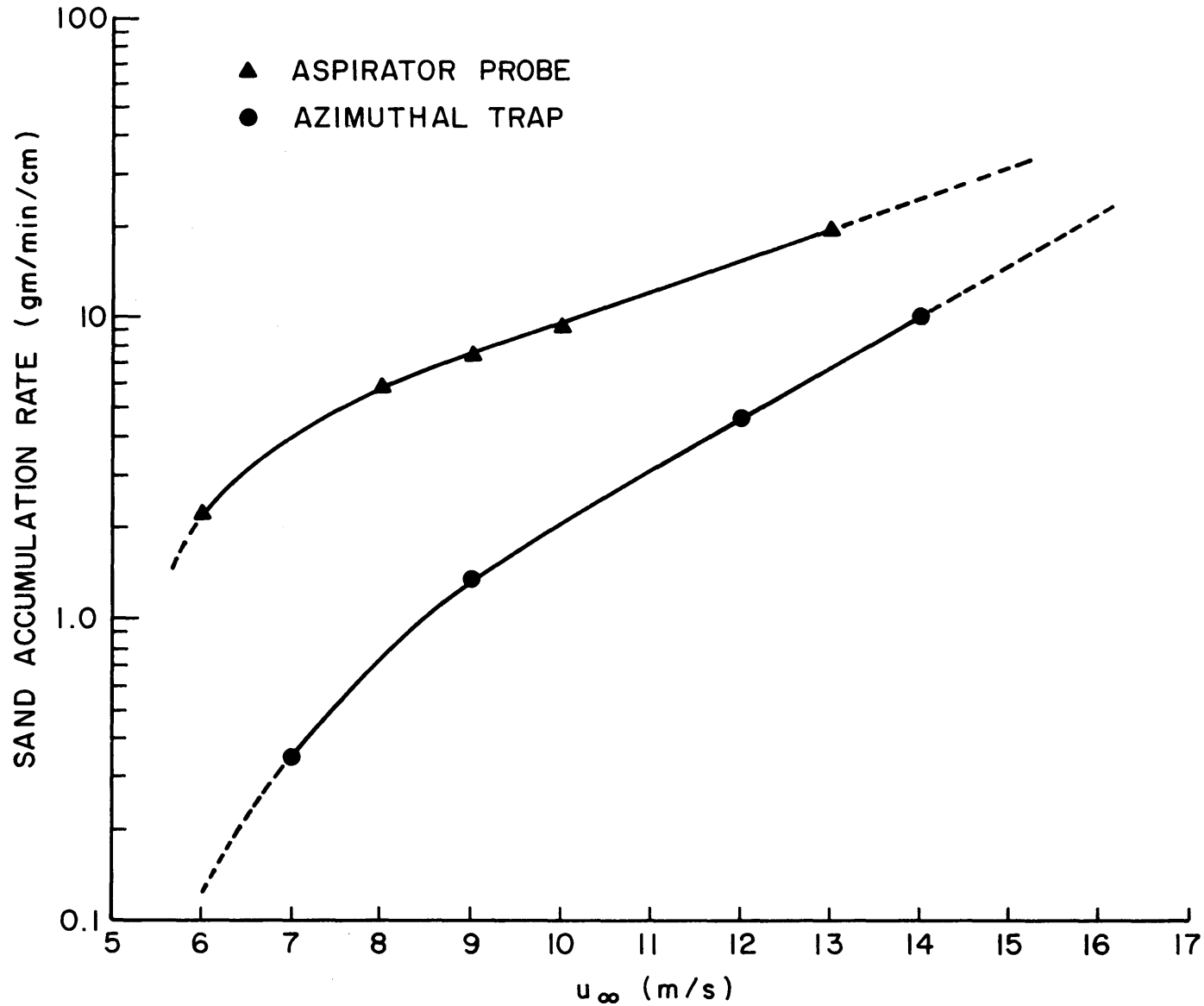

Figure 5-7. Comparison of sand accumlation rates from azimuthal trap with those from aspirator probe.

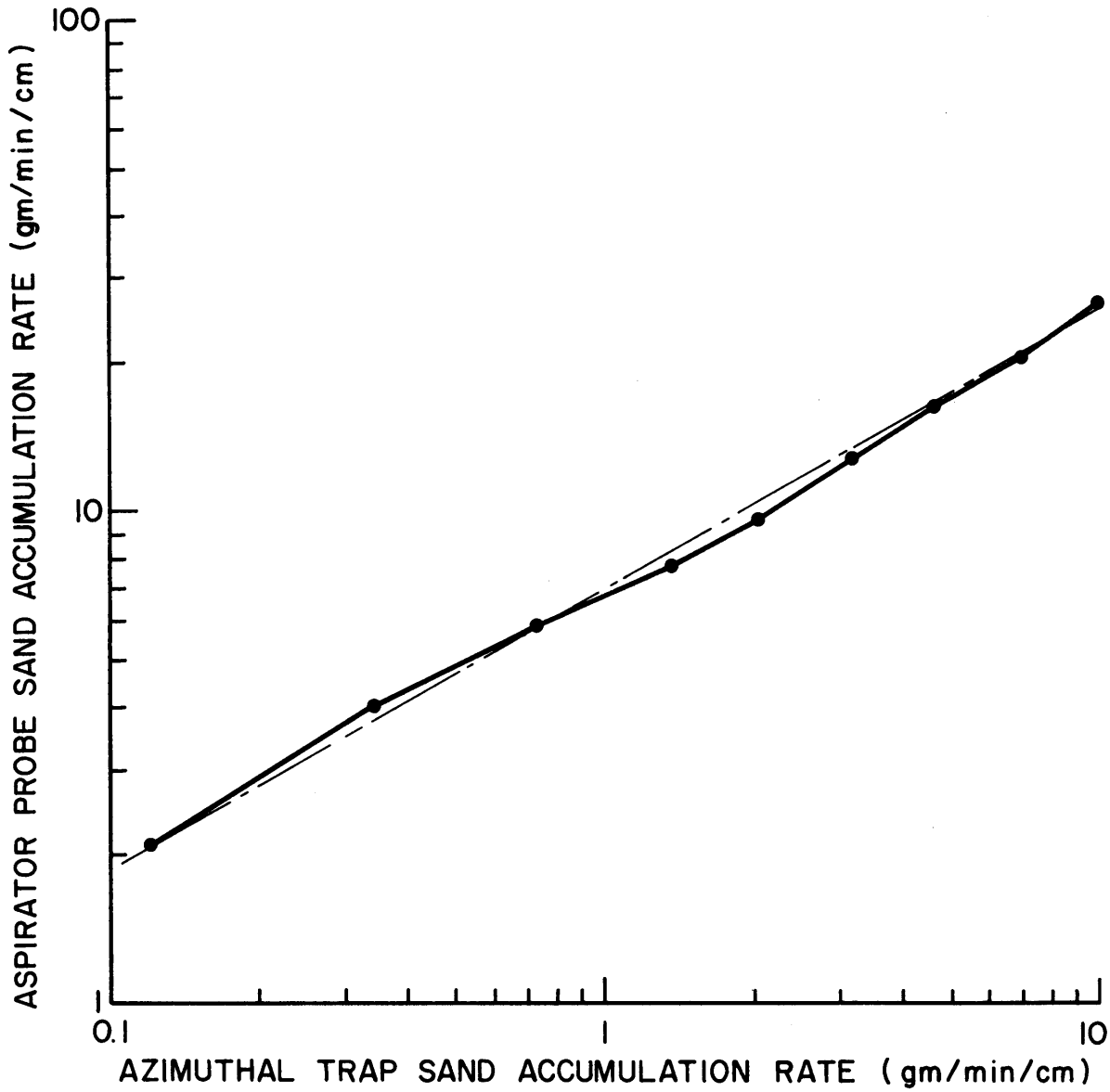

Figure 5-8. Relationship of azimuthal trap and aspirator probe accumulation rates as a function of wind-speed.

Table 5-3. Calculated efficiency of azimuthal sand trap.

Wind Speed (m/s)	Aspirator Probe (gm/min/cm)	Azimuthal Trap (gm/min/cm)	Efficiency (%)
6	2.22	(0.12)	5.5
7	(4.0)	0.34	8.5
8	5.94	(0.73)	12.5
9	7.62	1.37	18.0
10	9.48	(2.05)	22.0
11	(12.20)	(3.20)	26.0
12	(15.90)	4.69	29.5
13	20.4	(6.95)	34.0
14	(25.6)	10.21	40.0

NOTE: Numbers in parentheses obtained from sand accumulation rate vs. free-stream velocity curves.

Figure 5-9 contains a graph of the calculated efficiency of the azimuthal trap as a function of wind speed. This plot is also nearly linear, especially so in the velocity regime from 9-14 m/s.

5.5 Conclusions and Commentary

One factor which affects the efficiency of the azimuthal sand trap is its alignment with the wind. Misalignment of as little as 10° from the prevailing wind can reduce efficiency (sand collected vs. sand transported) as much as 50 percent. Additional misaligment will cause even greater errors in the accuracy of sand transport rates measured with the azimuthal trap.

Tests further indicated that efficiency of the azimuthal trap is directly related to the wind speed. That is to say, efficiency improves as the prevailing wind velocity increases. The trap's efficiency steadily increased from a low of 5.5 percent at 6 m/s to 40 percent at a speed of 14 m/s, in the laboratory tests.

It may be hypothesized from the graphs of Figures 5-7, 5-8 and 5-9 that efficiency of the azimuthal trap will continue to improve with wind

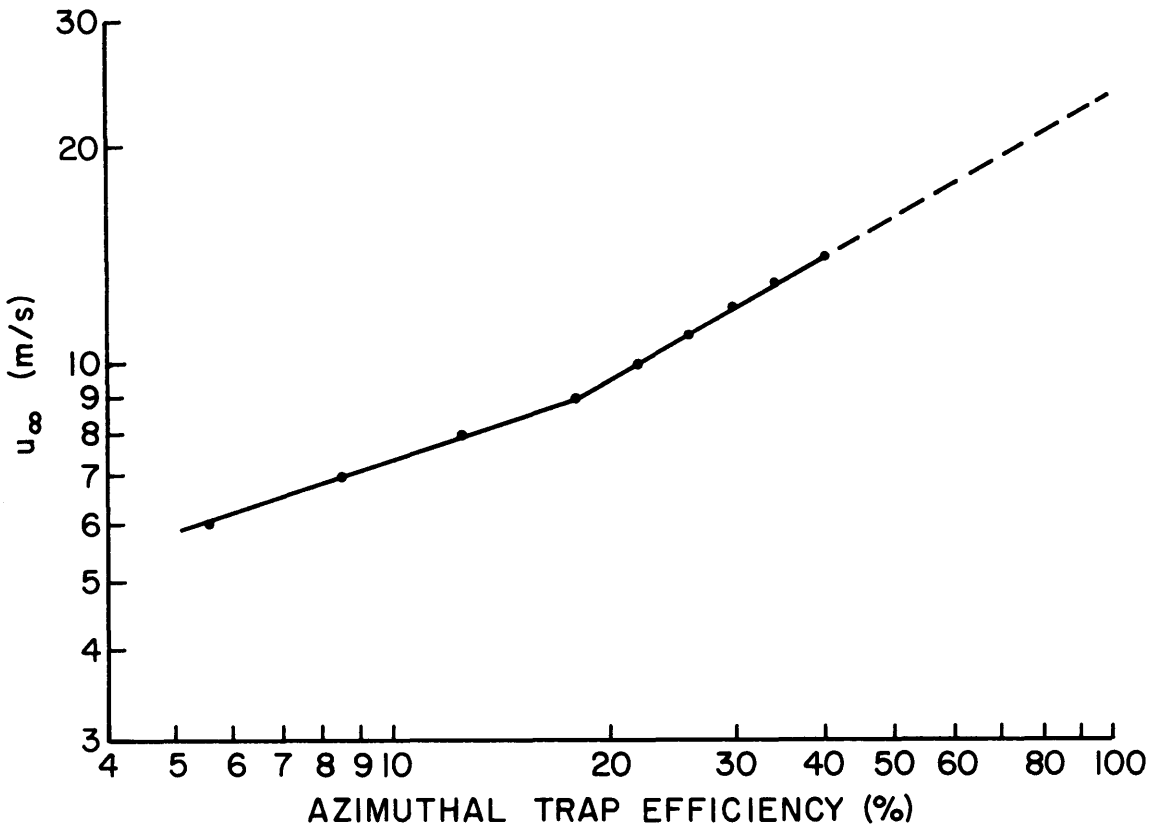

Figure 5-9. Calibration curve for large azimuthal sand trap.

speed. It is reasonable to assume that as speed increases, momentum of the sand particles are increasingly able to override some design deficiencies, although a trap's shape remains the primary factor of its efficiency. In the absence of further testing the foregoing hypotheses remain conjecture. However, the curve contained in Figure 5-9 should still provide good calibration of the existing azimuthal trap's efficiency within tested boundaries and even provide for some extrapolation of the upper limit without inducing large errors. It must be remembered, however, that scaling effects, if any, have not been considered for a tunnel-to-field conversion.

Wind-tunnel tests of the horizontal sand traps yielded a wide variety of results. Repeated tests produced results which varied trap efficiency by unacceptably large factors. The effects of scouring about the base of the traps, erosion from the trap, surface creep, wind-speed and all related variables each provide significant impact upon accuracy of the horizontal traps. The variables which affect efficiency of the cylindrical traps in the tunnel should be even more pronounced in the field where fluctuating wind-speeds and oscillating wind directions become additional factors.

As mentioned in the 1982 report, no significant confidence should be placed in any sand transport rates measured with the horizontal traps as they are subject to many uncontrollable/unexplainable vagaries.

6.0 CHEMICALLY TREATED SAND

6.1 Purpose

Chemicals "STOKOPOL C-4140" and "Sand Still" have been used in an effort to stabilize shifting sand surfaces in some Saudi Arabian locations. The chemical is normally sprayed on the sand in strips oriented perpendicular to the prevailing wind direction, alternated with similar untreated strips. The wind-tunnel experiment was designed to study the effects of sand erosion from the untreated surfaces.

6.2 Preliminary Discussions and Tests

It was originally suggested that the inclined upwind ramp surface extend for a distance of about 2.5 meters. After discussion with visiting representatives from the Research Institute, the length was ultimately reduced to 1.6 meters in order to minimize tunnel blockage effects. Additionally, due to the lack of availability of STOKOPOL C-4140, a decision was made to substitute COHEREX, as the sand stabilizing agent.

Tests were made outside the MWT to ascertain the suitability of a liquid agent, such as COHEREX, in a modelling situation. Strips of sand were saturated with solutions of the chemical which had been mixed with water in ratios of 1:2, 1:3 and 1:4. Each solution failed to dry, coalesce or otherwise harden to modify the sand surface, during the time available to observe its effects. (NOTE: The sand treated with COHEREX remains moist throughout, forty days after application). The decision to use a solid sandpaper covered material, in lieu of the available chemical stabilizing agent, was made at this time, due to time constraints.

6.3 Test Configuration

A plywood ramp with the upwind and downwind surfaces inclined at 13° and 33° to the floor, respectively, was installed across the width of the tunnel. A total of ten 20 cm wide strips of sandpaper covered styrofoam were used to simulate chemically stabilized sand. Strips one through four were located upwind, on a level surface, well out of the influence of the ramp. Strips five and six were positioned immediately ahead of the ramp, while the four remaining strips were evenly spaced along the ramp's upwind surface. Each of the 2.5 cm thick strips was placed atop a 2.5 cm deep bed of sand with the intervals between filled to provide an even sand surface. The tunnel roof was adjusted to provide as nearly constant a test section cross-sectional area in the vicinity of the model as structural limitations permitted. Figure 6-1 provides schematic views of the tunnel configuration for the sand stabilization tests.

6.4 Test Procedures

When model installation was complete the tunnel was permitted to run until the sand-bed stabilized (ripples were formed and in a state of dynamic equilibrium). Measurements for wind distribution (mean velocity) profiles and turbulence intensity were obtained at a wind speed at which saltation on the flat sand surface was discernible. With a reference of approximately 6.35 m/s established in the free-stream, velocities were sampled from the surface to a point above the ABL at four locations. The four positions (1 m upwind from ramp, and 20 cm, 80 cm, 140 cm up the ramp face) are identified on the elevation view of Figure 6-1 with the numerals 1, 2, 3 and 4.

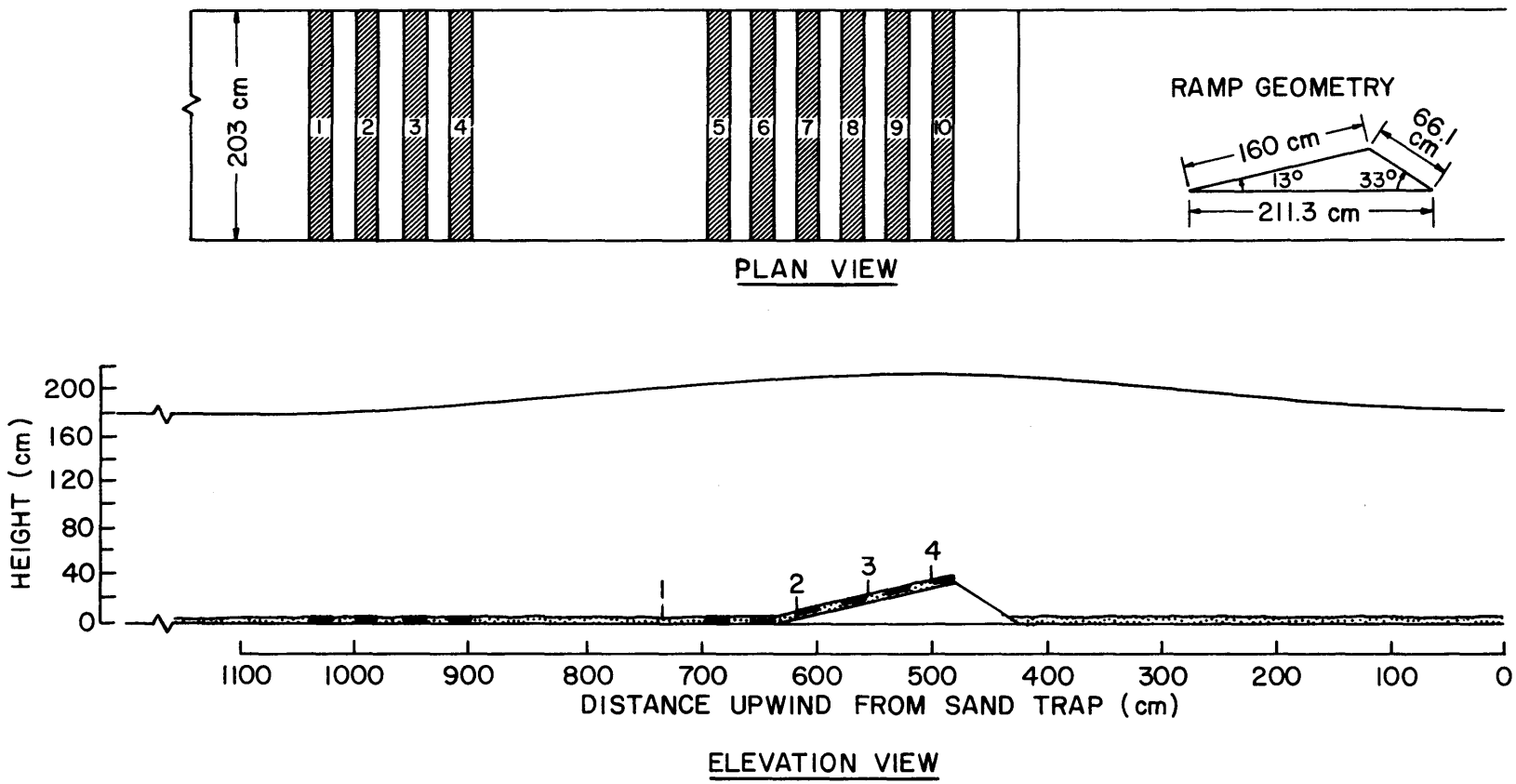

Figure 6-1. Plan and elevation views of 20 cm stabilized sand strips in tunnel test section.

After velocity measurements were completed the tunnel sand-bed was again screeded to provide a smooth sand-bed of 5 cm depth. The erosion tests were conducted by running the tunnel for thirty minute/one hour intervals and using a depth gauge to determine sand height between the simulated stable strips. A free-stream velocity of about 9 m/s was necessary to induce reasonable sand erosion on the inclined surface. Measurements were continued until a stable condition was realized on the untreated ramp surfaces.

6.5 Test Results

Mean velocity and turbulence intensity profiles for the four previously identified locations are presented in Figures 6-2a through 6-2d. Measurements ranged from 1.5 mm to 90-160 cm above the surface. The lowest 20 cm of each profile, where the most rapid changes take place, are reproduced in an expanded version as Figures 6-3a through 6-3d.

The influence of the inclined surface is revealed by an analysis of the mean velocities ($\bar{u}$) and turbulence intensities (TI) at a height about 2 cm above the surface. At Pos. #1, the $\bar{u}$ equaled 2.5 m/s with a corresponding TI of 19 percent. As the flow approached the transition area at the base of the ramp (Pos. #2), an increase in turbulence to 22 percent and decrease in velocity to 1.9 m/s were measured, as expected. Flow up the inclined surface was marked with progressive acceleration and diminishing turbulence. At midpoint of the ramp (Pos. #3), $\bar{u}$ increased to 3.1 m/s, enroute to 5 m/s near the top (Pos. #4), with corresponding decreases in the TI to 13 percent and 9 percent. Mean velocities at all four locations ranged from approximately 6-6.5 m/s at heights of 90-120 cm. Turbulence at the same four positions above the ABL were within the 4-6 percent range.

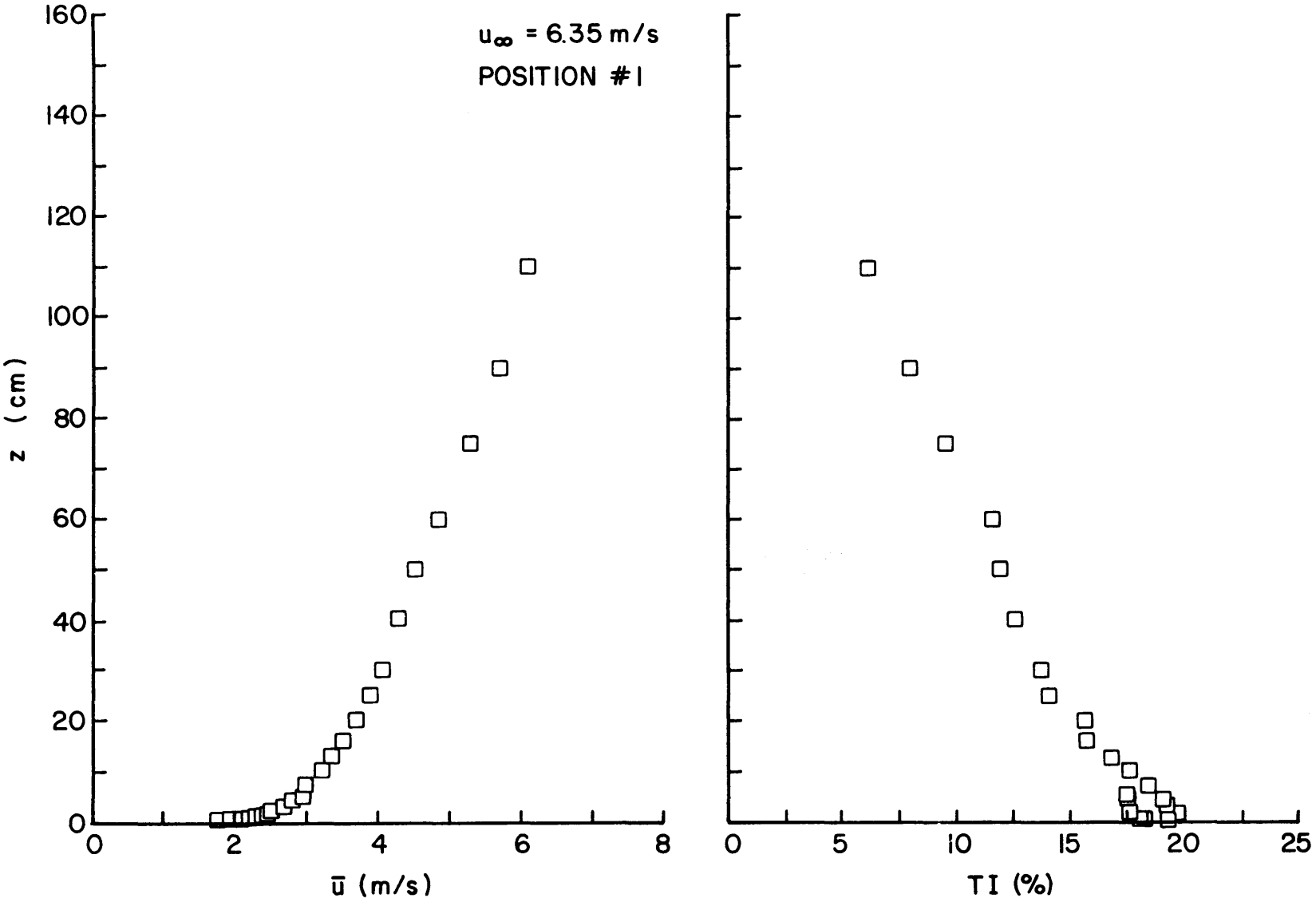

Figure 6-2a. Mean velocity and turbulence intensity profiles from the surface to 110 cm at a position 1 m upwind from simulated dune.

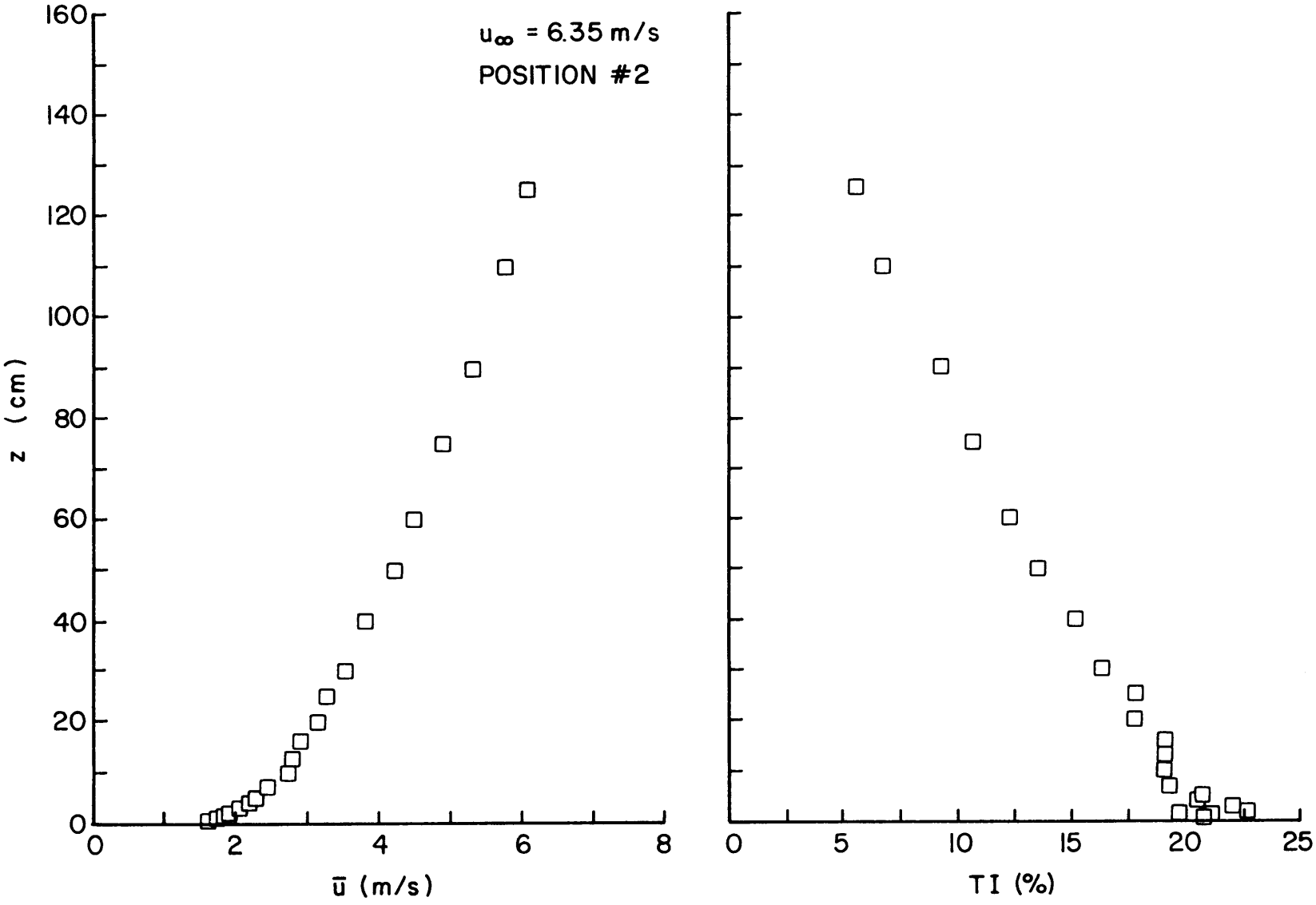

Figure 6-2b. Mean velocity and turbulence intensity profiles from the surface to 130 cm at a position 20 cm up stoss side of simulated dune.

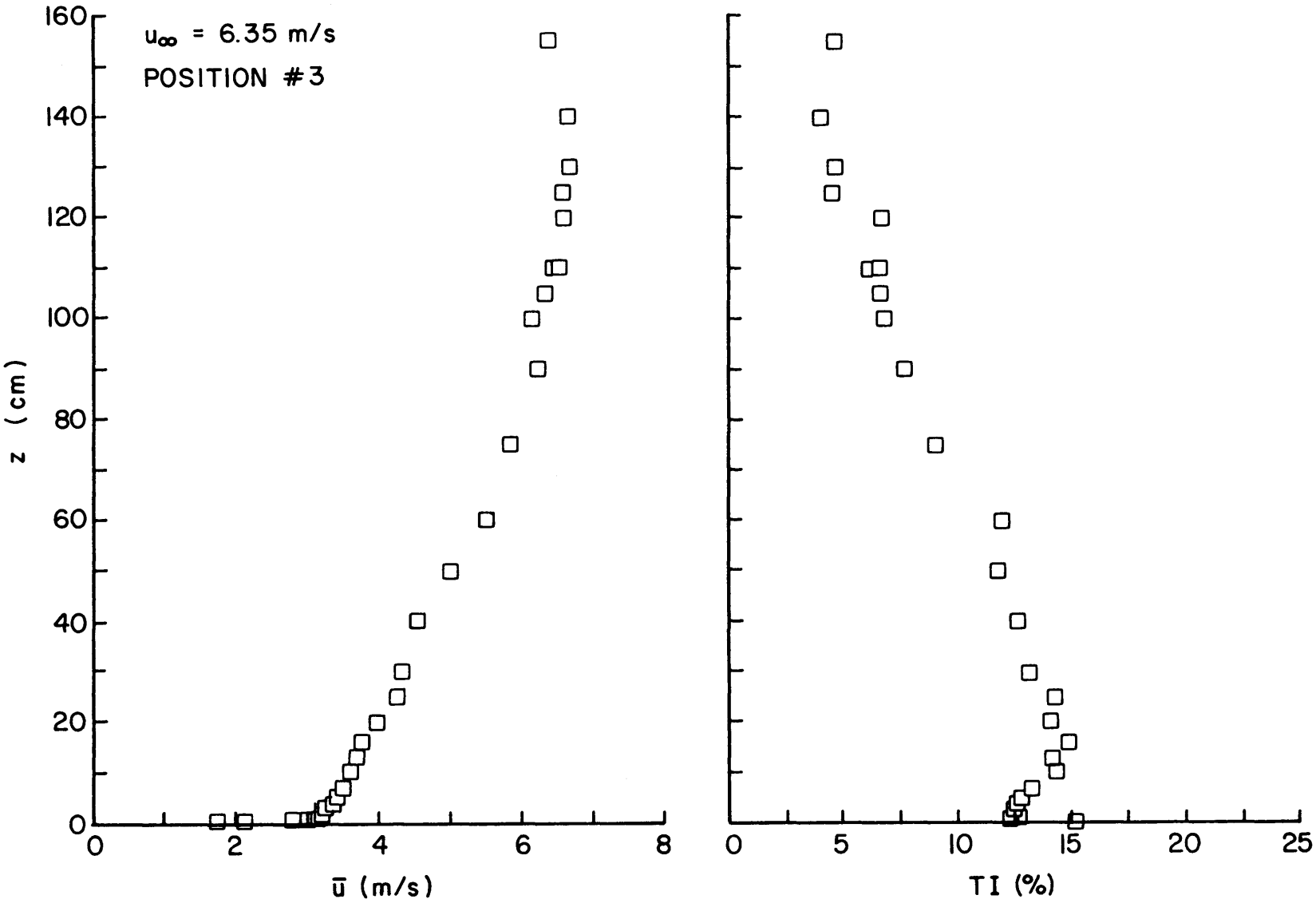

Figure 6-2c. Mean velocity and turbulence intensity profiles from the surface to 150 cm at a position midway up stoss side of simulated dune.

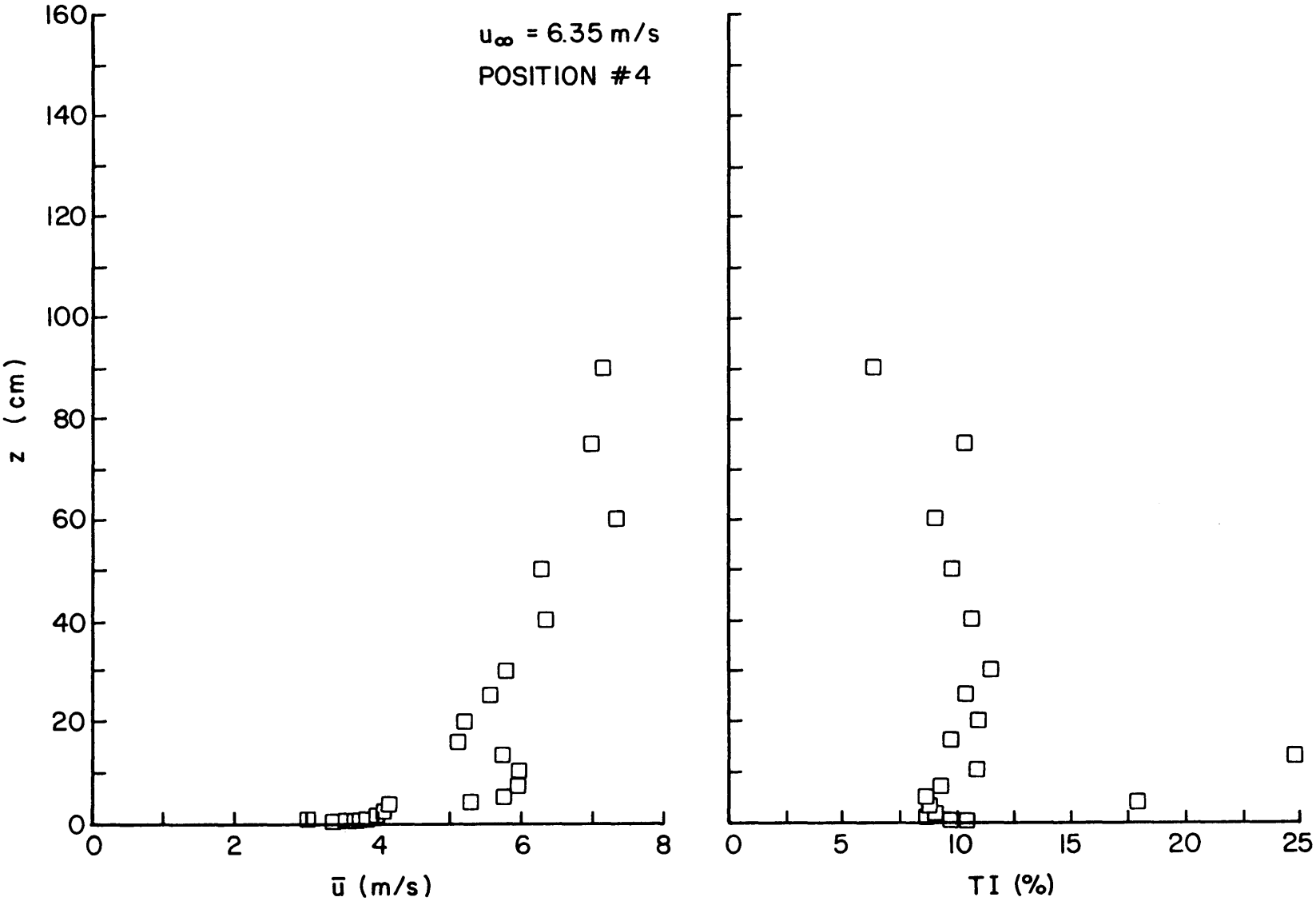

Figure 6-2d. Mean velocity and turbulence intensity profiles from the surface to 90 cm at a position 20 cm below crest on stoss side of simulated dune.

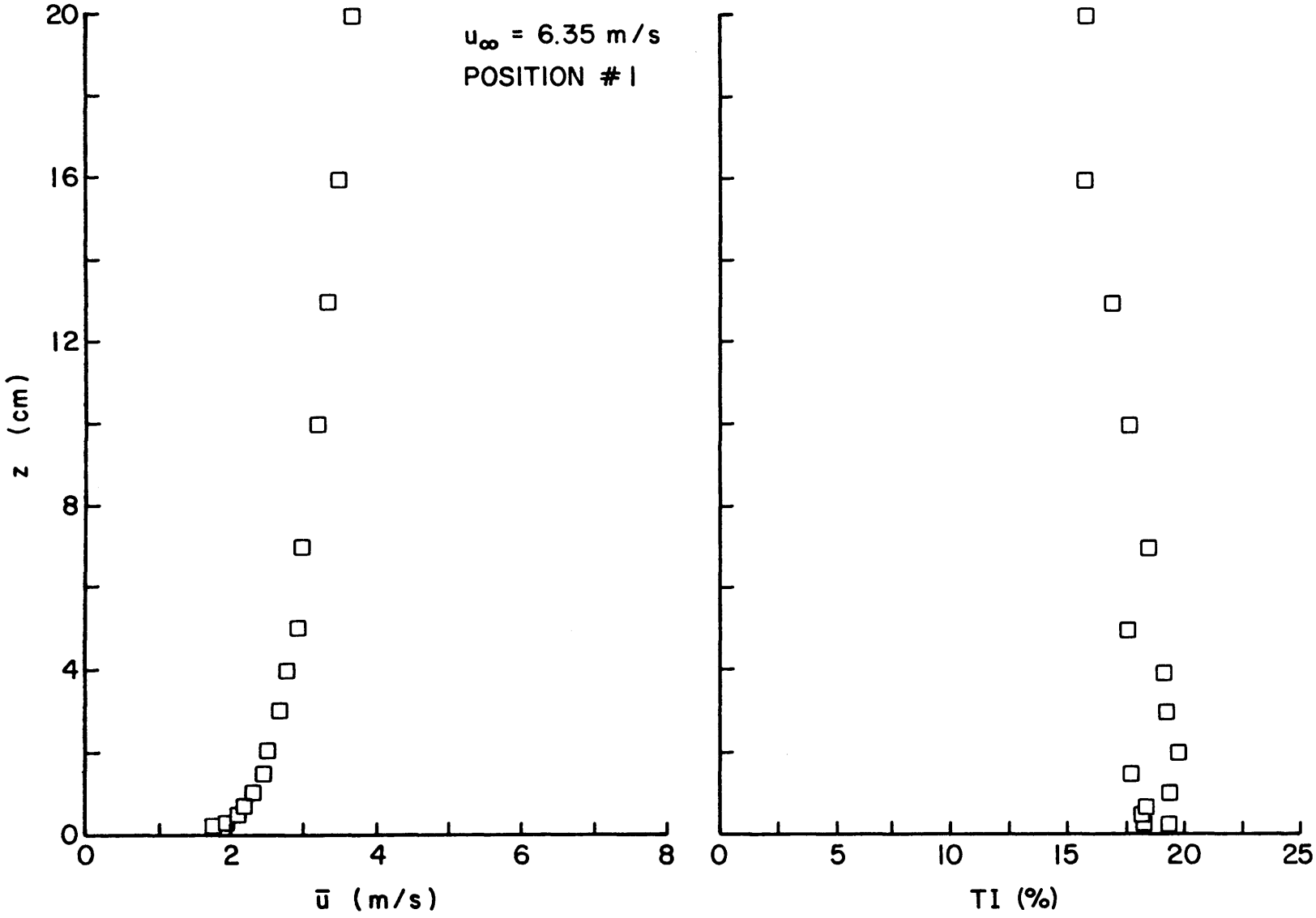

Figure 6-3a. Mean velocity and turbulence intensity profiles from the surface to 20 cm at a position 1 m upwind from simulated dune.

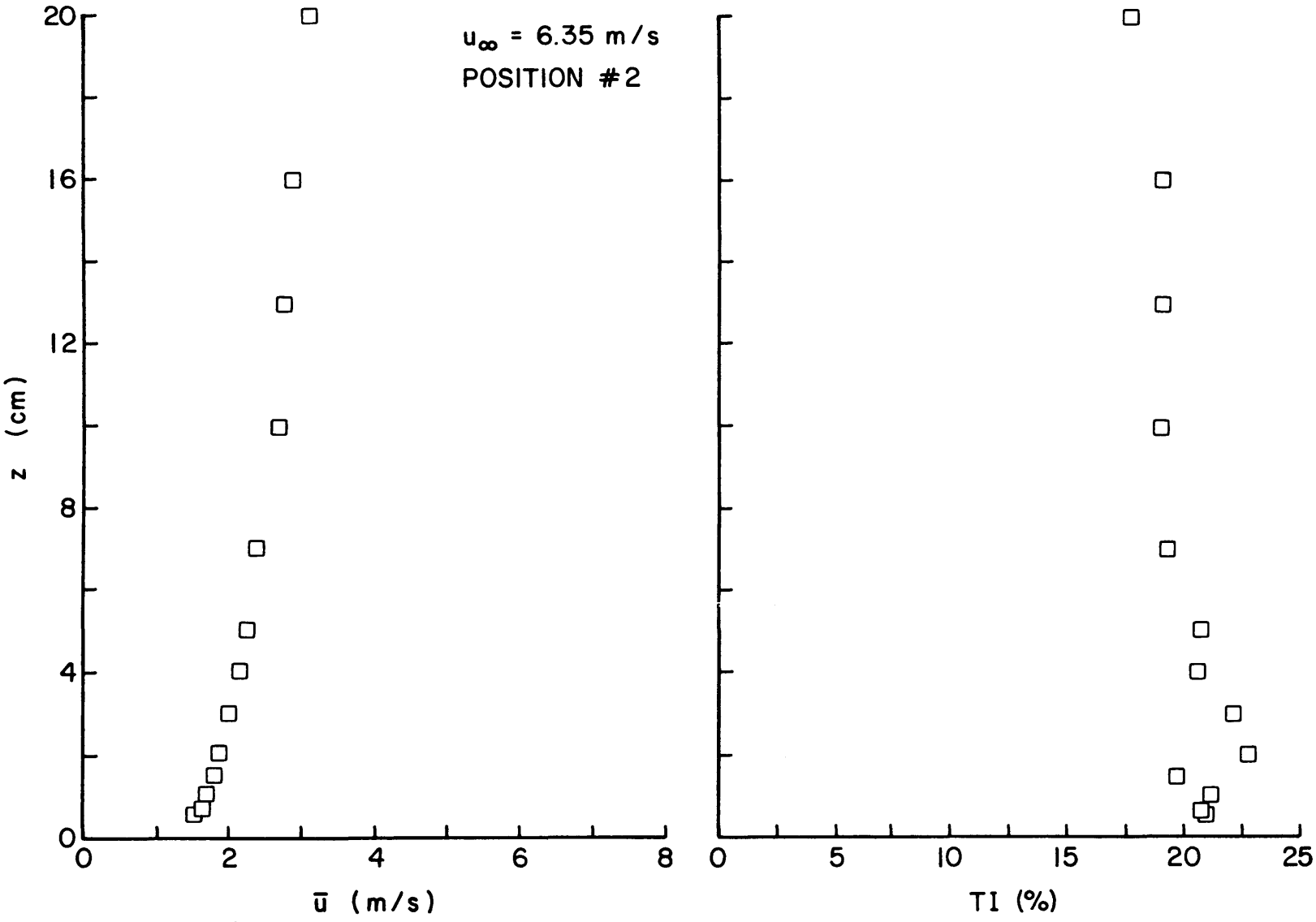

Figure 6-3b. Mean velocity and turbulence intensity profiles from the surface to 20 cm at a position 20 cm up stoss side of simulated dune.

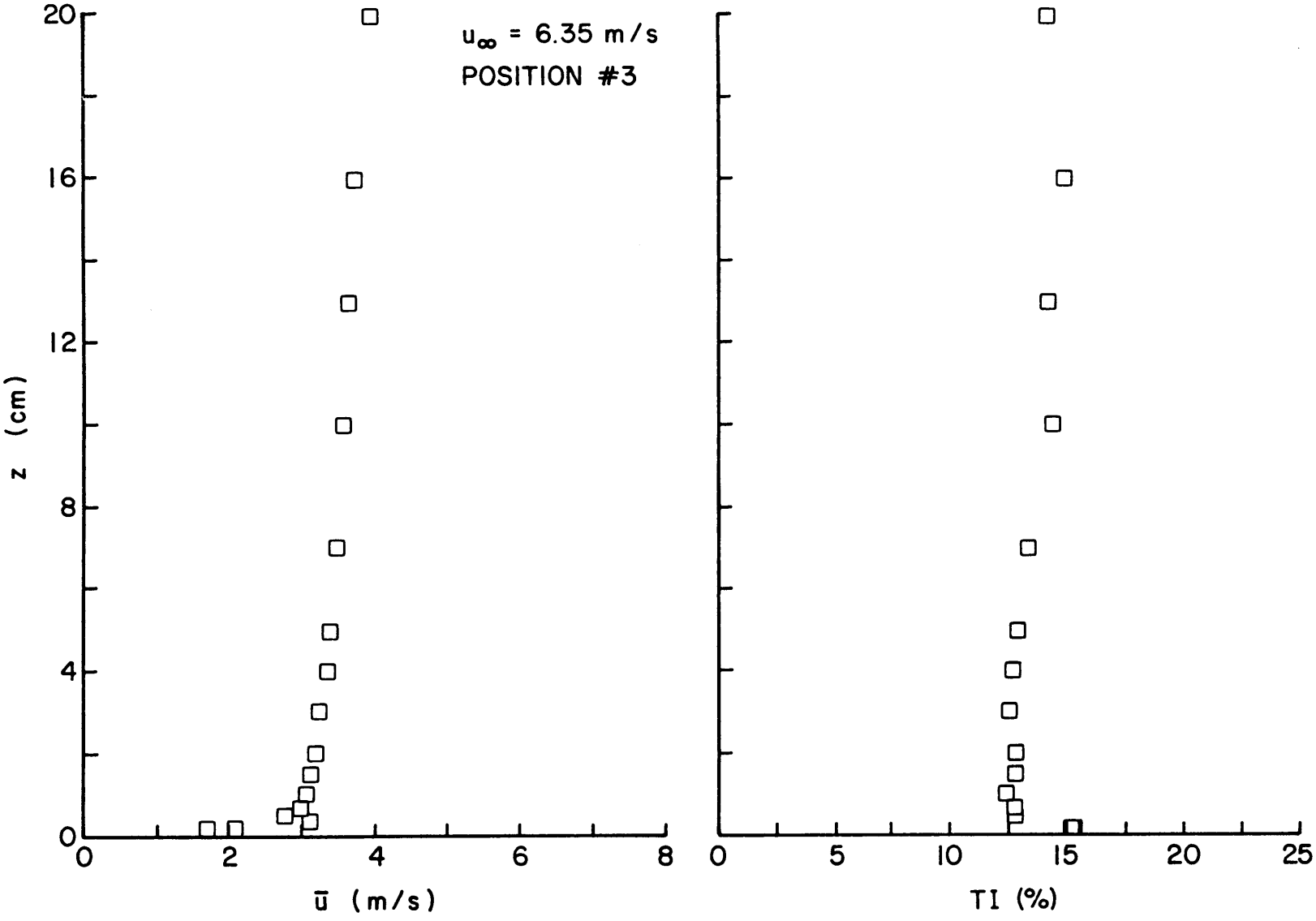

Figure 6-3c. Mean velocity and turbulence intensity profiles from the surface to 20 cm at a position midway up stoss side of simulated dune.

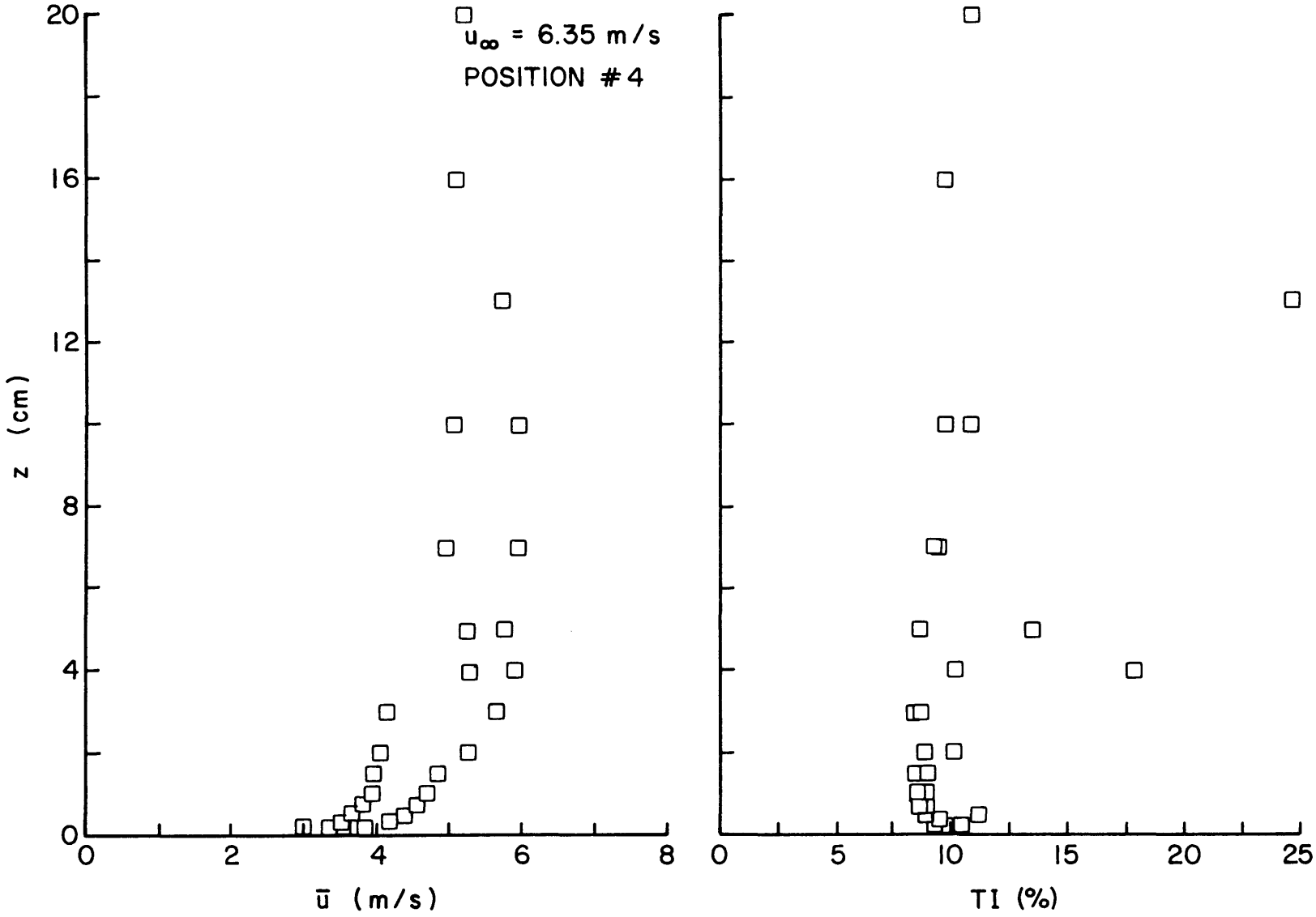

Figure 6-3d. Mean velocity and turbulence intensity profiles from the surface to 20 cm at a position 20 cm below crest on stoss side of simulated dune.

The sand erosion measurements are tabulated in Table 6-1, for each time interval. Erosion of sand between stabilized strips #1 through #4 occurred during the first hour and then a gradual build-up began which resulted in coverage of all four of these upwind strips after 5.5 hours running time.

Deposition of sand began immediately in the vicinity of stable strips #5 and #6. Decreased velocity in this area dictated a loss of sand from the cloud and resultant sand accumulation in the transition area from flat to inclined surface.

Erosion of sand from the unstabilized areas on the ramp began immediately. The rate of erosion increased with distance up the ramp, which is in excellent agreement with lower level velocities measured along this surface. Erosion between strips #7 through #10 continued until each reached a depth of 2.3 cm after 3.5 hours. No further erosion was detected in the remaining two hours of testing.

Figure 6-4 is a downwind view of the inclined surface which contains visual evidence of the sand deposition over the two strips preceding the ramp and erosion of the unstabilized areas on the ramp after 5.5 hours running time.

6.6 Conclusions and Commentary

From the limited wind-tunnel experiments which were performed on a simulated dune surface it is reasonable to conclude that erosion will occur naturally between stabilized strips of sand, particularly on inclined surfaces. As each modelled area eroded to identical depths, the extent of erosion may be related to the wind-speed. As the tests were conducted at only one velocity, this hypothesis requires further investigation. It is also quite possible that the extent of erosion may be influenced by strip width and this phenomenon was not investigated.

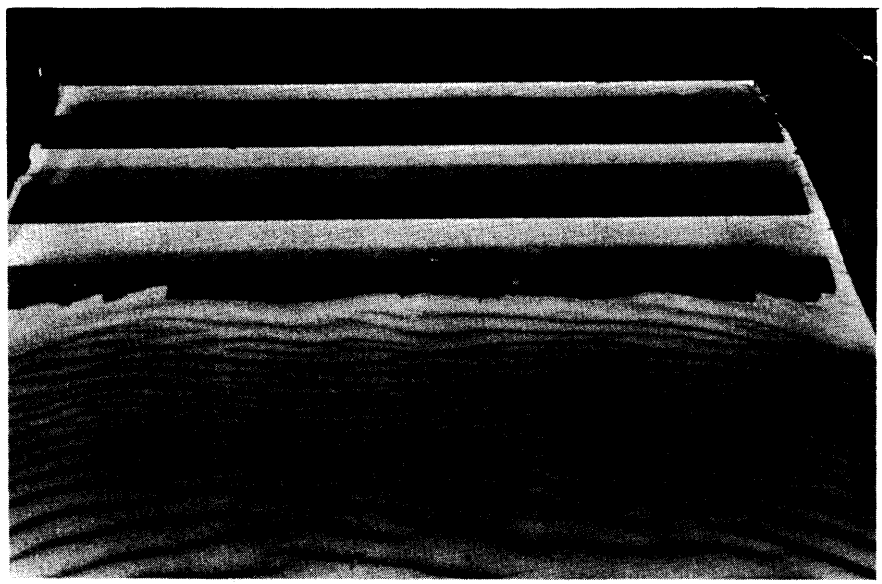

Figure 6-4. Upwind side of ramp (simulated dune) after 5 1/2 hours of running time at 9 m/s wind speed.

The modelling also indicated that sand accumulations at the upwind base may be anticipated when the windward side of the dune is stabilized, as occurred in the roadway tests.

COHEREX, the petroleum based agent, which was substituted for the STOKOPOL C-4140 stabilizer, did not form a surface crust. The agent penetrated the sand quite uniformly and formed a mixture which was an average of 3.5 cm thick. The agent dampened the sand, and in that manner, did provide some stabilization.

Table 6-1. Sand erosion (cm) between stabilized strips on a level surface and on a simulated dune stoss face, for a 9 m/s wind velocity.

Stable Strips	Run Time (hrs)							
	0.5	1.0	1.5	2.0	2.5	3.5	4.5	5.5
Between 1 & 2	-1.5	-1.5	-1.1	-0.9	-0.3	+1.0	+1.4	+1.9
Between 2 & 3	-1.8	-2.1	-1.9	-2.0	-1.7	-0.5	+0.9	+1.4
Between 3 & 4	-1.0	-2.1	-2.1	-2.0	-2.1	-1.4	-0.9	+1.4
Between 5 & 6	+0.3	+0.3	+0.5	+0.8	+0.7	+2.0	+2.5	+2.9
Between 7 & 8	-1.1	-1.4	-1.7	-2.1	-2.2	-2.3	-2.3	-2.3
Between 8 & 9	-1.4	-1.9	-2.0	-2.1	-2.2	-2.3	-2.3	-2.3
Between 9 & 10	-2.0	-2.2	-2.2	-2.1	-2.2	-2.3	-2.3	-2.3

7.0 REERENCES

1. Cermak, J. E. "Laboratory simulation of atmospheric boundary layer." AIAA Journal, Vol. 9, No. 9, September 1971, pp. 1746-1754.

2. Cermak, J. E. "Wind tunnel design for physical modeling of atmospheric boundary layer." Journal of the Engineering Mechanics Division, ASCE, Vol. 107, No. EM3, Proc. Paper 16340, June 1981, pp. 623-642.

3. Cermak, J. E. "Simulation of the natural wind." Preprint 82-518, ASCE Convention and Exhibit, New Orleans, Louisiana, 25-29 October, 1982.

4. Cermak, J. E., H. W. Shen, J. A. Peterka and L. F. Janin "Wind-tunnel research for IAP sand study project." CER82-83JEC-HWS-JAP-LFJ24, Colorado State University, September 1982.